universität wien

# DISSERTATION / DOCTORAL THESIS

Titel der Dissertation / Title of the Doctoral Thesis

„Depth distribution of benthic foraminifera in the mid to deeper sublittoral and uppermost bathyal around Okinawa, Japan“

verfasst von / submitted by

Wan Nurzalia Wan Saelan, BSc, MSc

angestrebter akademischer Grad / in partial fulfilment of the requirements for the degree of

Doctor of Philosophy (PhD)

Wien, 2016 / Vienna, 2016

| | |
|---|---|
| Studienkennzahl lt. Studienblatt / Degree programme code as it appears on the student record sheet: | A 794 685 437 |
| Dissertationsgebiet lt. Studienblatt / Field of study as it appears on the student record sheet: | Biologie |
| Betreut von / Supervisor | Ao. Univ. -Prof. Dr. Johann Hohenegger |

## ACKNOWLEDGEMENTS

Help from Him has been transformed in the form of awesome people throughout this whole journey. Thank you to the Malaysian government and Universiti Malaysia Terengganu for sponsoring my study. My former master's degree supervisor, Prof. Dr. Mohd Lokman Husain (Deputy Vice Chancellor of Universiti Malaysia Terengganu) was the one who pushed me to be involved in foraminiferal study in the very beginning. I am always grateful that he did that but more importantly I am grateful that I listened to him. Ao. Univ. -Prof. Dr. Johann Hohenegger, my PhD supervisor. Thanks to him I am able to learn more about foraminifera. He basically taught me how science should be pursued. His guidance and support are overflowing and I can't thank him enough. Thank you to my colleagues in the Department of Palaeontology, University of Vienna for the massive support. Everyone is so helpful. Alhamdulillah for such a great support system. Special mention to Kazuhika Fujita from the University of the Ryukyus for sending the samples to Vienna. Without the samples, this study will be impossible to perform.

Of course, who am I without my parents. Thank you Abah, Mak, Farhah, Zulhilmi and Shakirah for always believing in Angah, without fail. To the most important person in my life, my husband, Asrul Ramli. He helped me during lab work; he accompanied me in the office during weekends and holidays; he is basically my backbone. He did everything he can to smoothen this journey and for that I dedicate this thesis to him.

Last but not least, my friends in Kuala Lumpur, Kuantan, Kuala Terengganu and Vienna. Thank you so much guys. I would also like to mention Miss Fazlin Rahayu, a former secretary at the Scholarship Division, Ministry of Higher Education in Malaysia who made sure that I received my monthly allowance on time and not forgetting efficient reimbursement every single time. Thank you so much Ayu!

## TABLE OF CONTENTS

## ABSTRACT

Distribution of optimally preserved benthic foraminifera is related to depth in the sublittoral and uppermost bathyal around Okinawa, Japan. Depth is a composite factor that influences physical factors, i.e., temperature, salinity, substrate caused by hydrodynamics and illumination. Sediment samples between 64m and 275m depth were taken from the seafloor by grab sampler. Optimally preserved tests were analyzed using a Motic SMZ-168 microscope. Grain sizes < 63μm were analyzed using Micromeritics Sedigraph ET5100. Grain sizes > 63μm were analyzed by sieving. Statistical analysis performed on seven larger and 45 smaller benthic foraminiferal species includes canonical correspondence and correspondence analyses. Depth distributions are fitted by power transformed normal distributions. Distributions in grain size classes and percentages of silt and clay are depicted in circle graphs.

Taxonomic description grouped the benthic foraminiferal tests into seven orders, 55 families, 100 genera and 175 species. The first components of the bimodal distribution pattern of *Amphistegina lessonii, Calcarina hispida, A. bicirculata, A. radiata, A. papillosa* and *Operculina complanata* demonstrate optimal depth distributions in the mid sublittoral. *Planostegina longisepta* demonstrates optimal depth distribution in the deeper sublittoral. Dependence on coarse sand is demonstrated by *A. bicirculata, A. radiata* and *C. hispida*. Dependence on fine sand is demonstrated by *A. lessonii*. Dependence on very fine sand is demonstrated by *O. complanata* and *P. longisepta*. *A. papillosa* does not show dependence on any particular substrate type. Optimal depth distributions of the larger foraminifera are in agreement with the living individuals except for *A. lessonii, A. radiata* and *C. hispida*. Larger foraminiferal specimens picked between the 125 - 250μm sieve fraction demonstrate depth transport. Low depth transport is demonstrated by *A. lessonii* and *C. hispida*. Depth transports at 210m are demonstrated by *A. bicirculata, A. papillosa, O. complanata* and *P. longisepta* indicating similar test buoyancies. Highest depth transport at 270m is demonstrated by *A. radiata*.

Depth distributions of optimally preserved smaller benthic foraminiferal tests demonstrate optima in the mid sublittoral, deeper sublittoral and uppermost bathyal. Optimal depth distributions of the tests in the mid and deeper sublittoral is related to dependence on either coarse sand, medium sand or no dependence on specific substrate type. Optimal depth distributions of the tests in the uppermost bathyal is related to dependence on fine and very fine sand. Agglutinated foraminiferal tests have demonstrated agreement between optimal depth distribution and dependence on substrate type. Benthic foraminifera with secreted $CaCO_3$ tests have shown partial agreement between optimal depth distribution and dependence on substrate type. Life position of the smaller benthic foraminifera is influenced by test dominance in percentages of silt and clay. Test dominance in the high or highest percentages of silt and clay is reflected on infaunal life position. Test dominance in the low or lowest percentages of silt and clay is reflected on epifaunal life position. Test dominance in medium percentages or no dominance reflects on either epifaunal or infaunal life position. Test dominance in percentages of silt and clay is related to its dependence on substrate type.

## ZUSAMMENFASSUNG

Vor Okinawa (Japan) konnte im Sublittoral und obersten Bathyal eine tiefen-abhängige Verteilung benthischer Foraminiferen in optimaler Erhaltung erkannt werden. Die Parameter Temperatur, Salinität, Hydrodynamik und Licht sind tiefenabhängig. Sedimentproben wurden mittels eines Probengreifers ("grab sampler") in Tiefen zwischen 64m und 275m genommen. Optimal erhaltene Gehäuse wurden unter dem Motic SMZ-168 Mikroskop untersucht. Die Korngrößen <63µm wurden mit Hilfe des Sedigraphen (Micrometrics Sedigraph ET5100) untersucht; Korngrößen >63µm mittels der Siebmethode. Kanonische Korrespondenzanalyse und einfache Korrespondenzanalyse wurden an sieben Spezies von Großforaminiferen und 45 Kleinforaminiferenspezies durchgeführt. Die Tiefenverteilung wird über eine power-transformierte Normalverteilung erklärt. Die Korngrößenverteilung ist in Kreisdiagrammen dargestellt.

Taxonomisch ließen sich die Foraminiferen in 7 Ordnungen mit 55 Familien, 100 Gattungen und 175 Arten gliedern. Das bimodale Verteilungsschema von *Amphistegina lessonii, Calcarina hispida, A. bicirculata, A. radiata, A. papillosa* and *Operculina complanata* zeigt in der Tiefenverteilung ein Optimum im mittleren Sublittoral; *Planostegina longisepta* zeigt ein Optimum im tieferen Sublittoral. Das Auftreten der Arten *Amphistegina bicirculata*, *A. radiata* sowie *C. hispida* zeigt einen Zusammenhang mit grobsandigem Substrat; *A. lessonii* von mit feinsandigem Substrat und die Arten *Operculina complanata* und *P. longisepta* mit sehr feinsandigem Substrat. *Amphistegina papillosa* ist nicht an einen speziellen Substrattyp gebunden. Abgesehen von *Amphistegina lessoni*, *A. radiata* und *C. hispida*, stimmen die Tiefenverteilungen der Gehäuse mit den Verteilungen lebender Individuen überein. Ein deutlicher Tiefentransport ist bei allen Arten deren Gehäuse eine Größe zwischen 125µm und 250µm aufweisen, zu sehen. Bei den Arten *Amphistegina lessonii* und *C. hispida* ist dieser Tiefentransport vergleichsweise gering. Vermutlich wird der Tiefentransport der Arten *Amphistegina bicirculata, A. papillosa, O. complanata und P. longisepta* (210m Wassertiefe) durch die ähnliche hydrodynamische Beschaffenheit der Gehäuse beeinflusst. Den weitesten Transport weist *Amphistegina radiata* (270m Wassertiefe) auf.

Die Tiefenverteilungsoptima der Kleinforaminiferen liegen im mittleren bis tieferen Sublittoral und dem obersten Bathyal. Optima im obersten Bathyal sind an feinen und sehr feinen Sand gebunden, während Verteliungsoptima im mittleren und tieferen Sublittoral keine eindeutige Abhängigkeit von einem Substrattyp zeigen. Agglutinierende Foraminiferen zeigen in dieser Studie einen Zusammenhang zwischen ihren Tiefenverteilungsoptima und der Abhängigkeit von einem Substrattyp. Die Verteilung kalkschaliger Foraminiferen zeigt einen teilweisen Zusammenhang zwischen der optimalen Tiefenverteilung und der Abhängigkeit vom Substrattyp. Die Korngrößenverteilung im Substrat beeinflusst die Lebensweise der Kleinforaminiferen; Infaunal lebende Formen bevorzugen einen hohen Silt und Ton Anteil. In Sedimenten mit niederen Silt und Ton Anteilen dominieren Kleinforaminiferen mit epifaunaler Lebensweise.

# CHAPTER 1

# INTRODUCTION

## 1.1 Background of the study

Investigation on the depth distribution of optimally preserved benthic foraminifera in the mid to deeper sublittoral and uppermost bathyal is an articulation to the depth distribution of living larger symbiont bearing benthic foraminifera in the euphotic zone. The focus is on depth as the composite factor influencing benthic foraminiferal distribution. Distribution in grain size classes is investigated because depth distribution is influenced by substrate type. Distribution in percentages of silt and clay gives account into epifaunal and infaunal life position of the smaller benthic foraminifera.

Marine realm is divided into different zones (Figure 1.0). Basic division units such as depth and distance from the continent divide inshore zone from the open ocean. Marine organisms prefer specific marine zone to inhabit. This is due to the physics and chemistry constituting each marine zone. Depth is the composite factor influencing the distribution of organisms in the marine environment. Marine zones are divided into supralittoral, littoral, sublittoral, bathyal, abyssal and hadal (Lalli & Parsons 1997). The sublittoral zone is always inundated by seawater where it has significant wave and tidal actions. This zone starts at the end of the littoral zone and ends at the end of the continental shelf. Physical characteristics of this zone are; (1) light attenuation reaches the seafloor and (2) temperature and pressure are more consistent throughout the water column. Habitats for the majority of oceanic creatures are located in the sublittoral zone due to the high rate of primary productivity.

Foraminifera are unicellular microorganisms inhabiting the marine environment. The foraminiferal cell body is often protected by a test. The test is a unique characteristic due to the composition that can consist of either calcium carbonate ($CaCO_3$) or agglutinating grains (organic or inorganic). The test construction is as simple as a single chamber or in more complicated forms with multiple chambers and elaborate structures. Test form and function is an important aspect in benthic foraminiferal ecology. Specialized test form and function are foraminiferal adaptation to environmental condition. Foraminifera prefer specific environmental gradient in order to attain optimal distribution.

In the euphotic zone, illumination is controlled by depth and transparency of the water column. Illumination is the functional factor which influence the distribution of living larger symbiont bearing benthic foraminifera. On the other hand, distribution of smaller benthic foraminifera is mainly influenced by grain size distribution. Depth is regarded as a factor that indirectly influences the distribution of smaller benthic foraminifera in the sublittoral zone.

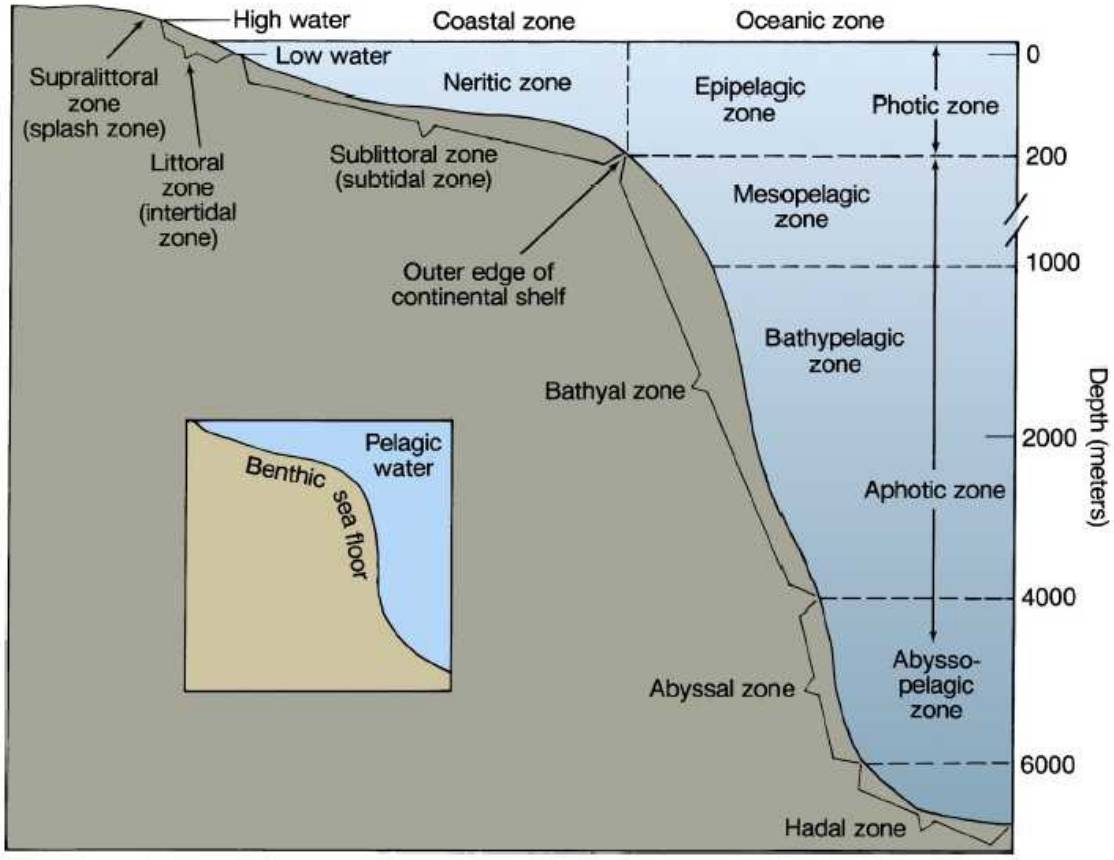


Figure 1.0 Marine environmental zonations (Lalli & Parsons 1997)

## 1.2 Depth distribution

Pioneering depth distribution investigations were performed by Hallock 1984 and Hohenegger 1994. They are the first workers quantitatively investigating the distribution of living larger foraminifera according to depth; with illumination and hydrodynamics as key environmental factors influencing the distribution (Hohenegger et al. 1999; Hohenegger 2000a). These foraminifera acquire specialized wall and test structures to adapt to illumination and hydrodynamics conditions. Larger foraminiferal tests are subjected to downslope transport along the depth gradient (Hohenegger & Yordanova 2001a; Hohenegger & Yordanova 2001b). Factors influencing transport and displacement of larger foraminiferal tests are offshore bottom current induced by cyclones, slope inclination and test bouyancies. Further experiments were conducted to determine settling and traction velocities of larger foraminiferal tests (Yordanova & Hohenegger 2007), e.g., strong biconvex tests of *Amphistegina lessonii* are less buoyant than flat tests of *A. bicirculata*. Relationship between living and optimally preserved empty tests of larger benthic foraminifera indicated that distributions of these two coincide with each other (Yordanova & Hohenegger 2002). Empty tests were classified into three preservation states, i.e., optimal, good and poor. Distribution of optimally preserved tests demonstrates usefulness in investigating benthic foraminiferal distribution. Wave motion and light decline exponentially with depth thus indicating tremendous potential of larger foraminifera in paleodepth estimation (Hallock et al. 1991).

## 1.3 Aim of the study

This is the first attempt to investigate depth distributions of benthic foraminifera in the mid to deeper sublittoral and uppermost bathyal. Approximate maximum depths attained in studies of living larger benthic foraminifera were 120m, whereas this study investigates the depth distributions of smaller benthic foraminifera occurring at maximum depth of 290m. This study aims to identify all benthic foraminiferal species sampled in the investigation area. Further analyses are performed on the most frequent benthic foraminiferal species consisted of seven larger foraminiferal species belonging to three families and 45 smaller foraminiferal species representing 21 families. The next aim is to determine the depth distribution and dependence on substrate types of these species. The final aim is to identify epifaunal and infaunal life position of smaller benthic foraminifera by investigating their distribution in percentages of silt and clay.

## 1.4 Thesis outline

An overview of the thesis structure is given as follows. The first chapter is the introduction. Chapter 2 outlines the methodology that has been adopted. Explanations are given on the investigation area, sampling procedure, laboratory analysis and data analysis. Chapter 3 discusses the environmental factors involved in this study. The factors are depth, inclination and sedimentological parameters. Chapter 4 contains the taxonomic description and plates of all benthic foraminiferal species found in the investigation area. Chapter 5 investigates the depth distribution and dependence on substrate type of larger benthic foraminiferal species. Chapter 6 investigates the depth distribution, dependence on substrate type and dominance in percentages of silt and clay of smaller benthic foraminiferal species. The final part of the thesis includes bibliography and species index.

# CHAPTER 2

# METHODOLOGY

## 2.1 Location and environmental setting

Okinawa is the largest island of the Ryukyu Island Arc. The Ryukyus are located in the southwest of mainland Japan and consist of hundreds of islands and islets. These islands are arranged in a curve hence the name Ryukyu Island Arc. The Ryukyus extend from Tanega Island (30°44'N, 131°0'E) in the northeast to Yonaguni Island (24°27'N, 123°0'E) in the southwest. The area is bounded by the East China Sea on the northwest and by the Pacific Ocean on the northeast. The Okinawa Trough (2000m depth) in the south separates the Ryukyu Arc from the East China Sea shelf. The Kuroshio warm current flows through the trough (Hatta & Ujiie 1992). The climate of Ryukyus is subtropical with monthly mean seawater temperature of 21.5 - 29.0°C (at the surface) and 20.4 - 21.4°C (at 150m depth). Annual mean seawater temperature is 25.2°C (at the surface) and 20.7°C (at 150m). Annual mean salinity is 34.6 at the surface and 34.8 at ~200m depth. The area is rimmed by coral fringing reefs with two basic topographic zones that can be divided into the reef flat and reef slope. The reef slope zone starts with a steep drop from the reef flat and it extends from the surface to 50m depth. The shelf around Ryukyus is flat and slope gently seaward. The seaward margin is located at the depth of 90m to 170m (Matsuda & Iryu 2011). The width of the shelf is from 0 to 25km. Okinawa is subjected to several typhoon events per year thus the sediments were always transported from the beach and reef moat area to the upper fore reef area (Yordanova & Hohenegger 2002).

The northern transects of the investigation area are located to the northwest of Okinawa with sampling stations located around the south of Izena Island (Figure 2.0). The southern transect is located to the west of Motobu Peninsula with sampling stations located in the south of Ie Island.

## 2.2 Sampling and preparation

Samples were collected by a grab sampler during a cruise of a Japanese research vessel investigating the seafloor around Okinawa. These samples were sent to the Department of Palaeontology, University of Vienna by Kazuhika Fujita from the University of the Ryukyus. The samples were collected between 64m and 275m depth. Parts of the surface sediments were stored in plastic jars, filled with seawater and formalin to fix the protoplasm of living organisms if they were present. A set of sieves with mesh sizes of 63μm, 125μm and 250μm was used to wash and sieve the samples. Samples were dried at 60°C. Universal sample splitter was used to split samples of 250μm fraction. Microsplitter was used to split samples of 125μm fraction. Only optimally preserved foraminiferal specimens were picked and identified using Motic SMZ-168 Series microscope. Taxonomic identification was performed by following Akimoto et al. 2002; Hatta & Ujiie 1992; Hohenegger 2011; Loeblich & Tappan 1994; Parker 2009.

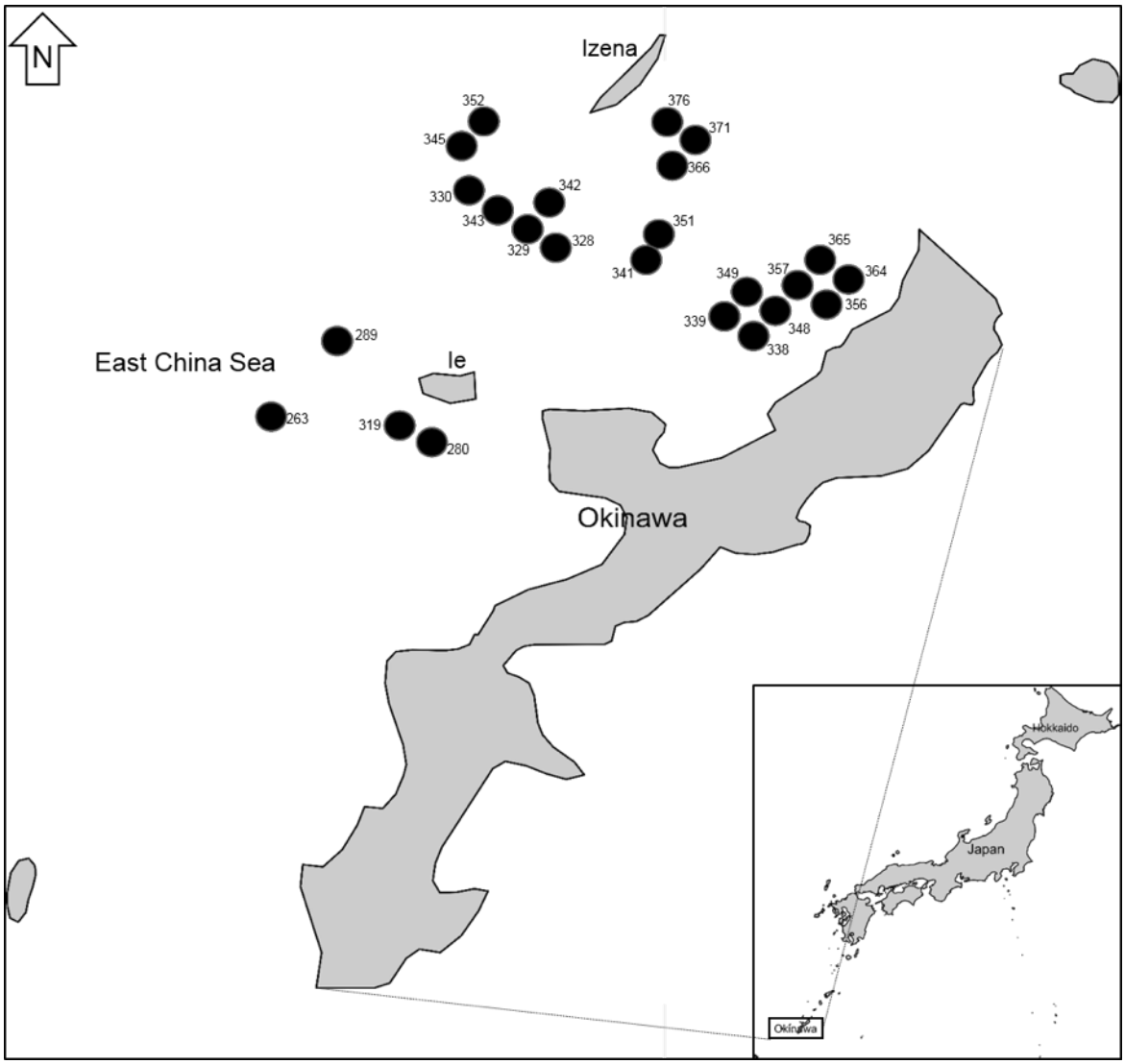


Figure 2.0 Location of sampling stations

Samples for grain size analysis were brought to the sedimentology laboratory of the Department of Sedimentology, University of Vienna for further analysis. Sediments that are < 63μm were analyzed using the Micromeritics Sedigraph ET5100. Sediments that are > 63μm were analyzed by sieving (Boggs 2006; Cheetham et al. 2008). Stack of sieves with mesh size diameters of 4mm, 2mm, 1mm, 0.5mm, 0.25mm, 0.125mm and 0.063mm were placed onto a sieve shaker with water running through the sieves that bring along the sediments. Sediments collected at each sieve were dried at 60°C.

## 2.3 Data analysis

Optimally preserved foraminiferal specimens (Yordanova & Hohenegger 2002) were identified and counted. Normalization of the test abundance to a standard weight of 100g was conducted due to differences in sample weights. Canonical correspondence analysis was performed in statistical software PAST 3.2 to identify the relationship between foraminiferal abundance and environmental factors (Hammer & Harper 2006). According

to the ordinations, the important environmental factors are depth and sedimentological parameters. Species distributions in relation to environmental factors, i.e., depth, grain size and percentages of silt and clay were analyzed by correspondence analysis in PAST 3.2 (Hammer & Harper 2006). Distributions in grain size classes and percentages of silt and clay are depicted in circle graphs that have been analyzed in Microsoft Excel.

Depth distributions of benthic foraminiferal species presented in histograms were analyzed in IBM SPSS Statistics 22 and Microsoft Excel 2013 for Windows. Frequency distributions are unimodal and can be fitted by power transformed normal distributions (Hohenegger 2000a; Hohenegger & Yordanova 2001b; Hohenegger 2006). The formula is:

$$\varphi\ (x) = d \exp[-(x^y - \mu)^2 / 2\sigma^2]$$

Where $d$ represents the abundance optimum, $\mu$ the mean and $\sigma^2$ the distribution variance. The power factor $y$ signalizes intensities of left ($y > 1$) or right side ($y < 1$) skewness. Values of the power factor higher than 1.5 or less than 0.1 indicate significant restriction by the gradient at higher scores in the former and lower scores in the latter.

# CHAPTER 3

# ENVIRONMENTAL FACTORS

## 3.1 Depth and inclination

Marine realm is divided into different depth zones. Basic division units such as depth and distance from the continent divides inshore zone from the open ocean. Depth is the basic unit that classifies these zones. Marine organisms have shown preference on which depth zone to inhabit. Therefore, depth is regarded as a factor that influences the distribution of marine organisms.

Depth distribution of benthic foraminifera is investigated as an articulation to depth distribution of living larger symbiont bearing benthic foraminifera. Illumination is the functional factor which influences the distribution of living larger benthic foraminifera. Illumination is controlled by depth in the euphotic zone, with the intensity decreases exponentially with increasing depth. On the contrary, distribution of smaller benthic foraminifera is influenced by grain size distribution. Grain size distribution at the seafloor is related to hydrodynamics, with wave motion decreases exponentially with depth. Depth is the composite factor controlling illumination and grain size distribution. Depth indirectly influences the distribution of smaller benthic foraminifera in the sublittoral.

Living larger benthic foraminifera are adapted to illumination by acquiring specialized wall structures (Hallock 1981; Hottinger 1983; Hohenegger 1994; Hohenegger et al. 1999; Pecheux 1995). Families with opaque test walls have the ability to reduce light penetration (Hohenegger 2004). Members of the Peneroplidae family show symbiotic relationships with rhodophyceans. *Peneroplis planatus* is the most abundant in the reef flat and uppermost reef slope. *P. pertusus* is less abundant in the reef flat but more abundant in slightly deeper environment down to 30m depth. *Dendritina ambigua* and *D. zhengae* are more restricted to the upper fore reef areas from 5 to 50m. Members of the Soritidae family show symbiotic relationships with zooxanthellae, i.e., *Sorites orbiculus, Amphisorus hemprichii* and *Marginopora vertebralis*, enabling these foraminifera to inhabit the highly illuminated area of the fore reef moat. Only *Parasorites orbitolitoides* avoids high-energy environment inhabiting at 10 - 60m depth.

Families with hyaline test walls show adaptation to light penetration (Hohenegger 2004). Members of the family Amphisteginidae host diatoms as symbionts such as *Amphistegina lobifera* which is dominant in shallowest reefs. *A. lessonii* also shows preference to shallow reef. *A. bicirculata* prefers much deeper environment from 40m to 110m, while *A. radiata* and *A. papillosa* that both exhibit symmetrical, biconvex tests and peripheral apertural position prefer deeper environment. Members of the Calcarinidae family which host endosymbiotic diatoms, i.e., *Baculogypsina sphaerulata* and *Calcarina gaudichaudii* are abundant in reef crest pools of the reef flat zone. *C. defrancii* is restricted to the calm water of the uppermost reef slope with lower depth limit at 20m. *C. hispida* is the most dominant calcarinid in the fore reef area with depth distribution range from 50 to 70m. The largest calcarinid *Baculogypsinoides spinosus* has a depth distribution of 50 to 70m. Members of the family Nummulitidae exhibit symbiotic relationships with diatoms. *Operculina ammonoides* is the most abundant in the fore reef area down to 20m depth. *Nummulites venosus* prefers deeper regions from 20m to 80m depth. *Heterostegina*

*depressa* is the only nummulitid inhabiting the frontal crest pools with depth distribution that started from the surface down to 70m. The largest living calcareous foraminifera, *Cycloclypeus carpenteri* is abundant in the deeper fore reef areas with depth distribution from 30m to 100m.

Inclination is another factor included in the canonical correspondence analysis. Inclination is defined as the calculated tangent of the angle ($\alpha$) that formed when the slope (*m*) makes an angle  with the *x* axis (Figure 3.0). The slope of a line can be calculated when horizontal run is divided by the vertical rise:

$$slope = \frac{vertical\ rise}{horizontal\ run}$$

The formula to calculate slope is as follows:

$$m = \frac{a}{b}$$

The formula to calculate the tangent of an angle ($\alpha$):

$$tan\ \alpha = \frac{opposite}{adjacent}$$

Since the formula to calculate slope (*m*) is also defined as opposite/adjacent, inclination ($\alpha$) can be calculated as follows:

$$tan\ \alpha = \frac{opposite}{adjacent} = m$$

$$tan\ \alpha = m$$

$$\alpha = \arctan m$$

Vertical rise represents depth and horizontal run represents the distance of sample location from the reef edge. Inclination is measured because it gives the information of transported materials. It is especially useful for larger foraminiferal distribution in this study that have shown influence of downslope transport.

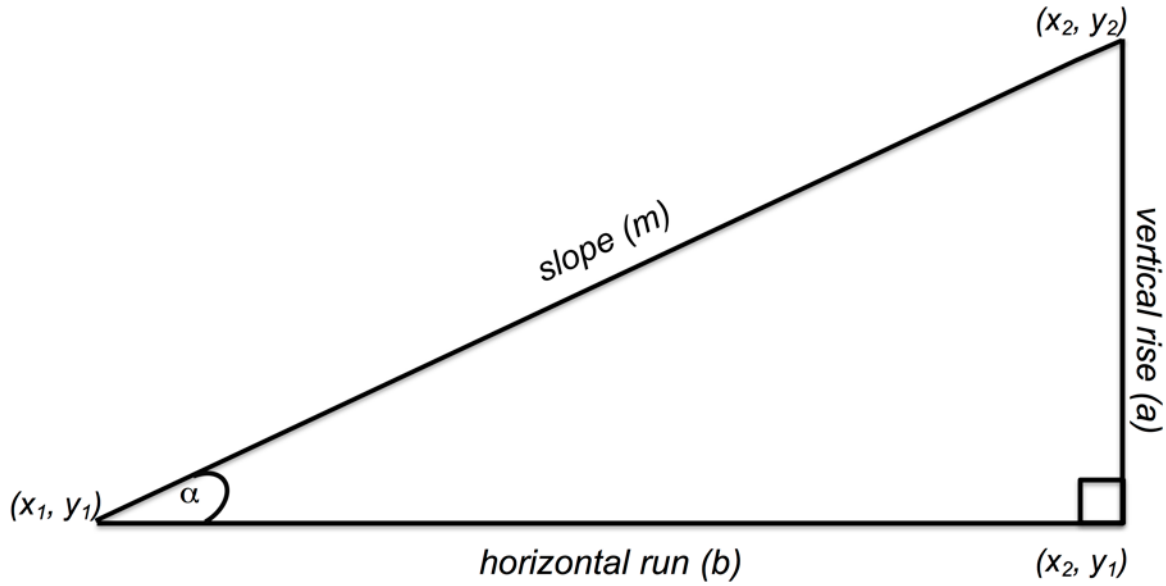


Figure 3.0 Tangent of angle for calculating inclination

3.2 Relationship between depth, inclination and grain size distribution

Canonical correspondence analysis investigates the relationships among depth, inclination, sedimentological parameters (Figure 3.1) and grain size distribution (Figure 3.2). The sedimentological parameters are mean, sorting, skewness, proportion of the main component, proportion of gravel and proportion of silt and clay. The sorting coefficient marks the range of grain sizes over the scale and magnitude of spread or scatter of these values; high values indicate poor sorting and low values indicate good sorting. Skewness indicates deviation from the symmetrical distribution; positive skewness indicates dominance of the finer grain sizes and negative skewness indicates dominance of the coarser grain sizes. Proportions have been linearized by arcsine-root transformation. These are done for the proportions of the main component, gravel class (phi < -1) and silt and clay class (phi > 4).

Depth and inclination are positively correlated with each other, with increasing depth correlates with increasing inclination (Figure 3.1). The arrow direction for depth which lies very close to the first axis (eigenvalue of 97.4%) indicates that depth is the most important factor in the ordination. The arrow direction for inclination which lies very close to the second axis (eigenvalue of 2.597%) indicates that inclination is not an important factor in this ordination. Depth shows positive correlations with increasing skewness, increasing mean grain size and increasing proportion of silt and clay. Increasing depth shows positive correlation with increasing skewness indicating samples from the deeper region are dominated by finer sediments, as shown by the position of skewness at the highest point in the first axis. Increasing depth also shows correlations with increasing mean grain size and increasing proportion of silt and clay. Mean grain size and proportion of silt and clay are located at the lowest position in the first axis thus demonstrating weak correlations with increasing depth. Negative correlations are shown between increasing depth and increasing proportion of gravel, as well as increasing sorting coefficient. This indicates that samples from the shallow region are dominated by coarser sediment

grains. Weak negative correlation is also shown between increasing proportion of the main component and increasing depth. An example of grain size distribution is shown in the ordination indicating samples from the deeper region are dominated by finer sediment grains.

Figure 3.2 shows the positions of grain size distributions in all samples which correspond to depth and inclination. The ordination is constructed on the same axis as in figure 3.1. It is demonstrated that depth and inclination positively correlated to one another. Depth is a more important factor than inclination due to its position in the ordination. Depth is located very close to axis 1 which has the highest eigenvalue of 97.4%. Inclination is located much nearer to axis 2 which has much lower eigenvalue of 2.597%. There are five samples located in the top-left of the ordination showing strong positive correlations with increasing depth. These samples represent the dominance of silt and clay in the deeper region. Three samples located in bottom-left of the ordination showing correlations with increasing depth. These samples represent dominance of sandy sediments. One of the samples show bimodal distribution pattern indicating that the sediments were transported from the shallow region, with the main component distributed as sand and the second component is consisted of low proportion of gravel.

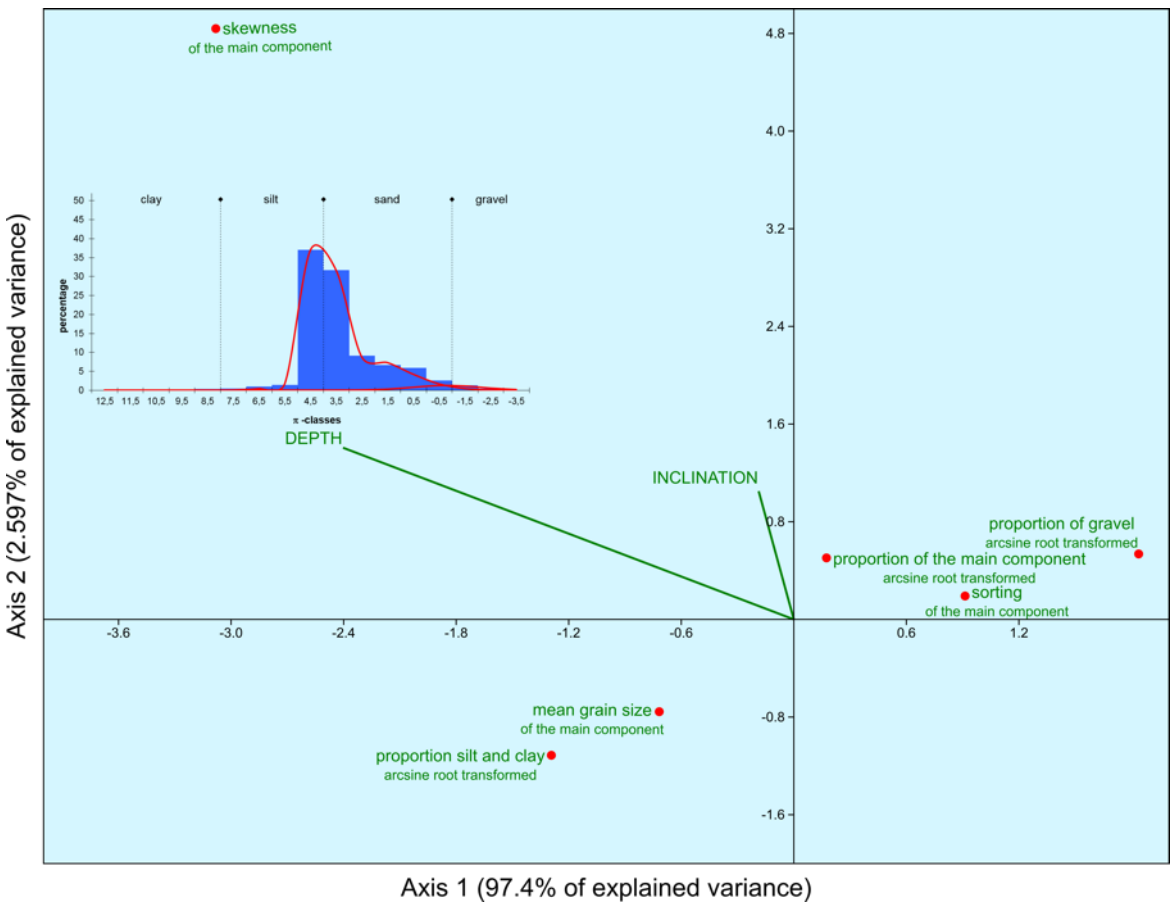


Figure 3.1 Ordination of sedimentological parameters showing correlations with depth and inclination

Most of the samples are located in the shallow region (Figure 3.2), as demonstrated by the positions of twelve samples in the bottom-right of the ordination. These samples have shown positive correlations with decreasing depth. Grain size distribution of these samples show strong dominance of coarser sediment grains, i.e., coarse sand and gravel. Five of these samples show bimodal pattern with the main component dominated by sand and the second component dominated by high proportion of gravel. The remaining four samples located in the top-right show weak correlations with decreasing depth. These samples show dominance of sandy component. One of the samples that is located very close to the first axis shows bimodal pattern with the main component distributed in sand class and the second component distributed in high proportion of gravel. The main component in the bimodal distributions indicate autochthonous material and the second component represents allochthonous material. Detailed explanations of the grain size distribution in the study area are discussed in the next section (3.3).

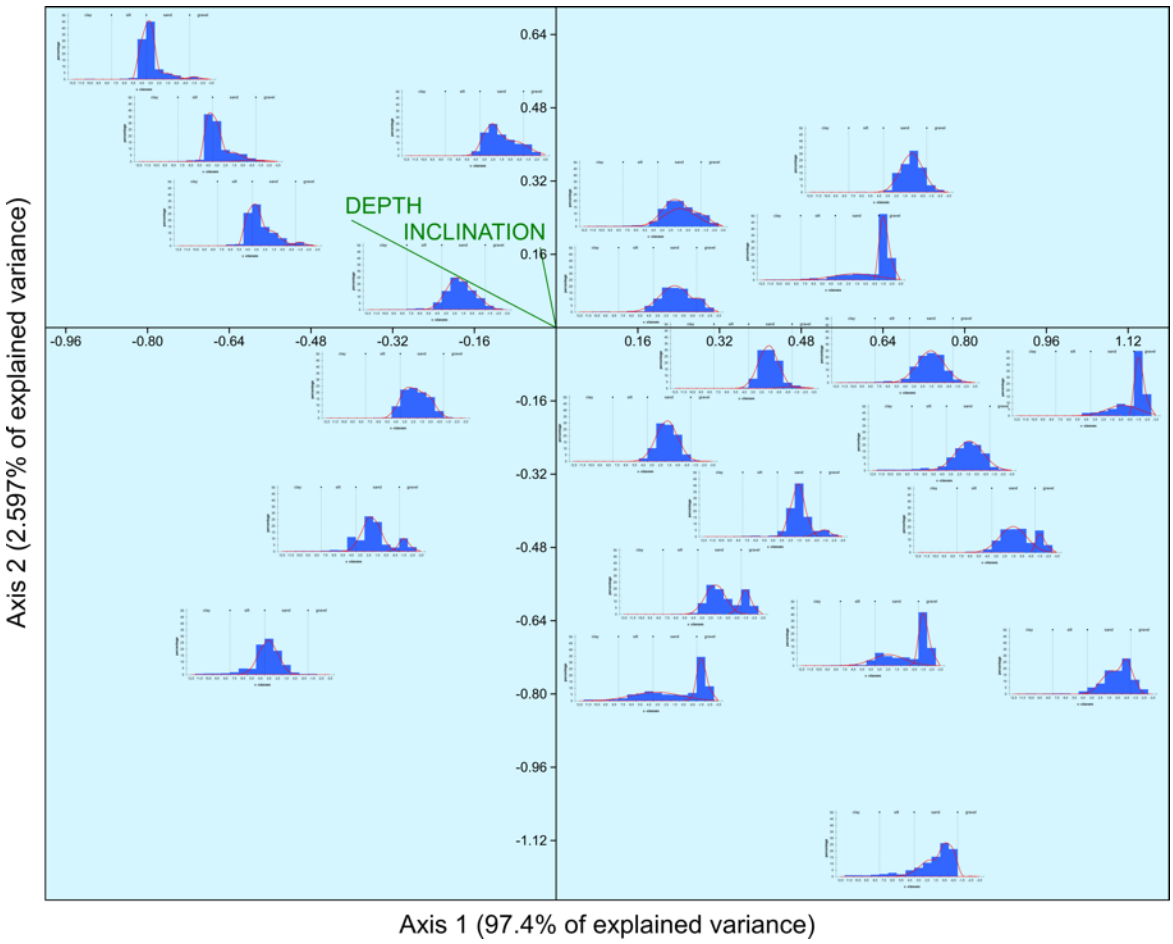


Figure 3.2 Ordination of grain size distribution showing correlations with depth and inclination

## 3.3 Grain size distribution

Sediment samples collected in the south of Ie Island (Figure 3.3) are all poorly sorted. All are symmetrically distributed except at 189m where the sediments are strongly fine skewed. Sediments at 69m depth belong to the very fine sand class. Sediments at 148m belong to the medium sand class. Deeper sediments at 189m and 203m are distributed

into very fine sand class. Bimodal distribution of the sediments is shown by the shallowest sample in this area at 69m depth. The bimodal pattern shows that the main component is composed of fine sand and the second component belongs to the coarse sand. Sediments of the south of Ie Island are mainly composed of very fine sand.

Sediments sampled in the southeast of Izena Island (Figure 3.4) are all poorly sorted. At less than 100m depth, symmetric distributions are found at 64m, 79m and 94m except at 95m, where sediments are fine-skewed. Between 100m and 200m; symmetric distributions are found at 134m. Sediments at 105m and 139m are fine-skewed. The deepest sample in this area is located at 211m. Sediments are strongly fine-skewed at this depth. Shallowest sediments sampled at less than 100m belong to the medium sand class except at 64m, where sediments belong to the fine sand class. Between 100m and 200m; sediments fit into the medium sand class except at 105m, where sediments belong to the fine sand class. The deepest sample at 211m consisted of very fine sand. Bimodal distributions of the sediments are shown at samples 64m and 95m. These bimodal distributions show that the main components are composed of fine-grained sediments and second component consists of coarse grains. Sediments of the transect in the southeast of Izena Island are composed of mainly medium sand grains.

Sediment samples collected in the south of Izena Island are all poorly sorted (Figure 3.5). The shallowest samples collected at 71m and 72m are nearly symmetrically distributed. A slightly deeper sample at 75m is strongly fine-skewed. Coarse-skewed sediments of the shallow depth are at 79m and 83m. Between 100m and 140m, sediments are nearly symmetrically distributed except at 117m, where sediments are fine-skewed. Sediment skewness of the deeper samples between 150m and 300m are as follows; strongly coarse-skewed at 168m, strongly fine-skewed at 227m and symmetrically distributed at 275m. Shallowest samples between 70m and 80m are distributed in different sand size classes; medium sand at 71m, coarse sand at 72m and 79m and very fine sand at 75m. Sediments at 100 - 140m fit to the medium sand class. Sediments at depth range of 150 - 300m belong to different sand classes; coarse sand at 168m, very fine sand at 189m, medium sand at 227m and fine sand at 275m. Bimodal distributions of the sediments are shown in samples at 71m, 79m, 115m and 275m, with main components distributed in the fine grain size classes and the second components belong to the coarse grain size classes. Sediments of the transect in the south of Izena Island are composed of mainly medium to coarse grain sizes at less than 100m, medium grain sizes at 100 - 150m and fine to very fine grain sizes at 150 - 300m.

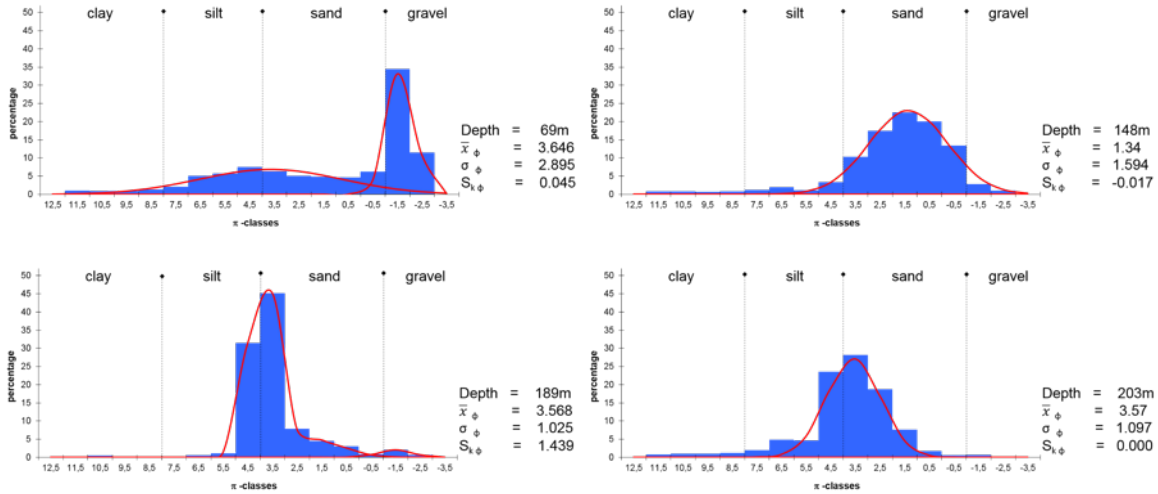


Figure 3.3 Grain size distribution of sediments sampled in the south of Ie Island. Decomposition of non-normal distributed frequencies into normal distributed components. All parameters (mean, sorting and skewness) in phi (ϕ) units

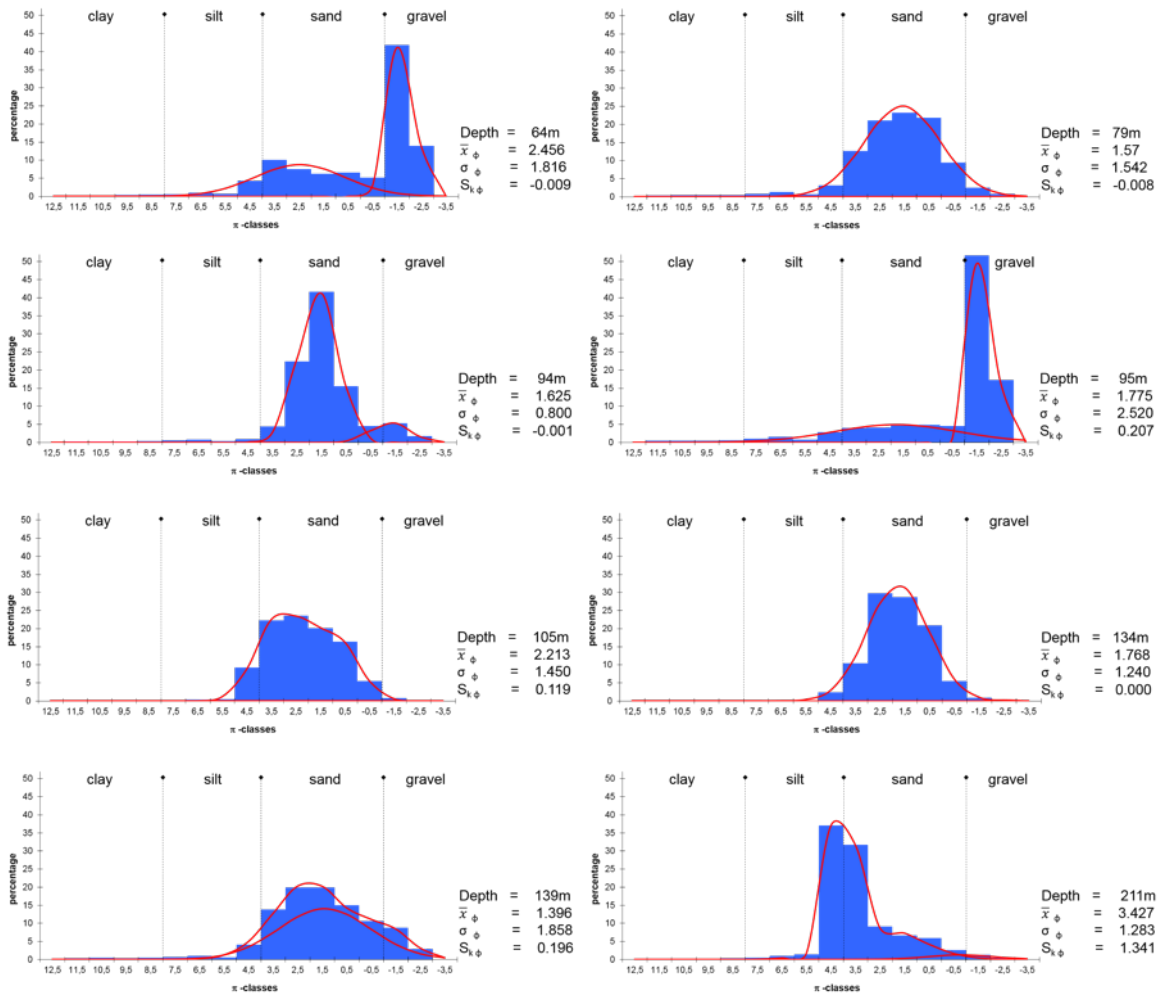


Figure 3.4 Grain size distribution of sediments sampled in the southeast of Izena Island. Decomposition of non-normal distributed frequencies into normal distributed components. All parameters (mean, sorting and skewness) in phi (ϕ) units

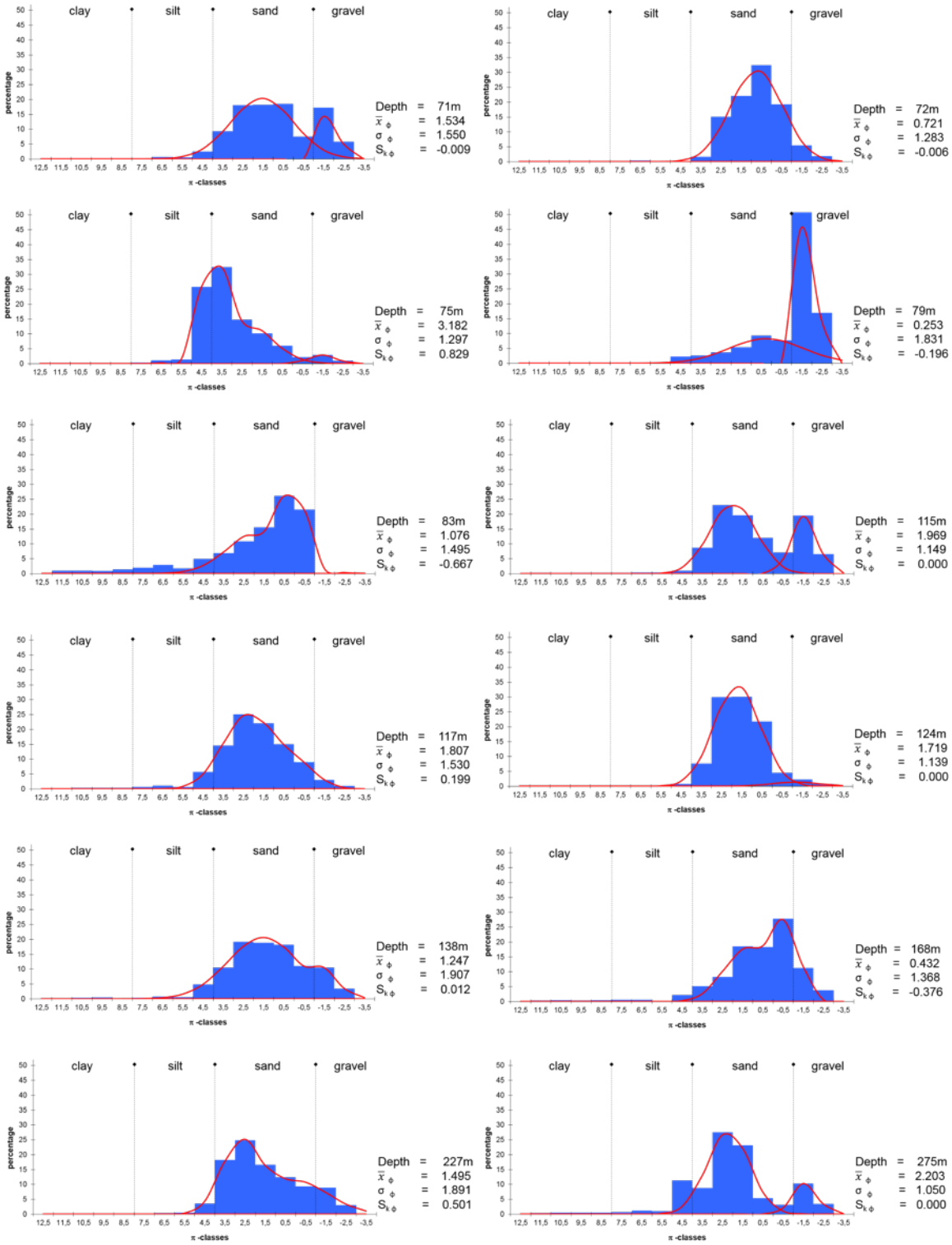


Figure 3.5 Grain size distribution of sediments sampled in the south of Izena Island. Decomposition of non-normal distributed frequencies into normal distributed components. All parameters (mean, sorting and skewness) in phi (ϕ) units

## CHAPTER 4

## BENTHIC FORAMINIFERA FROM THE MID TO DEEPER SUBLITTORAL AND UPPERMOST BATHYAL AROUND IZENA AND IE ISLANDS, OKINAWA, JAPAN

Optimally preserved specimens of benthic foraminifera found in 24 surface sediments sampled from the marine environment surrounding Izena and Ie Islands of Okinawa, Ryukyu Island Arc of the west Pacific are described. Taxonomic description (Section 4.1) and identification plates (Section 4.2) of the benthic foraminifera are presented. Benthic foraminiferal species found in the investigation area are grouped into 7 orders, 55 families, 100 genera and 175 species. Larger benthic foraminifera are comprised of 17 species while the remaining of them are smaller benthic foraminiferal species.

### 4.1 Taxonomic description

Order: LITUOLIDA Lankester 1885
Family: Lituolidae de Blainville 1827
Genus: *Ammotium* Loeblich & Tappan 1953

*Ammotium* sp. (pl. 1, fig. 1a-b)
Reference: Parker 2009, p. 18, fig. 13

Family: Pseudobolivinidae Wiesner 1931
Genus: *Pseudobolivina* Wiesner 1931

*Pseudobolivina* sp. (pl. 1, fig. 2a-b)
Reference: Hatta & Ujiie 1992, p. 83, fig. 8

Family: Reophacidae Cushman 1927
Genus: *Reophax* de Montfort 1808

*Reophax* aff. *nodulosa* Brady 1884 (pl. 1, fig. 3a-b)
Reference: Hatta & Ujiie 1992, p. 83, fig. 1

*Reophax scorpiurus* de Montfort 1808 (pl. 1, fig. 4)
Reference: Hatta & Ujiie 1992, p. 83, figs. 2-3

Family: Spiroplectamminidae Cushman 1927
Genus: *Spiroplectinella* Kisel'man 1927

*Spiroplectinella higuchii* Takayanagi 1953 (pl. 1, fig. 5a-b)
Reference: Akimoto et al. 2002, p. 37, fig. 1

*Spiroplectinella kerimbaensis* Said 1949 (pl. 1, fig. 6a-b)
Reference: Loeblich & Tappan 1994, p. 251, figs. 9-14

Genus: *Spirotextularia* Saidova 1975

*Spirotextularia floridana* Cushman 1922 (pl. 1, fig. 7a-b)
Reference: Loeblich & Tappan 1994, p. 253, figs. 10-16

*Spirotextularia fistulosa* Brady 1884 (pl. 1, fig. 8a-b)
Reference: Hatta & Ujiie 1992, p. 83, fig. 7

Family: Verneuillinidae Cushman 1911
Genus: *Gaudryina* d'Orbigny 1839

*Gaudryina quadrangularis* Bagg 1908 (pl. 1, fig. 9a-b)
Reference: Loeblich & Tappan 1994, p. 254, figs. 22-23

Order: TEXTULARIIDA Delage & Hérouard 1896
Family: Eggerellidae Cushman 1937
Genus: *Dorothia* Plummer 1931

*Dorothia rotunda* Chapman 1902 (pl. 2, fig. 1a-b)
Reference: Loeblich & Tappan 1994, p. 266, figs. 1-15

Family: Pseudogaudryinidae Loeblich & Tappan 1985
Genus: *Clavulinoides* Cushman 1936

*Clavulinoides* aff. *indiscreta* Brady 1922 (pl. 2, fig. 2)
Reference: Hatta & Ujiie 1992, p. 87, fig. 3

Genus: *Plotnikovina* Mikhalevich 1981

*Plotnikovina compressa* Cushman 1935 (pl. 2, fig. 4)
Reference: Ujiie & Hatta 1994, p. 19, figs. 1-3

Genus: *Pseudogaudryina* Cushman 1936

*Pseudogaudryina atlanta pacifica* Cushman & McCulloch 1939 (pl. 2, fig. 3a-b)
Reference: Akimoto et al. 2002, p. 40, fig. 2

Genus: *Siphoniferoides* Saidova 1981

*Siphoniferoides siphonifera* Brady 1881 (pl. 2, fig. 5a-b)
Reference: Hatta & Ujiie 1992, p. 87, fig. 5

Family: Textulariidae Ehrenberg 1838
Genus: *Sahulia* Hofker 1978

*Sahulia barkeri* Loeblich & Tappan 1985 (pl. 2, fig. 6a-b)
Reference: Hatta & Ujiie 1992, p. 85, fig. 2

Genus: *Textularia* Defrance 1824

*Textularia agglutinans* d'Orbigny 1839 (pl. 2, fig. 7a-c)
Reference: Akimoto et al. 2002, p. 38, fig. 1

*Textularia articulata* d'Orbigny 1846 (pl. 2, fig. 8a-c)
Reference: Akimoto et al. 2002, p. 38, fig. 2

*Textularia candeiana* d'Orbigny 1839 (pl. 2, fig. 9a-c)
Reference: Parker 2009, p. 46, fig. 34

*Textularia conica* d'Orbigny 1839 (pl. 3, fig. 1a-b)
Reference: Akimoto et al. 2002, p. 38, fig. 4

*Textularia crenata* Cheng & Zheng 1978 (pl. 3, figs. 2a-b, 3)
Reference: Hatta & Ujiie 1992, p. 87, fig. 2

*Textularia dupla* Todd 1954 (pl. 3, figs. 4a-b, 5)
Reference: Hatta & Ujiie 1992, p. 85, fig. 6

*Textularia foliacea* Heron-Allen & Earland 1915 (pl. 3, fig. 6a-b)
Reference: Hatta & Ujiie 1992, p. 85, fig. 7

*Textularia lateralis* Lalicker 1935 (pl. 3, fig. 7a-b)
Reference: Loeblich & Tappan 1994, p. 270, figs. 13-16

*Textularia neorugosa* Thalmann 1950 (pl. 3, fig. 8a-c)
Reference: Hatta & Ujiie, 1992, p. 85, fig. 8

*Textularia schencki* Cushman & Valentine 1930 (pl. 3, fig. 9a-b)
Reference: Akimoto et al. 2002, p. 39, fig. 1

*Textularia saulcyana* d'Orbigny 1839 (pl. 3, fig. 10a-b)
Reference: Akimoto et al. 2002, p. 40, fig. 1

*Textularia stricta* Cushman 1911 (pl. 3, fig. 11a-b)
Reference: Loeblich & Tappan 1994, p. 275, figs. 1-9

Family: Valvulinidae Berthelin 1880
Genus: *Cylindroclavulina* Bermúdez & Key 1952

*Cylindroclavulina bradyi* Cushman 1911 (pl. 3, fig. 12)
Reference: Hatta & Ujiie 1992, p. 87, fig. 8

Order: SPIRILLINIDA Hohenegger & Piller 1975
Family: Spirillinidae Reuss & Fritsch 1861
Genus: *Spirillina* Ehrenberg 1843

*Spirillina decorata* Brady, 1884 (pl. 4, fig. 1)
Reference: Akimoto et al. 2002, p. 41, fig. 6

*Spirillina vivipara* Ehrenberg 1843 (pl. 4, fig. 2)
Reference: Hatta & Ujiie 1992, p. 225, fig. 3

Order: MILIOLIDA Delage & Hérouard 1896
Family: Alveolinidae Ehrenberg 1839
Genus: *Alveolinella* H. Douvillea 1907

*Alveolinella quoyi* d'Orbigny 1826 (pl. 4, fig. 3)

Reference: Hatta & Ujiie 1992, p. 109, figs. 11-12

Family: Cornuspiridae Schultze 1854
Genus: *Cornuspira* Schultze 1854

*Cornuspira involvens* Reuss 1850 (pl. 4, fig. 4)
Reference: Hatta & Ujiie 1992, p. 89, fig. 1

Family: Fischerinidae Millett 1898
Genus: *Nodobaculariella* Cushman & Hazawa 1937

*Nodobaculariella insignis* Brady 1884 (pl. 4, fig. 5a-b)
Reference: Hatta & Ujiie 1992, p. 89, figs. 4-5

Genus: *Vertebralina* d'Orbigny 1826

*Vertebralina striata* d'Orbigny 1826 (pl. 4, fig. 6a-b)
Reference: Hatta & Ujiie 1992, p. 89, fig. 6

Genus: *Wiesnerella* Cushman 1933

*Wiesnerella ujiiei* Hatta 1992 (pl. 4, fig. 7)
Reference: Hatta & Ujiie 1992, p. 89, fig. 8

Family: Hauerinidae Schwager 1876
Genus: *Articulina* d'Orbigny 1826

*Articulina alticostata* Cushman 1944 (pl. 4, fig. 8)
Reference: Hatta & Ujiie 1992, p. 109, fig. 2

*Articulina pacifica* Cushman 1944 (pl. 4, fig. 9a-b)
Reference: Hatta & Ujiie 1992, p. 109, figs. 3-4

Genus: *Massilina* Schlumberger 1893

*Massilina granulocostata* Germeraad 1946 (pl. 4, fig. 10a-b)
Reference: Loeblich & Tappan 1994, p. 316, figs. 1-12

Genus: *Miliolinella* Wiesner 1931

*Miliolinella* cf. *M. chiastocytis* Loeblich & Tappan 1994 (pl. 4, fig. 11a-c)
Reference: Parker 2009, p. 118-119, figs. 83-84

*Miliolinella circularis* Bornemann 1855 (pl. 4, fig. 12a-b)
Reference: Hatta & Ujiie 1992, p. 101, figs. 1-2

*Miliolinella oceanica* Cushman 1932 (pl. 4, fig. 13a-b)
Reference: Hatta & Ujiie 1992, p. 101, figs. 3-4

*Miliolinella subrotunda* Montagu 1803 (pl. 5, fig. 1a-b)
Reference: Parker 2009, p. 125, fig. 88

*Miliolinella webbiana* d'Orbigny 1839 (pl. 5, fig. 2a-b)
Reference: Hatta & Ujiie 1992, p. 101, fig. 5

*Miliolinella* sp. (pl. 5, fig. 3)
Reference: Hatta & Ujiie 1992, p. 101, fig. 6

Genus: *Parrina* Cushman 1931

*Parrina bradyi* Millett 1898 (pl. 5, fig. 4)
Reference: Loeblich & Tappan 1994, p. 301, figs. 1-3

Genus: *Planispirinella* Wiesner 1931

*Planispirinella exigua* Brady 1879 (pl. 5, fig. 5a-b)
Reference: Hatta & Ujiie 1992, p. 89, fig. 3

Genus: *Pyrgo* Defrance 1824

*Pyrgo denticulata* Brady 1884 (pl. 5, fig. 6a-c)
Reference: Hatta & Ujiie 1992, p. 103, figs. 1-2

*Pyrgo sarsi* Schlumberger 1891 (pl. 5, fig. 7a-b)
Reference: Parker 2009, p. 171, fig. 121

*Pyrgo striolata* Brady 1884 (pl. 5, fig. 8a-b)
Reference: Parker 2009, p. 173, fig. 122

*Pyrgo* sp. (pl. 5, figs. 9a-b, 10)
Reference: Parker 2009, p. 174, fig. 123

Genus: *Quinqueloculina* d'Orbigny 1826

*Quinqueloculina arenata* Said 1949 (pl. 6, fig. 1)
Reference: Hatta & Ujiie 1992, p. 93, figs. 6-7

*Quinqueloculina bicarinata* d'Orbigny 1826 (pl. 6, fig. 2a-b)
Reference: Hatta & Ujiie 1992, p. 95, figs. 1-2

*Quinqueloculina crassicarinata* Collins 1958 (pl. 6, fig. 3a-b)
Reference: Loeblich & Tappan 1994, p. 314, figs. 4-12

*Quinqueloculina elongata* Natland 1938 (pl. 6, fig. 4a-b)
Reference: Akimoto et al. 2002, p. 50, fig. 4

*Quinqueloculina granulocostata* Germeraad 1946 (pl. 6, fig. 5a-b)
Reference: Parker 2009, p. 214-215, figs. 150-151

*Quinqueloculina incisa* Vella 1957 (pl. 6, fig. 6a-b)
Reference: Loeblich & Tappan 1994, p. 317, figs. 13-15

*Quinqueloculina laevigata* d'Orbigny 1839 (pl. 6, fig. 7a-b)

Reference: Akimoto et al. 2002, p. 51, fig. 4

*Quinqueloculina lamarckiana* d'Orbigny 1839 (pl. 6, fig. 8a-c)
Reference: Akimoto et al. 2002, p. 52, fig. 1

*Quinqueloculina neostriatula* Thalmann 1956 (pl. 6, fig. 9a-c)
Reference: Hatta & Ujiie 1992, p. 97, fig. 2

*Quinqueloculina parkeri* Brady 1881 (pl. 6, fig. 10a-b)
Reference: Hatta & Ujiie 1992, p. 97, figs. 3-4

*Quinqueloculina philippinensis* Cushman 1921 (pl. 6, fig. 11a-c)
Reference: Loeblich & Tappan 1994, p. 318, figs. 1-10

*Quinqueloculina poeyana* d'Orbigny 1839 (pl. 6, fig. 12a-c)
Reference: Akimoto et al. 2002, p. 52, fig. 2

*Quinqueloculina polygona* d'Orbigny 1839 (pl. 7, fig. 1a-b)
Reference: Hatta & Ujiie 1992, p. 97, fig. 5

*Quinqueloculina rugosa* d'Orbigny 1839 (pl. 7, fig. 2a-d)
Reference: Hatta & Ujiie 1992, p. 97, fig. 6

*Quinqueloculina seminulum* Linnaeus 1758 (pl. 7, fig. 3a-c)
Reference: Hatta & Ujiie 1992, p. 99, figs. 1-2

*Quinqueloculina tubus* Todd 1957 (pl. 7, fig. 4a-c)
Reference: Parker 2009, p. 278-279, figs. 198-199

*Quinqueloculina venusta* Karrer 1868 (pl. 7, fig. 5a-b)
Reference: Akimoto et al. 2002, p. 54, fig.4

Genus: *Sigmoilinella* Zheng 1979

*Sigmoilinella tortuosa* Zheng 1979 (pl. 7, fig. 6a-b)
Reference: Hatta & Ujiie 1992, p. 107, figs. 9-10

Genus: *Sigmoilopsis* Finlay 1947

*Sigmoilopsis schlumbergeri* Silvestri 1904 (pl. 7, fig. 7a-b)
Reference: Akimoto et al. 2002, p. 58, fig. 1

Genus: *Spirosigmoilina* Parr 1942

*Spirosigmoilina speciosa* Karrer 1868 (pl. 7, fig. 8a-b)
Reference: Hatta & Ujiie 1992, p. 109, fig. 1

Genus: *Triloculina* d'Orbigny 1826

*Triloculina affinis* d'Orbigny 1826 (pl. 8, fig. 1a-b)
Reference: Hatta & Ujiie 1992, p. 103, fig. 4

*Triloculina* cf. *T. tricarinata* d'Orbigny 1826 (pl. 8, fig. 2a-b)
Reference: Parker 2009, p. 368, fig. 265

*Triloculina marshallana* Todd 1954 (pl. 8, fig. 3a-b)
Reference: Hatta & Ujiie 1992, p. 105, fig. 5

*Triloculina serrulata* McCulloch 1977 (pl. 8, fig. 4a-b)
Reference: Parker 2009, p. 367, fig. 265

*Triloculina tricarinata* d'Orbigny 1826 (pl. 8, fig. 5a-b)
Reference: Hatta & Ujiie 1992, p. 105, fig. 8

Family: Peneroplidae Shultze 1854
Genus: *Peneroplis* de Montfort 1808

*Peneroplis pertusus* Forskål 1775 (pl. 8, fig. 6)
Reference: Hatta & Ujiie 1992, p. 113, fig. 1

*Peneroplis planatus* Fichtel & Moll 1798 (pl. 8, fig. 7)
Reference: Hatta & Ujiie 1992, p. 113, fig. 2

Genus: *Spirolina* Lamarck 1804

*Spirolina acicularis* Batsch 1791 (pl. 8, fig. 8a-b)
Reference: Hatta & Ujiie 1992, p. 113, fig. 3

Family: Riveroinidae Saidova 1981
Genus: *Pseudohauerina* McCulloch 1977

*Pseudohauerina orientalis* Cushman 1946 (pl. 8, fig. 9a-b)
Reference: Hatta & Ujiie 1992, p. 109, figs. 10

Family: Soritidae Ehrenberg 1839
Genus: *Parasorites* Seiglie & Rivera 1977

*Parasorites orbitolitoides* Hofker 1930 (pl. 9, fig. 1)
Reference: Hatta & Ujiie 1992, p. 115, figs. 1-2

Genus: *Sorites* Ehrenberg 1839

*Sorites orbiculus* Forskål 1775 (pl. 9, fig. 2a-b)
Reference: Hatta & Ujiie 1992, p. 115, figs. 5-6

Family: Spiroloculinidae Wiesner 1920
Genus: *Mikrobelodontos* Loeblich & Tappan 1994

*Mikrobelodontos bradyi* Parker 1960 (pl. 9, fig. 3)
Reference: Loeblich & Tappan 1994, p. 303, figs. 1-8

Genus: *Nummulopyrgo* Hofker 1983

*Nummulopyrgo globulus* Hofker 1976 (pl. 9, fig. 4a-b)
Reference: Loeblich & Tappan 1994, p. 302, figs. 8-16

Genus: *Spiroloculina* d'Orbigny 1826

*Spiroloculina corrugata* Cushman & Todd 1944 (pl. 9, fig. 5a-b)
Reference: Hatta & Ujiie 1992, p. 91, fig. 5

*Spiroloculina manifesta* Cushman & Todd 1944 (pl. 9, fig. 6a-d)
Reference: Hatta & Ujiie 1992, p. 91, fig. 7

*Spiroloculina subimpressa* Parr 1950 (pl. 9, fig. 7a-d)
Reference: Loeblich & Tappan 1994, p. 305, figs. 9-15

Order: LAGENIDA Delage & Hérouard 1896
Family: Glandulinidae Reuss 1860
Genus: *Glandulina* d'Orbigny 1839

*Glandulina antarctica* Parr 1950 (pl. 10, fig. 1)
Reference: Loeblich & Tappan 1994, p. 405, figs. 9-11

Family: Nodosariidae Ehrenberg 1838
Genus: *Laevidentalina* Loeblich & Tappan 1986

*Laevidentalina bradyensis* Dervieux 1894 (pl. 10, fig. 2)
Reference: Loeblich & Tappan 1994, p. 351, figs. 1-9

Genus: *Lingulina* d'Orbigny 1826

*Lingulina carinata* d'Orbigny 1826 (pl. 10, fig. 3)
Reference: Hatta & Ujiie 1992, p. 21, fig. 1

Genus: *Pyramidulina* Fornasini 1894

*Pyramidulina pauciloculata* Cushman 1917 (pl. 10, fig. 4a-b)
Reference: Loeblich & Tappan 1994, p. 354, figs. 7-8

Family: Polymorphinidae d'Orbigny 1839
Genus: *Guttulina* d'Orbigny 1839

*Guttulina bartschi* Cushman & Ozawa 1930 (pl. 10, fig. 5a-b)
Reference: Loeblich & Tappan 1994, p. 382, figs. 5-15

Genus: *Sigmoidella* Cushman & Ozawa 1928

*Sigmoidella elegantissima* Parker & Jones 1865 (pl. 10, fig. 6)
Reference: Loeblich & Tappan 1994, p. 385, figs. 4-12

Family: Vaginulinidae Reuss 1860
Genus: *Amphicoryna* Schlumberger in Milne-Edwards 1881

*Amphicoryna scalaris* Batsch 1791 (pl. 10, fig. 7)
Reference: Hatta & Ujiie 1992, p. 227, fig. 8

Genus: *Astacolus* de Monfort 1808

*Astacolus insolitus* Schwager 1866 (pl. 10, fig. 8)
Reference: Hatta & Ujiie 1992, p. 227, figs. 9-10

*Astacolus japonicus* Asano 1936 (pl. 10, fig. 9)
Reference: Loeblich & Tappan 1994, p. 367, figs. 14-19

*Astacolus sublegumen* Parr 1950 (pl. 10, fig. 10)
Reference: Hatta & Ujiie 1992, p. 229, figs. 1-2

Genus: *Lenticulina* Lamarck 1804

*Lenticulina calcar* Linnaeus 1767 (pl. 10, fig. 11a-b)
Reference: Loeblich & Tappan 1994, p. 57, figs. 1-8

*Lenticulina domantayi* McCulloch 1977 (pl. 10, fig. 12a-b)
Reference: Loeblich & Tappan 1994, p. 121, figs. 1-8

*Lenticulina limbosa* Reuss 1863 (pl. 10, fig. 13a-b)
Reference: Hatta & Ujiie 1992, p. 227, fig. 2

*Lenticulina vortex* Fichtel & Moll 1798 (pl. 10, fig. 14a-b)
Reference: Loeblich & Tappan 1994, p. 358, figs. 9-14

*Lenticulina suborbicularis* Parr 1950 (pl. 10, fig. 15a-b)
Reference: Loeblich & Tappan 1994, p. 360, figs. 1-9

Order: ROBERTINIDA Loeblich & Tappan 1984
Family: Ceratobuliminidae Cushman 1927
Genus: *Lamarckina* Berthelin 1881

*Lamarckina ventricosa* Brady 1884 (pl. 11, fig. 1a-b)
Reference: Hatta & Ujiie 1992, p. 233, fig. 4

Family: Epistominidae Wedekind 1937
Genus: *Hoeglundina* Brotzen 1948

*Hoeglundina elegans* d'Orbigny 1878 (pl. 11, fig. 2a-b)
Reference: Hatta & Ujiie 1992, p. 233, fig. 3a-c

Family: Robertinidae Reuss 1850
Genus: *Geminospira* Makiyama & Nakagawa 1941

*Geminospira bradyi* Bermúdez 1952 (pl. 11, fig. 3)
Reference: Hatta & Ujiie 1992, p. 233, figs. 5-7

Order: ROTALIIDA Delage & Hérouard 1896
Family: Almaenidae Myatlyuk 1959
Genus: *Anomalinella* Cushman 1927

*Anomalinella rostrata* Brady 1881 (pl. 12, fig. 1a-b)
Reference: Hatta & Ujiie 1992, p. 271, fig. 3

Family: Amphisteginidae Cushman 1927
Genus: *Amphistegina* d'Orbigny 1826

*Amphistegina bicirculata* Larsen 1976 (pl. 12, fig. 2a-b)
Reference: Hohenegger 2011, p. 53

*Amphistegina lessonii* d'Orbigny in Guerin-Meneville 1843 (pl. 12, fig. 3a-b)
Reference: Hohenegger 2011, p. 52

*Amphistegina papillosa* Said 1949 (pl. 12, fig. 4a-b)
Reference: Hohenegger 2011, p. 54

*Amphistegina radiata* Fichtel & Moll 1798 (pl. 12, fig. 5)
Reference: Hohenegger 2011, p. 53

Family: Anomalinidae Cushman 1927
Genus: *Cibicidoides* Thalmann 1939

*Cibicidoides pachyderma* Rzehak 1886 (pl. 12, fig. 6a-b)
Reference: Hatta & Ujiie 1992, p. 255, fig. 5

Genus: *Hanzawaia* Asano 1944

*Hanzawaia coronata* Heron-Allen & Earland 1932 (pl. 12, fig. 7a-b)
Reference: Loeblich & Tappan 1994, p. 603, figs. 1-13

*Hanzawaia nipponica* Asano 1944 (pl. 13, fig. 1a-b)
Reference: Akimoto et al. 2002, p. 99, fig. 3

Genus: *Heterolepa* Franzenau 1884

*Heterolepa haidingerii* d'Orbigny 1846 (pl. 13, fig. 2a-b)
Reference: Akimoto et al. 2002, p. 98, fig. 2

*Heterolepa subpraecinctus* Akimoto 2002 (pl. 13, fig. 3a-b)
Reference: Akimoto et al. 2002, p. 98, fig. 3

Family: Bolivinellidae Hayward & Brazier 1980
Genus: *Rugobolivinella* Hayward 1990

*Rugobolivinella elegans* Parr 1932 (pl. 13, fig. 4)
Reference: Hatta & Ujiie 1992, p. 237, fig. 4a-b

Family: Bolivinitidae Cushman 1927
Genus: *Bolivina* d'Orbigny 1839

*Bolivina punctata* d'Orbigny 1848 (pl. 13, fig. 5)
Reference: Akimoto et al. 2002, p. 74, fig. 4

*Bolivina semicostata* Cushman 1911 (pl. 13, fig. 6)
Reference: Akimoto et al. 2002, p. 74, fig. 3

*Bolivina spathulata* Williamson 1858 (pl. 13, fig. 7a-b)
Reference: Akimoto et al. 2002, p. 74, fig. 1

*Bolivina vadescens* Cushman 1933 (pl. 13, fig. 8)
Reference: Loeblich & Tappan 1994, p. 451, figs. 1-4; 7-12

Genus: *Brizalina* Costa 1856

*Brizalina spinea* Cushman 1936 (pl. 13, fig. 9a-b)
Reference: Hatta & Ujiie 1992, p. 237, fig. 1

Family: Buliminoididae Seiglie 1970
Genus: *Buliminoides* Cushman 1911

*Buliminoides milleti* Cushman 1933 (pl. 13, fig. 10a-b)
Reference: Hatta & Ujiie 1992, p. 253, figs. 4-5

Family: Calcarinidae d'Orbigny 1826
Genus: *Baculogypsina* Sacco 1893

*Baculogypsina sphaerulata* Parker & Jones 1860 (pl. 13, fig. 11)
Reference: Hohenegger 2011, p. 61

Genus: *Baculogypsinoides* Sacco 1893

*Baculogypsinoides spinosus* Yabe & Hanzawa 1930 (pl. 13, fig. 12)
Reference: Hohenegger 2011, p. 60

Genus: *Calcarina* d'Orbigny 1826

*Calcarina calcar* d'Orbigny 1826 (pl. 14, fig. 1)
Reference: Hatta & Ujiie 1992, p. 275, figs. 1-5

*Calcarina hispida* Brady 1876 (pl. 14, fig. 2)
Reference: Hohenegger 2011, p. 58

Family: Cancrisidae Chapman, Parr & Collins 1934
Genus: *Cancris* de Monfort 1808

*Cancris auriculus* Fichtel & Moll 1798 (pl. 14, fig. 3a-b)
Reference: Akimoto et al. 2002, p. 83, fig. 2

Family: Cassidulinidae d'Orbigny 1839
Genus: *Globocassidulina* Voloshinova 1960

*Globocassidulina bisecta* Nomura 1983 (pl. 14, fig. 4a-b)
Reference: Loeblich & Tappan 1994, p. 459, figs. 7-13

Genus: *Paracassidulina* Nomura 1983

*Paracassidulina neocarinata* Nomura 1983 (pl. 14, fig. 5a-b)
Reference: Akimoto et al. 2002, p. 78, fig. 2

Family: Cibicididae Cushman 1927
Genus: *Cibicides* de Monfort 1808

*Cibicides* cf. *C. refulgens* de Monfort 1808 (pl. 14, fig. 6a-b)
Reference: Parker 2009, p. 536, figs. 378-379

*Cibicides lobatulus* Walker & Jacob 1798 (pl. 14, fig. 7a-b)
Reference: Hatta & Ujiie 1992, p. 259, figs. 4-5

Genus: *Paracibicides* Perelis & Reiss 1975

*Paracibicides hebeslucidus* Akimoto 2002 (pl. 14, fig. 8a-c)
Reference: Akimoto et al. 2002, p. 90, fig. 1

Family: Cymbaloporidae Cushman 1927
Genus: *Cymbaloporetta* Cushman 1928

*Cymbaloporetta bradyi* Cushman 1924 (pl. 14, fig. 9a-b)
Reference: Hatta & Ujiie 1992, p. 263, fig. 4

*Cymbaloporetta squammosa* d'Orbigny 1826 (pl. 14, fig. 10a-b)
Reference: Hatta & Ujiie 1992, p. 265, fig. 3

Family: Discorbidae Ehrenberg 1838
Genus: *Rotorbis* Sellier de Civrieux 1977

*Rotorbis pacifica* Hofker 1951 (pl. 15, fig. 1a-b)
Reference: Loeblich & Tappan 1994, p. 514, figs. 7-11

Genus: *Trochulina* d'Orbigny 1839

*Trochulina campanulata amabilis* Akimoto 2002 (pl. 15, fig. 2a-b)
Reference: Akimoto et al. 2002, p. 84, fig. 4

Family: Discorbinellidae Sigal 1952
Genus: *Discorbinella* Cushman & Martin 1935

*Discorbinella* sp. (pl. 15, fig. 3a-b)
Reference: Parker 2009, p. 558-559, fig. 396-396

Family: Elphidiidae Galloway 1933
Genus: *Cellanthus* de Montfort 1808

*Cellanthus craticulatus* Fichtel & Moll 1798 (pl. 15, fig. 4)
Reference: Hatta & Ujiie 1992, p. 283, fig. 7

Genus: *Elphidium* de Montfort 1808

*Elphidium* cf. *E. macellum* Fichtel & Moll 1798 (pl. 15, fig. 5a-b)
Reference: Parker 2009, p. 583, fig. 410

*Elphidium crispum* Linnaeus 1758 (pl. 15, fig. 6a-b)
Reference: Hatta & Ujiie 1992, p. 283, fig. 5

Family: Epistomariidae Hofker 1954
Genus: *Asanonella* Huang 1965

*Asanonella tubulifera* Heron-Allen & Earland 1915 (pl. 15, fig. 7a-b)
Reference: Hatta & Ujiie 1992, p. 269, fig. 1

Family: Eponididae Hofker 1954
Genus: *Eponides* de Montfort 1808

*Eponides cribrorepandus* Asano & Uchio 1951 (pl. 15, fig. 8a-b)
Reference: Akimoto et al. 2002, p. 84, fig. 1

*Eponides repandus* Fichtel & Moll 1798 (pl. 15, fig. 9a-b)
Reference: Hatta & Ujiie 1992, p. 245, figs. 1-2

Family: Gavelinellidae Hofker 1956
Genus: *Gyroidinoides* Brotzen 1942

*Gyroidinoides cushmani* Boomgart 1949 (pl. 15, fig. 10a-b)
Reference: Akimoto et al. 2002, p. 98, figs. 4-5

Family: Mississippinidae Saidova 1981
Genus: *Stomatorbina* Dorreen 1948

*Stomatorbina concentrica* Parker & Jones 1864 (pl. 15, fig. 11a-b)
Reference: Hatta & Ujiie 1992, p. 245, fig. 5

Family: Notorotaliidae Hornibrook 1961
Genus: *Parellina* Thalmann 1951

*Parellina pacifica* Collins 1958 (pl. 16, fig. 1a-b)
Reference: Hatta & Ujiie 1992, p. 283, fig. 8

Family: Nonionidae Schultze 1854
Genus: *Melonis* de Montfort 1808

*Melonis nicobarense* Cushman 1936 (pl. 16, fig. 2a-b)

Reference: Hatta & Ujiie 1992, p. 271, fig. 2

Family: Nummulitidae de Blainville 1827
Genus: *Nummulites* Lamarck 1801

*Nummulites venosus* Fichtel & Moll 1978 (pl. 16, fig. 3)
Reference: Hohenegger 2011, p. 62

Genus: *Cycloclypeus* W. B. Carpenter 1856

*Cycloclypeus carpenteri* Brady 1881 (pl. 16, fig. 4)
Reference: Hohenegger 2011, p. 69

Genus: *Operculina* d'Orbigny 1826

*Operculina complanata* Defrance in de Blainville 1822 (pl. 16, fig. 5)
Reference: Hohenegger 2011, p. 65

Genus: *Planostegina* Banner & Hodgkinson 1991

*Planostegina longisepta* Zheng 1979 (pl. 16, fig. 6)
Reference: Hohenegger 2011, p. 69

Family: Planorbulinidae Schwager 1877
Genus: *Caribeanella* Bermúdez 1952

*Caribeanella celsusraphes* Akimoto 2002 (pl. 16, fig. 7a-b)
Reference: Akimoto et al. 2002, p. 92, fig. 1

*Caribeanella ogiensis* Matsunaga 1954 (pl. 16, fig. 8a-b)
Reference: Akimoto et al. 2002, p. 91, fig. 2

*Caribeanella phillippinensis* McCulloch 1977 (pl. 16, fig. 9)
Reference: Akimoto et al. 2002, p. 91, fig. 3

*Caribeanella shimabarensis* Akimoto 2002 (pl. 16, fig. 10a-b)
Reference: Akimoto et al. 2002, p. 92, fig. 2

Genus: *Planorbulina* d'Orbigny 1826

*Planorbulina mediterranensis* d'Orbigny 1826 (pl. 16, fig. 11a-b)
Reference: Hatta & Ujiie 1992, p. 261, fig. 2

Genus: *Planorbulinella* Cushman 1927

*Planorbulinella larvata* Parker & Jones 1865 (pl. 16, fig. 12a-b)
Reference: Hatta & Ujiie 1992, p. 261, fig. 3

Family: Pseudoparrelliidae Voloshinova 1952
Genus: *Facetocochlea* Loeblich & Tappan 1994

*Facetocochlea pulchra* Cushman 1933 (pl. 16, fig. 13a-b)
Reference: Debenay 2012, p. 196

Family: Siphogenerinoididae Saidova 1981
Genus: *Rectobolivina* Cushman 1927

*Rectobolivina raphana* Parker & Jones 1865 (pl. 16, fig. 14)
Reference: Hatta & Ujiie 1992, p. 237, figs. 11-12

Family: Siphoninidae Cushman 1927
Genus: *Siphonina* Reuss 1850

*Siphonina tubulosa* Cushman 1924 (pl. 16, fig. 15a-b)
Reference: Parker 2009, p. 737, fig. 515

Family: Reussellidae Cushman 1933
Genus: *Chrysalidinella* Schubert 1908

*Chrysalidinella pacifica* Uchio 1952 (pl. 16, fig. 16)
Reference: Parker 2009, p. 445, fig. 320

Genus: *Fijella* Loeblich & Tappan 1962

*Fijella simplex* Cushman 1929 (pl. 16, fig. 17)
Reference: Hatta & Ujiie 1992, p. 241, fig. 1

Family: Rosalinidae Reiss 1963
Genus: *Neoconorbina* Hofker 1951

*Neoconorbina communis* Ujiie 1992 (pl. 17, fig. 1a-b)
Reference: Hatta & Ujiie 1992, p. 249, figs. 1-2

*Neoconorbina tuberocapitata* Chapman 1900 (pl. 17, fig. 2a-b)
Reference: Hatta & Ujiie 1992, p. 249, fig. 3

Genus: *Planodiscorbis* Bermúdez 1952

*Planodiscorbis rarescens* Brady 1884 (pl. 17, fig. 3a-b)
Reference: Hatta & Ujiie 1992, p. 249, fig. 4

Genus: *Rosalina* d'Orbigny 1826

*Rosalina globularis* d'Orbigny 1826 (pl. 17, fig. 4a-b)
Reference: Akimoto et al. 2002, p. 85, fig. 6

*Rosalina globuliniformis* Akimoto 2002 (pl. 17, fig. 5a-b)
Reference: Akimoto et al. 2002, p. 85, fig. 1

*Rosalina petasiformis* Cheng & Zheng 1978 (pl. 17, fig. 6a-b)
Reference: Hatta & Ujiie 1992, p. 251, figs. 1-2

*Rosalina vilardeboana* d'Orbigny 1839 (pl. 17, fig. 7a-b)
Reference: Akimoto et al. 2002, p. 85, fig. 7

Family: Rotaliidae Ehrenberg 1839
Genus: *Ammonia* Brünnich 1772

*Ammonia ariakensis* Akimoto 2002 (pl. 17, fig. 8a-b)
Reference: Akimoto et al. 2002, p. 100, fig. 3

*Ammonia beccarii* Linnaeus 1758 (pl. 17, fig. 9a-b)
Reference: Hatta & Ujiie 1992, p. 273, figs. 1-2

Family: Uvigerinidae Haeckel 1894
Genus: *Neouvigerina* Thalmann 1952

*Neouvigerina ampullacea* Brady 1884 (pl. 17, fig. 10)
Reference: Hatta & Ujiie 1992, p. 239, fig. 5

Genus: *Trifarina* Cushman 1923

*Trifarina bradyi* Cushman 1923 (pl. 17, fig. 11)
Reference: Akimoto et al. 2002, p. 81, fig. 6

Genus: *Uvigerina* d'Orbigny 1826

*Uvigerina schencki* Asano 1950 (pl. 17, fig. 12)
Reference: Akimoto et al. 2002, p. 81, fig. 4

*Uvigerina schwageri* Brady 1884 (pl. 17, fig. 13)
Reference: Hatta & Ujiie 1992, p. 239, fig. 7

Family: Victoriellidae Chapman & Crespin 1930
Genus: *Rupertina* Loeblich & Tappan 1961

*Rupertina pustulosa* Hatta 1992 (pl. 17, fig. 14a-b)
Reference: Hatta & Ujiie 1992, p. 267, figs. 2-4

4.2 Identification plates

## Plate 1

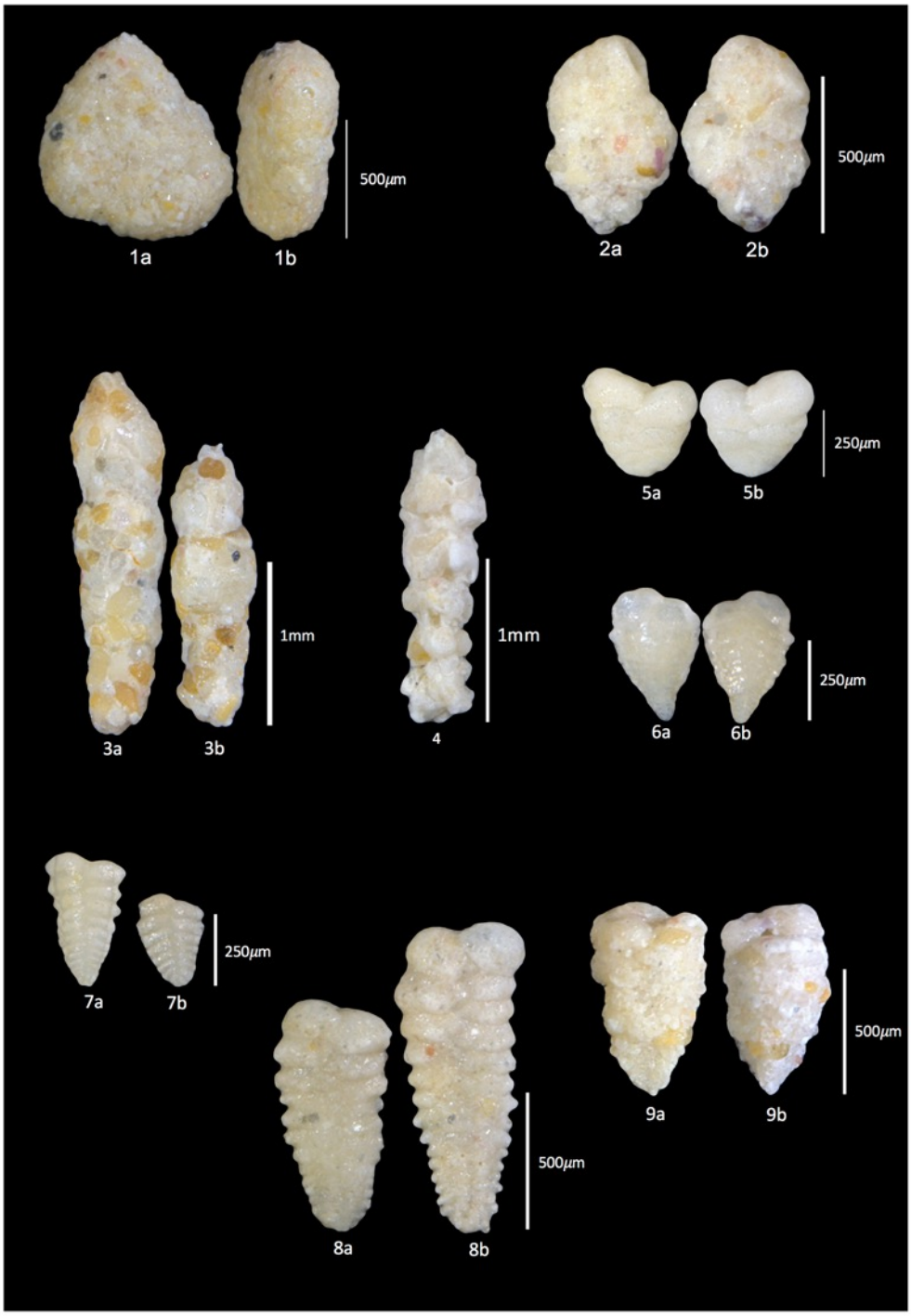


1. *Ammotium* sp. fig. 1a-b
2. *Pseudobolivina* sp. fig. 2a-b
3. *Reophax* aff. *nodulosa* fig. 3a-b
4. *Reophax scorpiurus* fig. 4
5. *Spiroplectinella higuchii* fig. 5a-b
6. *Spiroplectinella kerimbaensis* fig. 6a-b
7. *Spirotextularia floridana* fig. 7a-b
8. *Spirotextularia fistulosa* fig. 8a-b
9. *Gaudryina quadrangularis* fig. 9a-b

## Plate 2

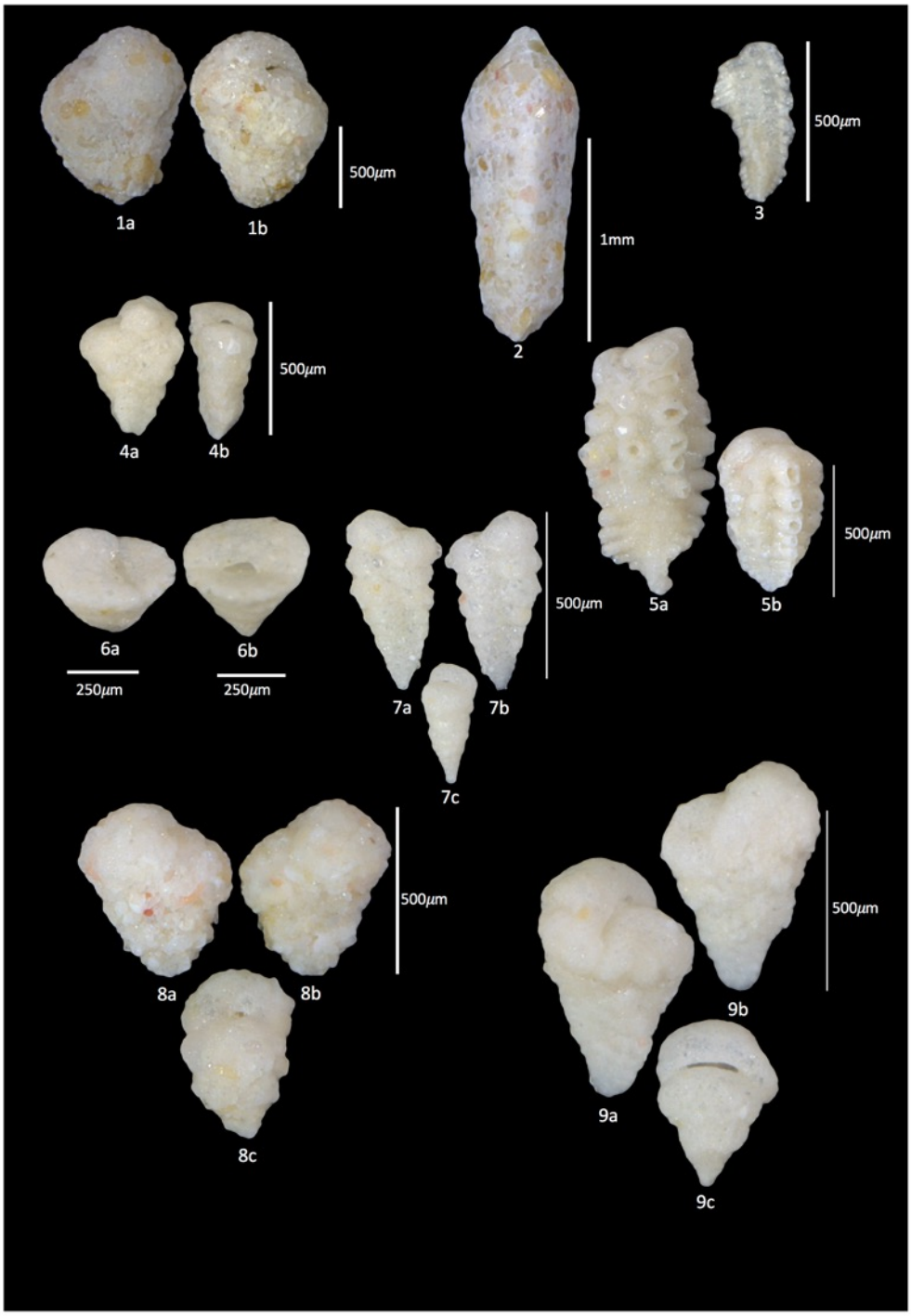


1. *Dorothia rotunda* fig. 1a-b
2. *Clavulinoides* aff. *indiscreta* fig. 2
3. *Plotnikovina compressa* fig. 4
4. *Pseudogaudryina atlanta pacifica* fig. 3a-b
5. *Siphoniferoides siphonifera* fig. 5a-b
6. *Sahulia barkeri* fig. 6a-b
7. *Textularia agglutinans* fig. 7a-c
8. *Textularia articulata* fig. 8a-c
9. *Textularia candeiana* fig. 9a-c

## Plate 3

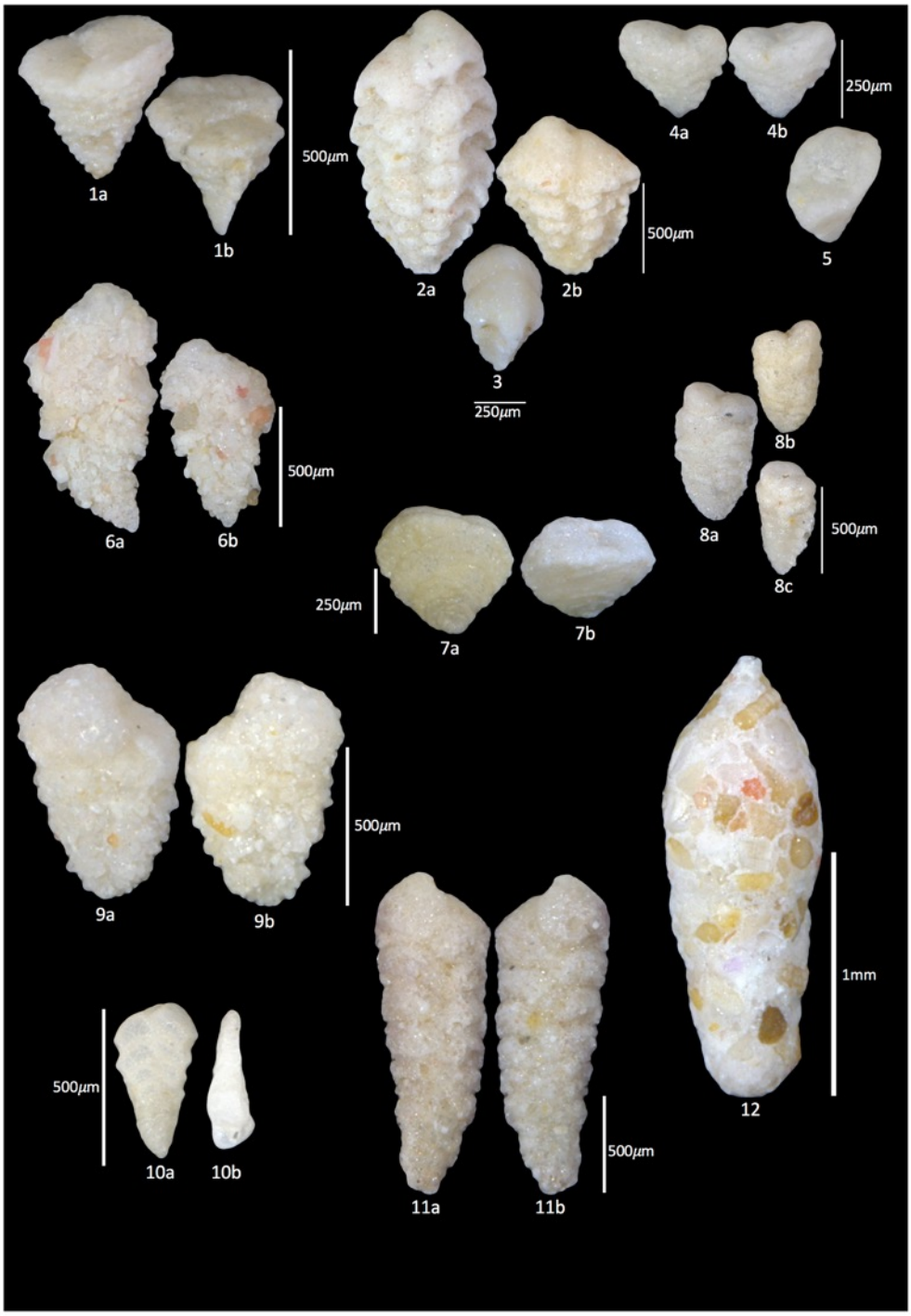


1. *Textularia conica* fig. 1a-b
2. *Textularia crenata* figs. 2a-b, 3
3. *Textularia dupla* figs. 4a-b, 5
4. *Textularia foliacea* fig. 6a-b
5. *Textularia lateralis* fig. 7a-b
6. *Textularia neorugosa* fig. 8a-c
7. *Textularia schencki* fig. 9a-b
8. *Textularia saulcyana* fig. 10a-b
9. *Textularia stricta* fig. 11a-b
10. *Cylindroclavulina bradyi* fig. 12

## Plate 4

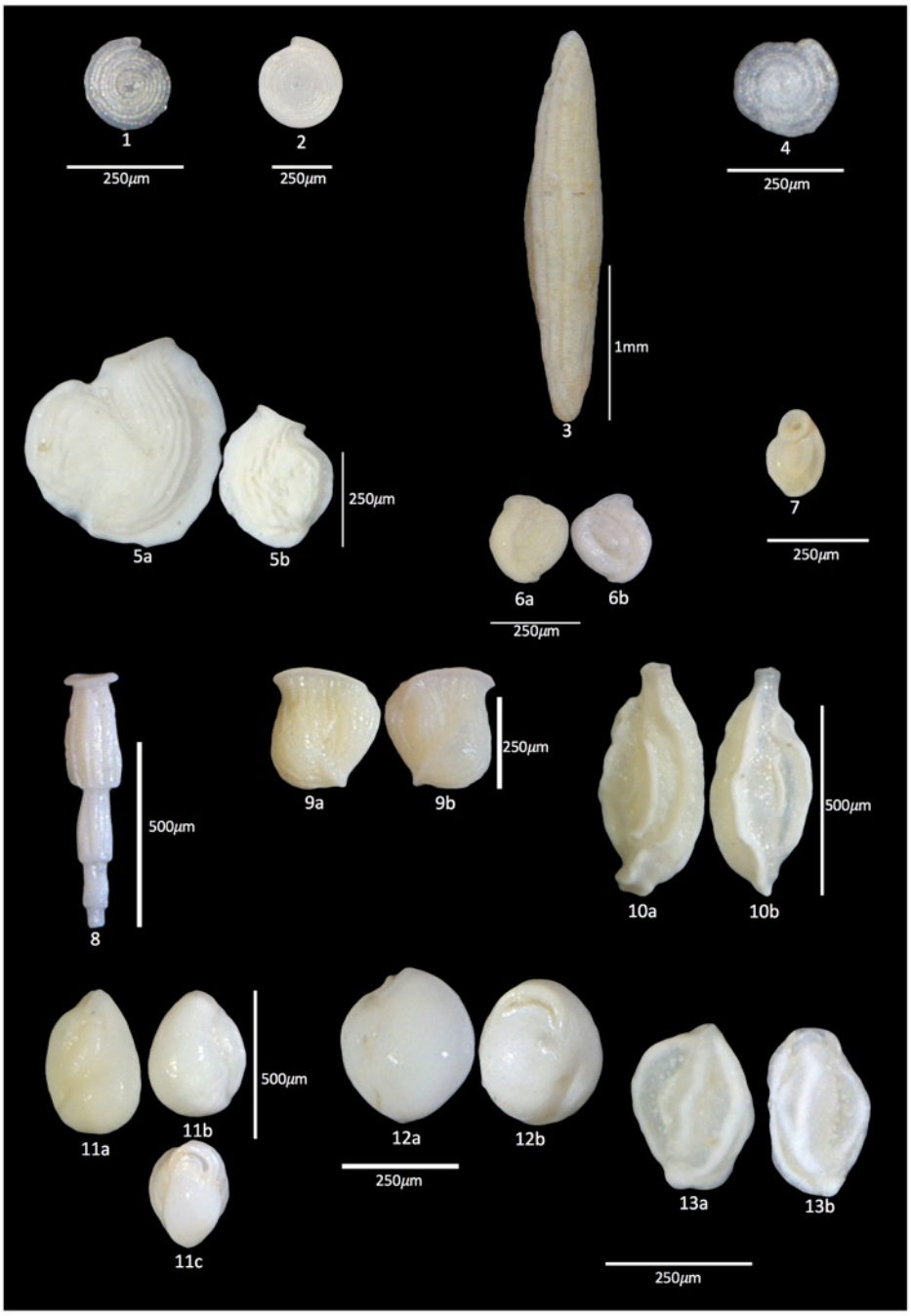


1. *Spirillina decorata* fig. 1
2. *Spirillina vivipara* fig. 2
3. *Alveolinella quoyi* fig. 3
4. *Cornuspira involvens* fig. 4
5. *Nodobaculariella insignis* fig. 5a-b
6. *Vertebralina striata* fig. 6a-b
7. *Wiesnerella ujiiei* fig. 7
8. *Articulina alticostata* fig. 8
9. *Articulina pacifica* fig. 9a-b
10. *Massilina granulocostata* fig. 10a-b
11. *Miliolinella* cf. *M. chiastocytis* fig. 11a-c
12. *Miliolinella circularis* fig. 12a-b
13. *Miliolinella oceanica* fig. 13a-b

## Plate 5

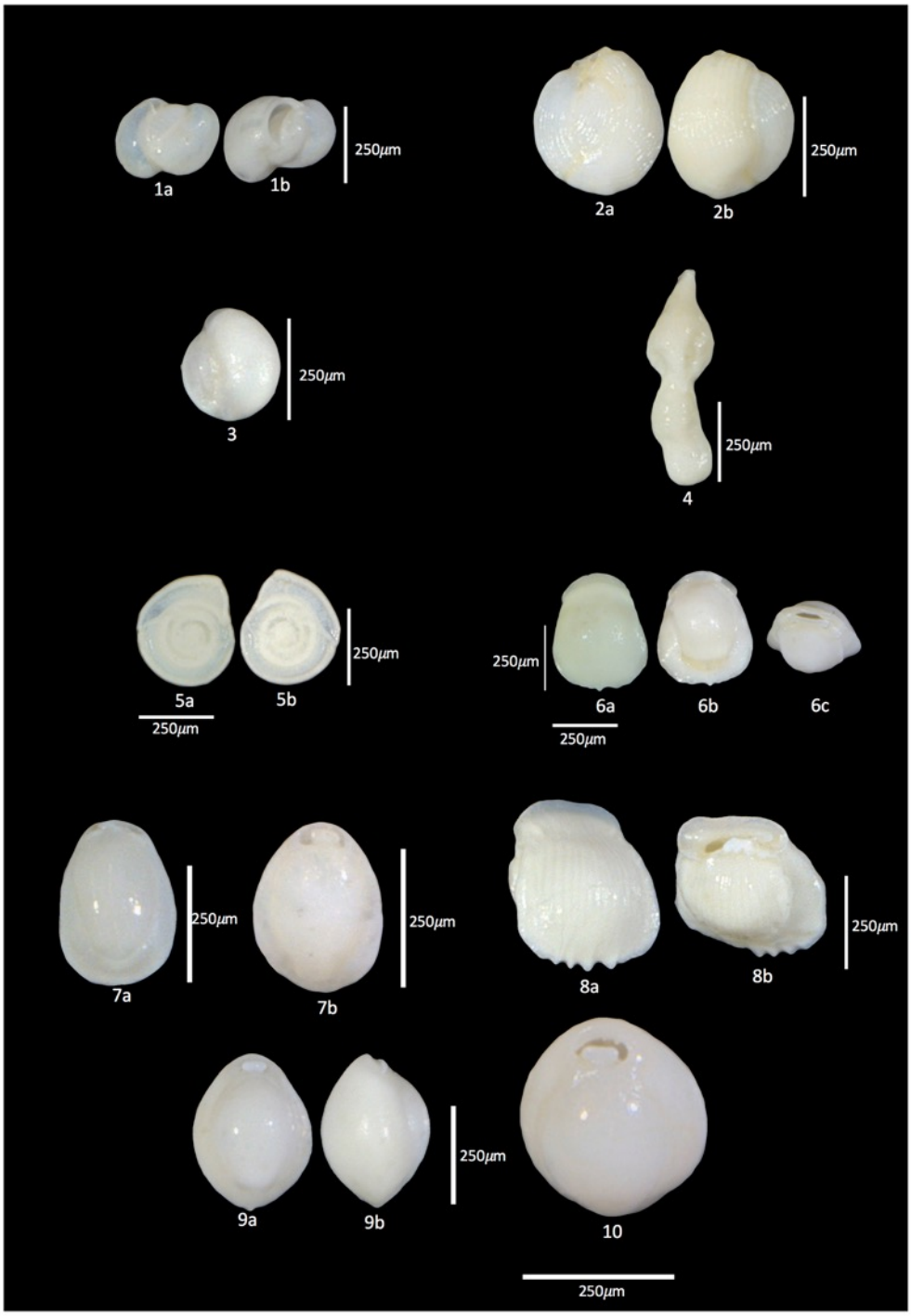


1. *Miliolinella subrotunda* fig. 1a-b
2. *Miliolinella webbiana* fig. 2a-b
3. *Miliolinella* sp. fig. 3
4. *Parrina bradyi* fig. 4
5. *Planispirinella exigua* fig. 5a-b
6. *Pyrgo denticulata* fig. 6a-c
7. *Pyrgo sarsi* fig. 7a-b
8. *Pyrgo striolata* fig. 8a-b
9. *Pyrgo* sp. 9a-b, 10

## Plate 6

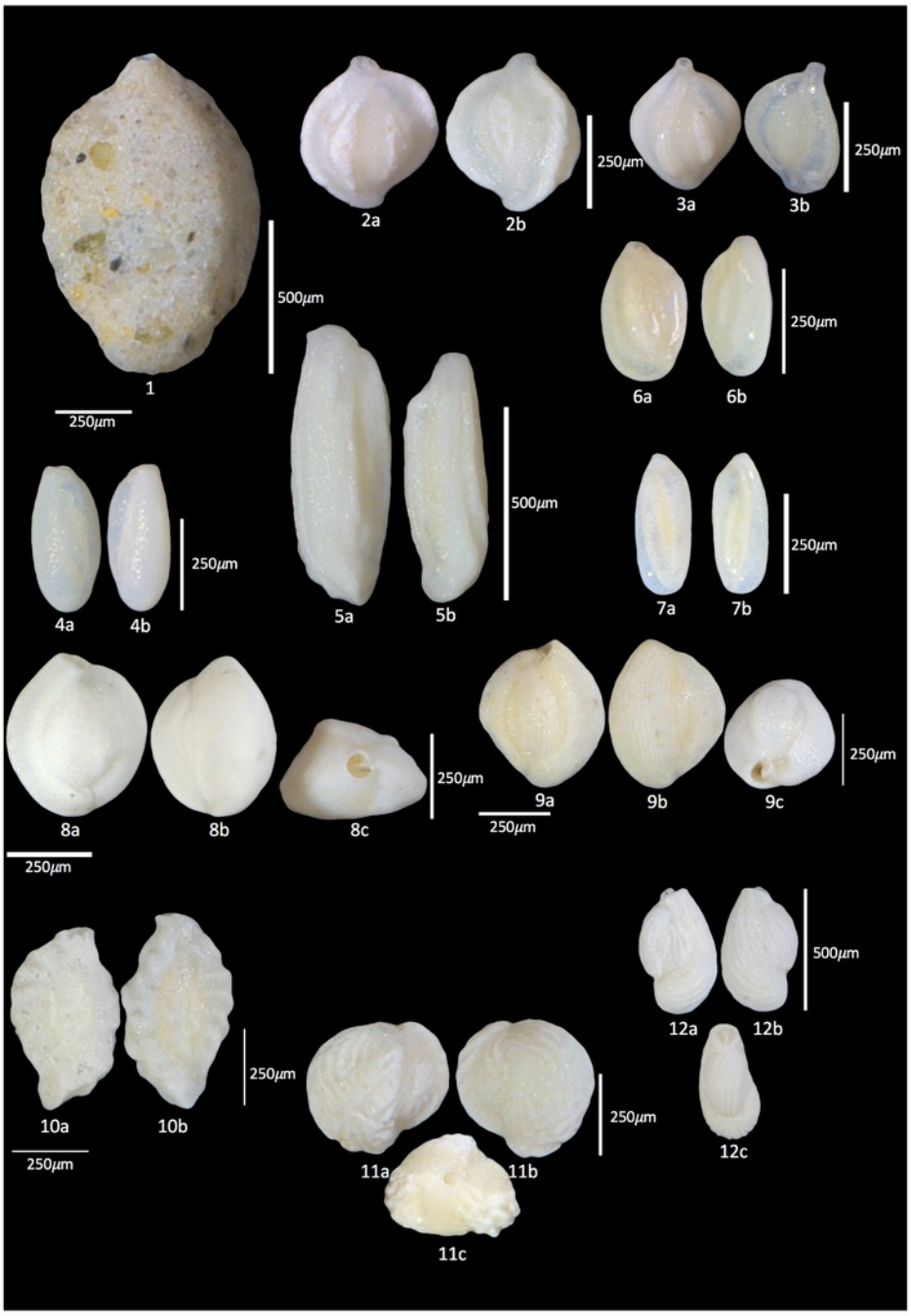


1. *Quinqueloculina arenata* fig. 1
2. *Quinqueloculina bicarinata* fig. 2a-b
3. *Quinqueloculina crassicarinata* fig. 3a-b
4. *Quinqueloculina elongata* fig. 4a-b
5. *Quinqueloculina granulocostata* fig. 5a-b
6. *Quinqueloculina incisa* fig. 6a-b
7. *Quinqueloculina laevigata* fig. 7a-b
8. *Quinqueloculina lamarckiana* fig. 8a-c
9. *Quinqueloculina neostriatula* fig. 9a-c
10. *Quinqueloculina parkeri* 10a-b
11. *Quinqueloculina philippinensis* fig. 11a-c
12. *Quinqueloculina poeyana* fig. 12a-c

## Plate 7

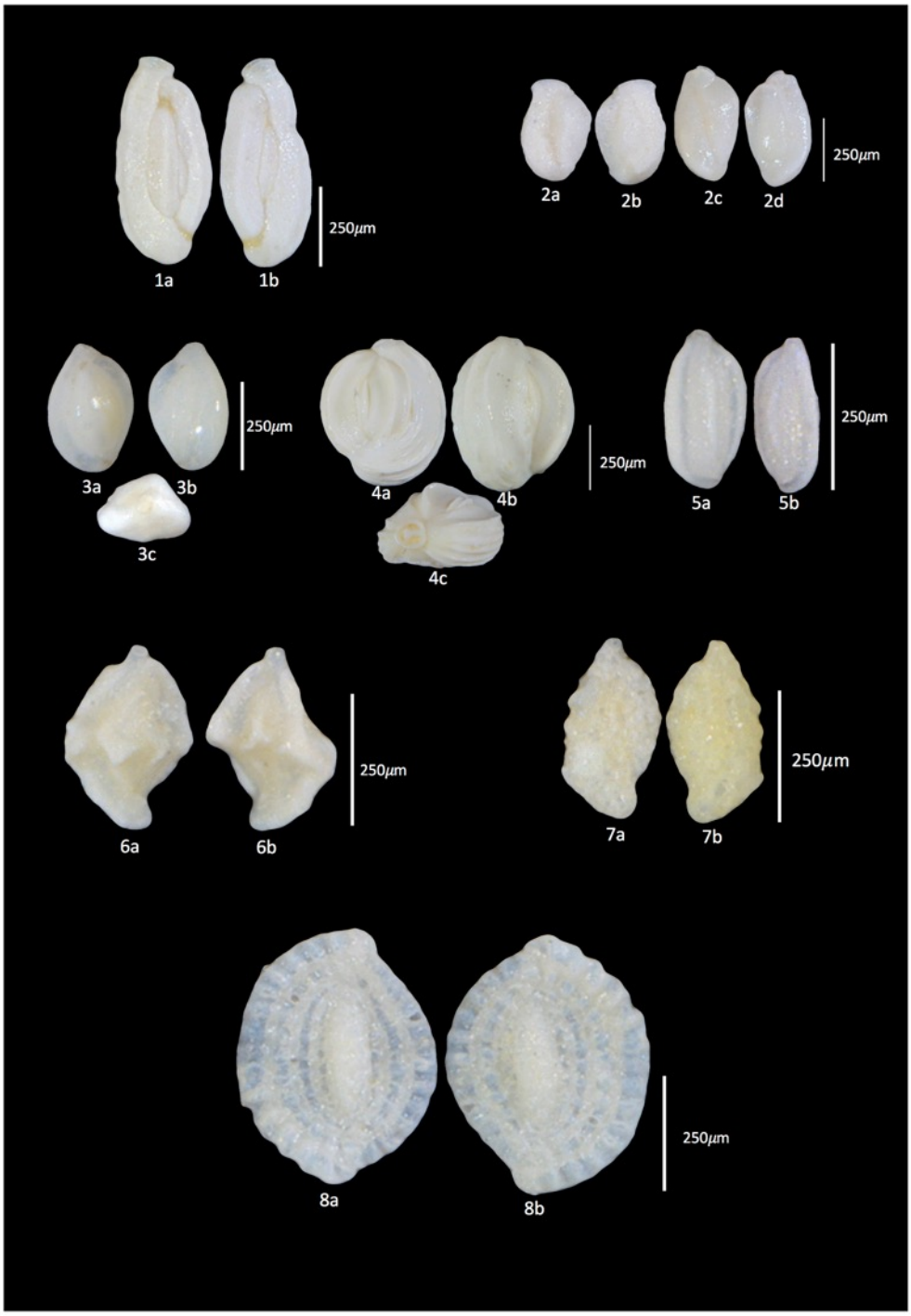


1. *Quinqueloculina polygona* fig. 1a-b
2. *Quinqueloculina rugosa* fig. 2a-d
3. *Quinqueloculina seminulum* fig. 3a-c
4. *Quinqueloculina tubus* fig. 4a-c
5. *Quinqueloculina venusta* fig. 5a-b
6. *Sigmoilinella tortuosa* fig. 6a-b
7. *Sigmoilopsis schlumbergeri* fig. 7a-b
8. *Spirosigmoilina speciosa* fig. 8a-b

## Plate 8

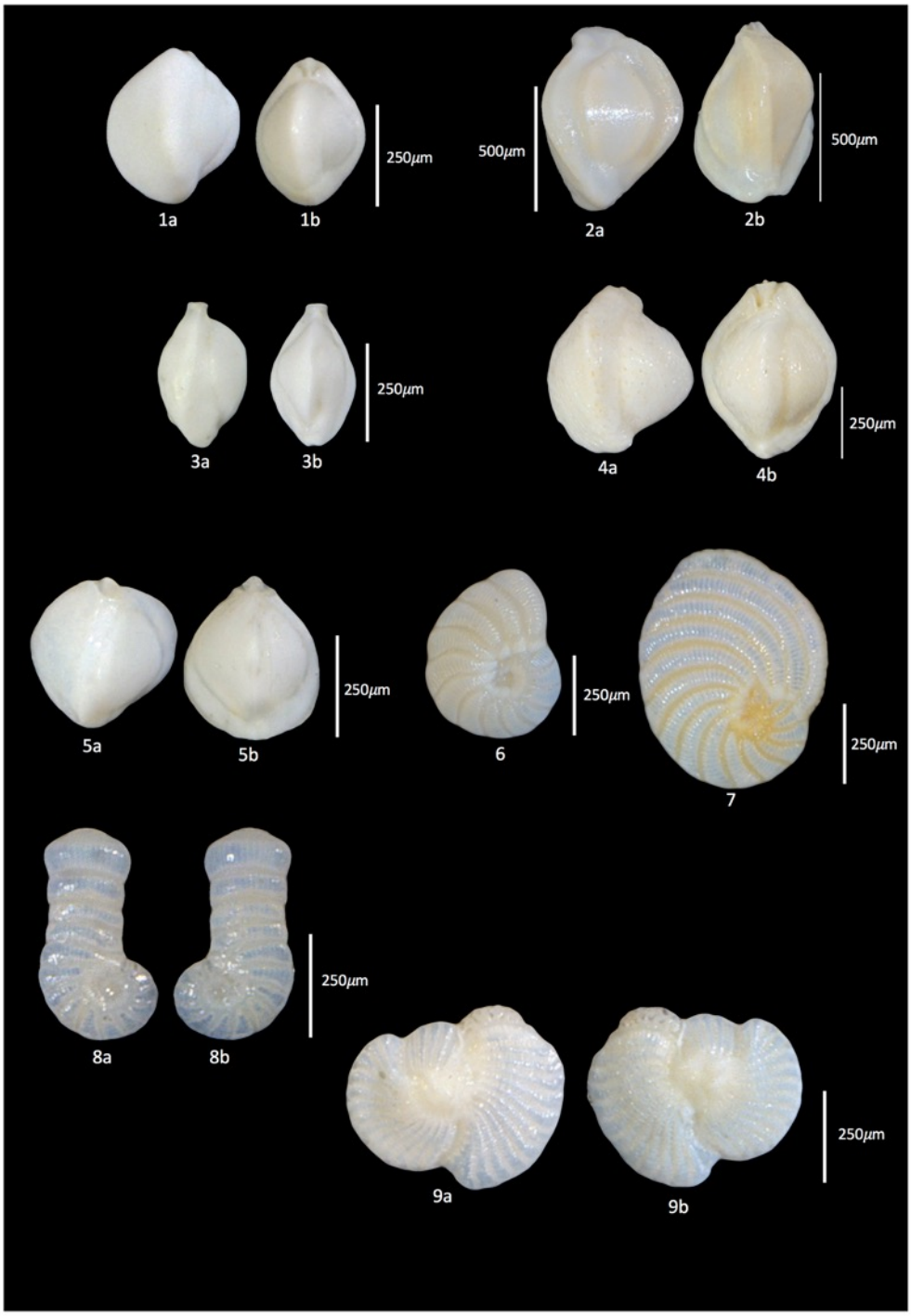


1. *Triloculina affinis* fig. 1a-b
2. *Triloculina* cf. *T. tricarinata* fig. 2a-b
3. *Triloculina marshallana* fig. 3a-b
4. *Triloculina serrulata* fig. 4a-b
5. *Triloculina tricarinata* fig. 5a-b
6. *Peneroplis pertusus* fig. 6
7. *Peneroplis planatus* fig. 7
8. *Spirolina acicularis* fig. 8a-b
9. *Pseudohauerina orientalis* fig. 9a-b

## Plate 9

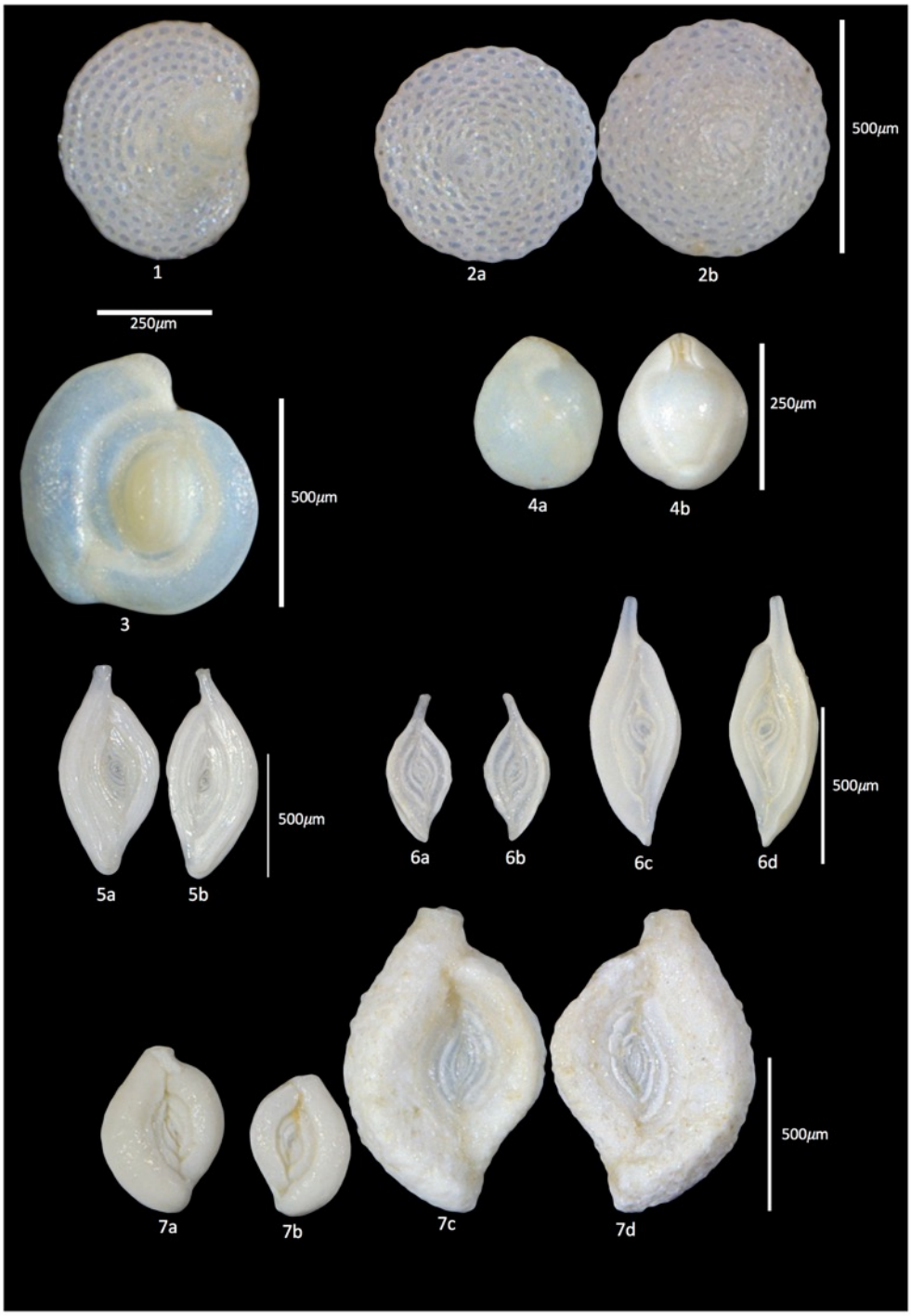


1. *Parasorites orbitolitoides* fig. 1
2. *Sorites orbiculus* fig. 2a-b
3. *Mikrobelodontos bradyi* fig. 3
4. *Nummulopyrgo globulus* fig. 4a-b
5. *Spiroloculina corrugata* fig. 5a-b
6. *Spiroloculina manifesta* fig. 6a-d
7. *Spiroloculina subimpressa* fig. 7a-d

## Plate 10

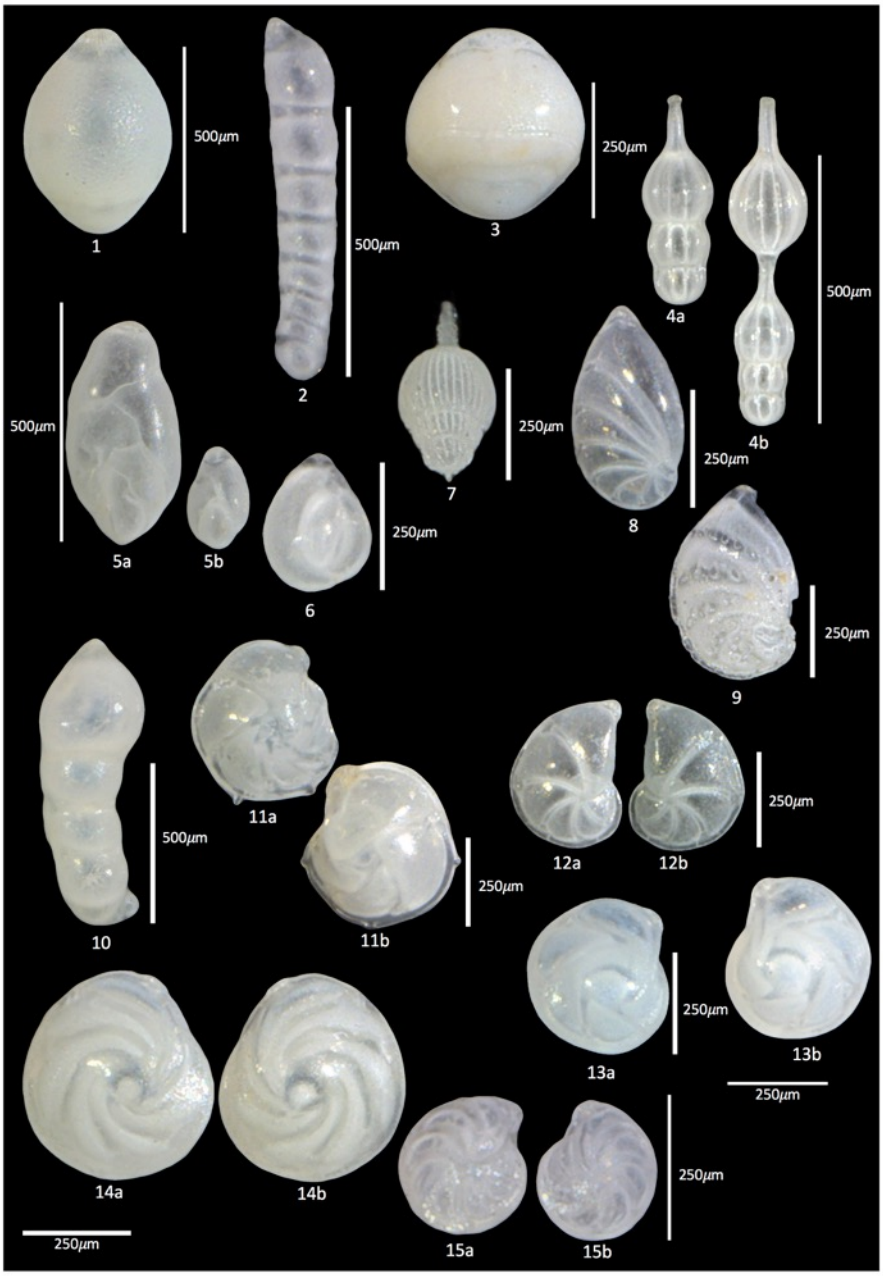


1. *Glandulina antarctica* fig. 1
2. *Laevidentalina bradyensis* fig. 2
3. *Lingulina carinata* fig. 3
4. *Pyramidulina pauciloculata* fig. 4a-b
5. *Guttulina bartschi* fig. 5a-b
6. *Sigmoidella elegantissima* fig. 6
7. *Amphicoryna scalaris* fig. 7
8. *Astacolus insolitus* fig. 8
9. *Astacolus japonicus* fig. 9
10. *Astacolus sublegumen* fig. 10
11. *Lenticulina calcar* fig. 11a-b
12. *Lenticulina domantayi* fig. 12a-b
13. *Lenticulina limbosa* fig. 13a-b
14. *Lenticulina vortex* fig. 14a-b
15. *Lenticulina suborbicularis* fig. 15a-b

## Plate 11

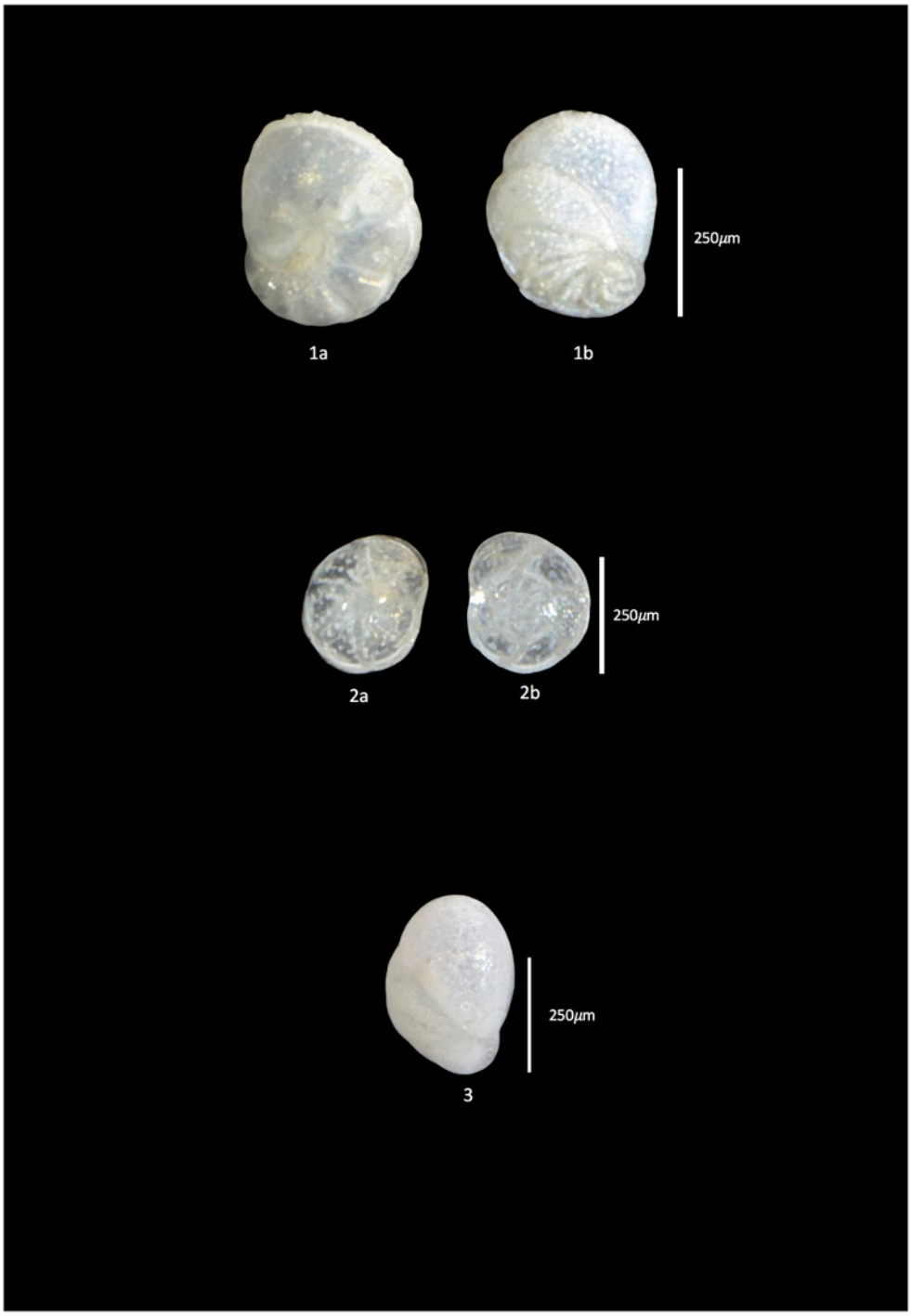


1. *Lamarckina ventricosa* fig. 1a-b
2. *Hoeglundina elegans* fig. 2a-b
3. *Geminospira bradyi* fig. 3

## Plate 12

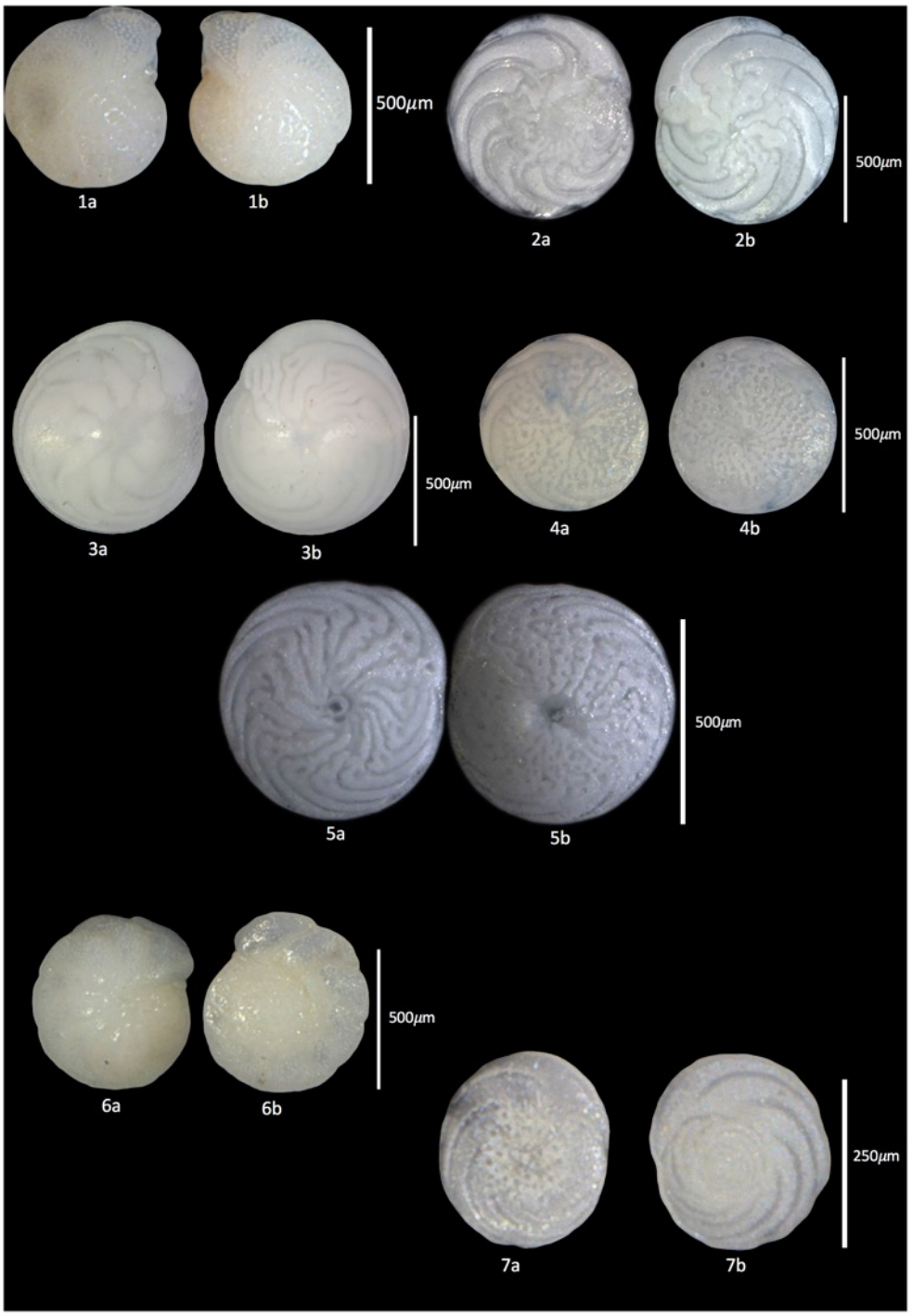


1. *Anomalinella rostrata* fig. 1a-b
2. *Amphistegina bicirculata* fig. 2a-b
3. *Amphistegina lessonii* fig. 3a-b
4. *Amphistegina papillosa* fig. 4a-b
5. *Amphistegina radiata* fig. 5
6. *Cibicidoides pachyderma* fig. 6a-b
7. *Hanzawaia coronata* fig. 7a-b

## Plate 13

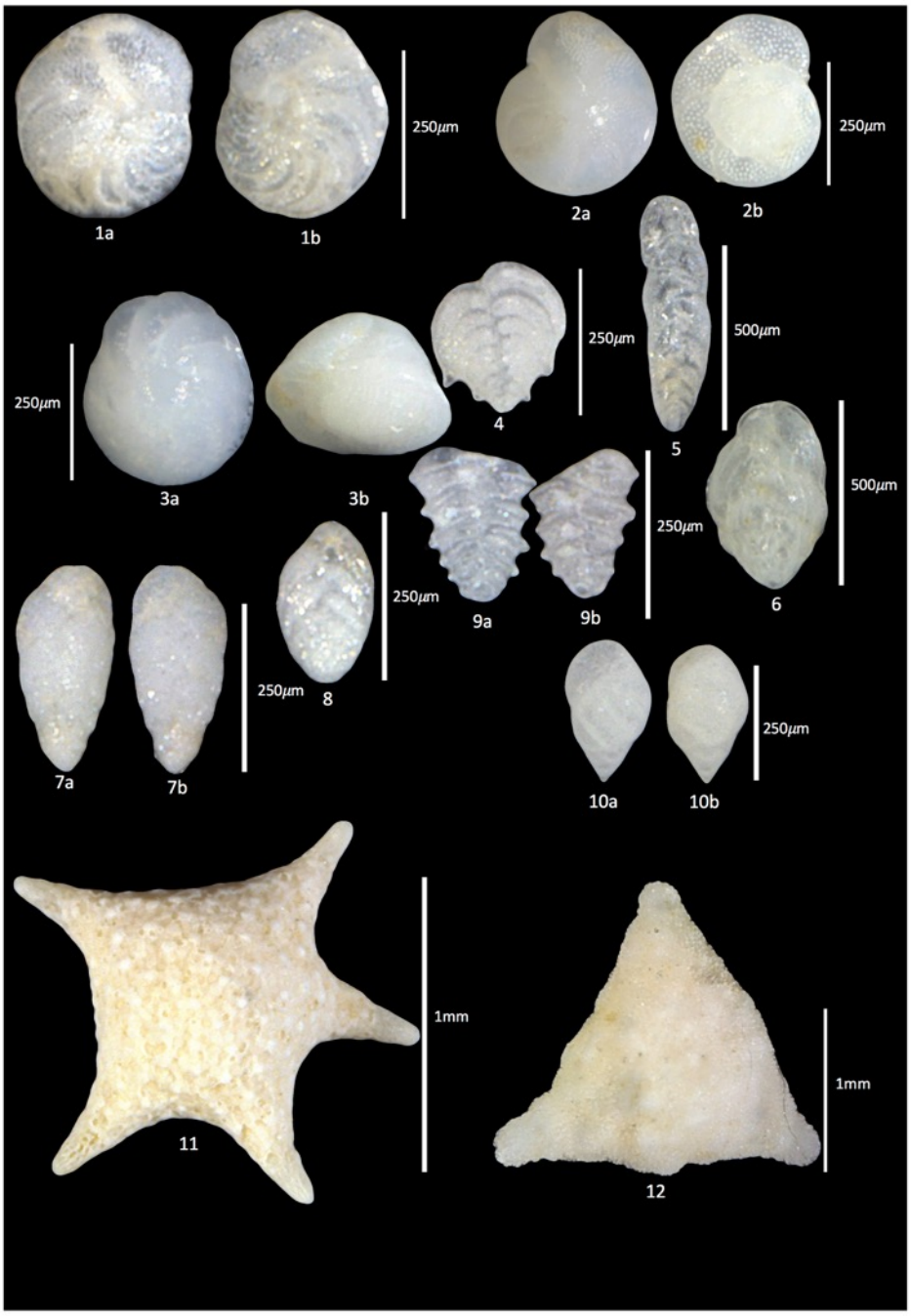


1. *Hanzawaia nipponica* fig. 1a-b
2. *Heterolepa haidingerii* fig. 2a-b
3. *Heterolepa subpraecinctus* fig. 3a-b
4. *Rugobolivinella elegans* fig. 4
5. *Bolivina punctata* fig. 5
6. *Bolivina semicostata* fig. 6
7. *Bolivina spathulata* fig. 7a-b
8. *Bolivina vadescens* fig. 8
9. *Brizalina spinea* fig. 9a-b
10. *Buliminoides milleti* fig. 10a-b
11. *Baculogypsina sphaerulata* fig. 11
12. *Baculogypsinoides spinosus* fig. 12

## Plate 14

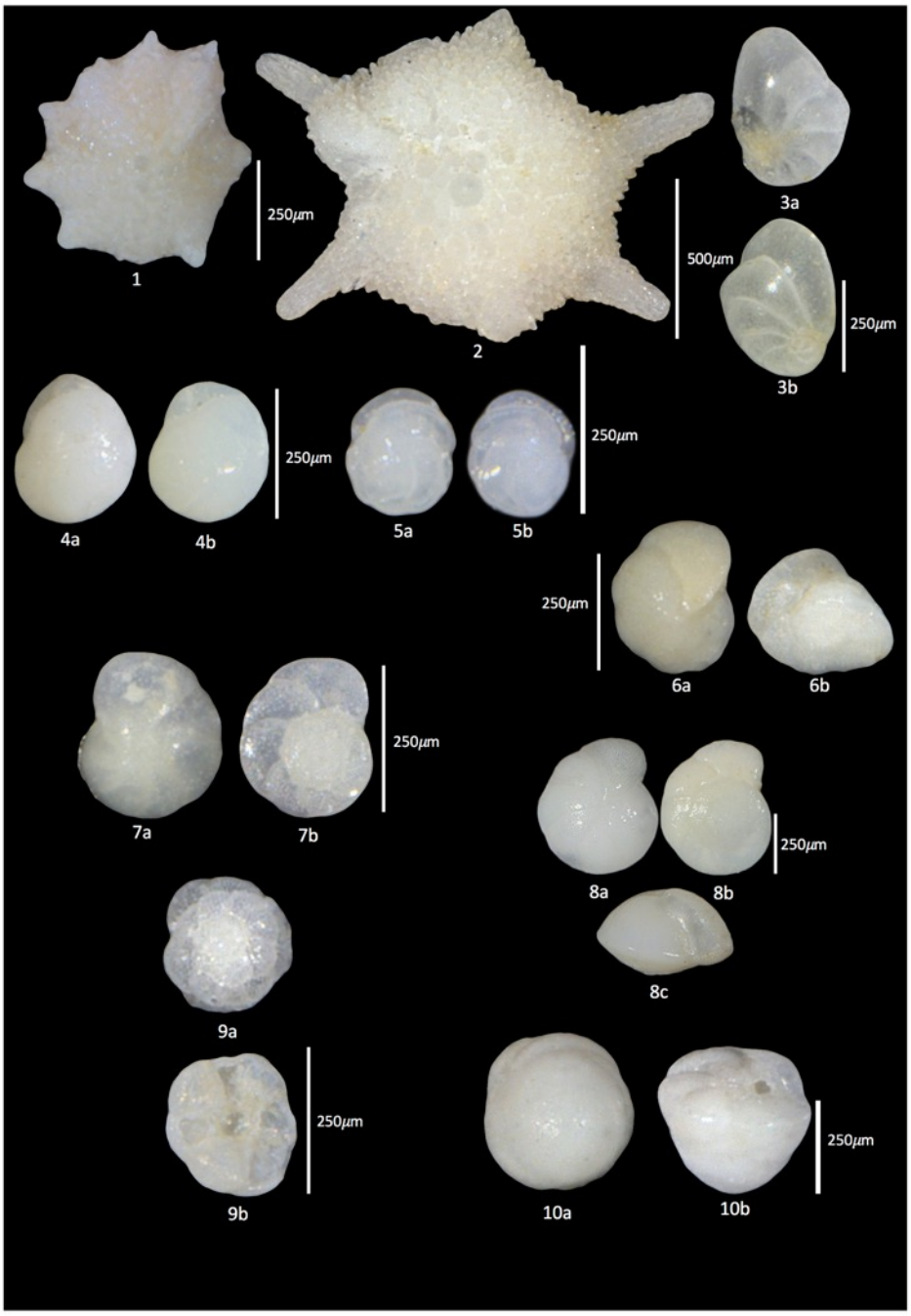


1. *Calcarina calcar* fig. 1
2. *Calcarina hispida* fig. 2
3. *Cancris auriculus* fig. 3a-b
4. *Globocassidulina bisecta* fig. 4a-b
5. *Paracassidulina neocarinata* fig. 5a-b
6. *Cibicides* cf. *C. refulgens* fig. 6a-b
7. *Cibicides lobatulus* fig. 7a-b
8. *Paracibicides hebeslucidus* fig. 8a-c
9. *Cymbaloporetta bradyi* fig. 9a-b
10. *Cymbaloporetta squammosa* fig. 10a-b

## Plate 15

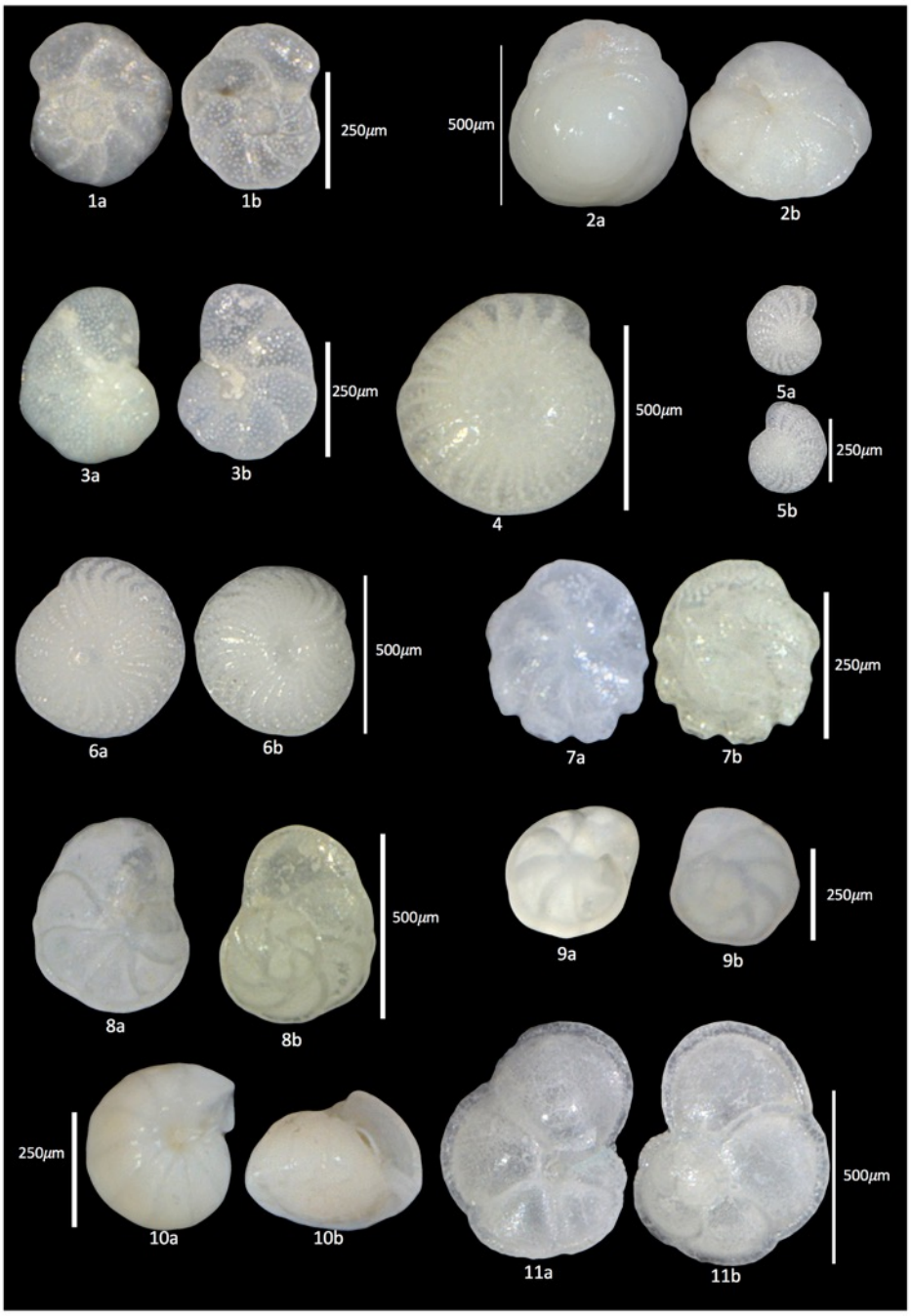


1. *Rotorbis pacifica* fig. 1a-b
2. *Trochulina campanulata amabilis* fig. 2a-b
3. *Discorbinella* sp. fig. 3a-b
4. *Cellanthus craticulatus* fig. 4
5. *Elphidium* cf. *E. macellum* fig. 5a-b
6. *Elphidium crispum* fig. 6a-b
7. *Asanonella tubulifera* fig. 7a-b
8. *Eponides cribrorepandus* fig. 8a-b
9. *Eponides repandus* fig. 9a-b
10. *Gyroidinoides cushmani* fig. 10a-b
11. *Stomatorbina concentrica* fig. 11a-b

## Plate 16


1. *Parellina pacifica* fig. 1a-b
2. *Melonis nicobarense* fig. 2a-b
3. *Nummulites venosus* fig. 3
4. *Cycloclypeus carpenteri* fig. 4
5. *Operculina complanata* fig. 5
6. *Planostegina longisepta* fig. 6
7. *Caribeanella celsusraphes* fig. 7a-b
8. *Caribeanella ogiensis* fig. 8a-b
9. *Caribeanella phillippinensis* fig. 9
10. *Caribeanella shimabarensis* fig. 10a-b
11. *Planorbulina mediterranensis* fig. 11a-b
12. *Planorbulinella larvata* fig. 12a-b
13. *Facetocochlea pulchra* fig. 13a-b
14. *Rectobolivina raphana* fig. 14
15. *Siphonina tubulosa* fig. 15a-b
16. *Chrysalidinella pacifica* fig. 16
17. *Fijella simplex* fig. 17

## Plate 17


1. *Neoconorbina communis* fig. 1a-b
2. *Neoconorbina tuberocapitata* fig. 2a-b
3. *Planodiscorbis rarescens* fig. 3a-b
4. *Rosalina globularis* fig. 4a-b
5. *Rosalina globuliniformis* fig. 5a-b
6. *Rosalina petasiformis* fig. 6a-b
7. *Rosalina vilardeboana* fig. 7a-b
8. *Ammonia ariakensis* fig. 8a-b
9. *Ammonia beccarii* fig. 9a-b
10. *Neouvigerina ampullacea* fig. 10
11. *Trifarina bradyi* fig. 11
12. *Uvigerina schencki* fig. 12
13. *Uvigerina schwageri* fig. 13
14. *Rupertina pustulosa* fig. 14a-b

# CHAPTER 5

# DEPTH DISTRIBUTION OF LARGER BENTHIC FORAMINIFERA

## 5.1 Introduction

### 5.1.1 Depth distribution

Depth is a composite factor influencing illumination rate, water movement and grain size distribution in the marine environment. Living larger benthic foraminifera inhabiting the euphotic zone have shown depth dependence distribution (Hallock 1984; Hohenegger 1994). Illumination is the functional factor which influences living larger benthic foraminiferal distribution in the euphotic zone (Hallock 1981; Hohenegger et al. 1999; Hohenegger 2000a). Intensity of illumination decreases exponentially with increasing depth (Kirk 1994). Adaptation to illumination is handled by specialized wall structure of the tests. Highly illuminated region is dominated by larger foraminifera with porcelaneous tests. Reduced illumination at the base of the euphotic zone is dominated by hyaline larger foraminifera. Depth distribution of larger foraminifera is also influenced by hydrodynamics. Coarse grains dominating the shallow water region are caused by strong water movement. Calmer water is associated with finer sediment grains caused by weak water movement. Shallow euphotic zone experiences strong water movement therefore the larger foraminifera must build strong tests to counteract the effect of strong water movement.

### 5.1.2 Depth transport

Distribution of larger foraminifera in the deeper sublittoral indicates optimal tests that have been transported along the depth gradient. Three factors may have caused depth transport: (1) traction caused by offshore bottom currents or frequent tropical cyclones that cross the area, (2) slope steepness and (3) test buoyancies (Hohenegger & Yordanova 2001b). Different species have different transport intensities along the depth gradient. Transport intensity of each larger foraminiferal species is resulted from different test buoyancy. Test buoyancies are determined by differences in test shapes and settling velocities (Briguglio & Hohenegger 2011).

### 5.1.3 Important environmental factors

According to the canonical correspondence analysis in chapter 3 (Figures 3.1 and 3.2), depth is determined as the most important factor in the ordination. Increasing depth shows positive correlations with increasing skewness, increasing mean grain size and increasing proportion of silt and clay. Increasing depth shows negative correlations with increasing sorting coefficient, increasing proportion of gravel and increasing proportion of the main component. These correlations show that samples in the deeper water region are dominated by fine sediment grains and in the shallow water region, coarse sediment grains are more prevalent.

### 5.1.4 Aim of the chapter

This chapter investigates the depth distribution and dependence on substrate of seven optimally preserved larger benthic foraminiferal species. Canonical correspondence analysis is performed to determine important factors influencing the distributions of *Amphistegina lessonii, A. bicirculata, A. radiata, A. papillosa, Calcarina hispida, Operculina complanata* and *Planostegina longisepta*. The factors are depth, inclination and sedimentological parameters, i.e., mean grain size, sorting, skewness, proportion of the main component, proportion of gravel and proportion of silt and clay. Depth distributions are depicted in correspondence analysis and frequency distribution fitted by power transformed normal distributions. Distributions in grain size classes are investigated in correspondence analysis and circle graphs.

### 5.1.5 Larger benthic foraminiferal species

Families of larger foraminiferal species in the investigation include Amphisteginidae, Calcarinidae and Nummulitidae. Members of Amphisteginidae sush as *A. lessonii, A. bicirculata, A. radiata* and *A. papillosa* possess trochospiral chamber arrangement and involute chambers that lead to lenticular test shape. Chambers are strongly arched at the periphery forming prolongations. Wall of each chamber covers the older test parts. Thickening of the test wall is easily achieved by the lamellar structure. Members of this family house diatoms as symbionts (Lee et al. 1989). Members of Calcarinidae such as *C. hispida* are very abundant in the tropical West Pacific region. The test form is flat and trochospiral with thick chamber walls. Test material is deposited on both lateral sides creating globular shape. Additional chambers can be found in the test creating a three-dimensional cyclic arrangement. Strong spines are arranged in the coiling plane that give the appearance of little stars. Members of this family exhibit symbiotic relationship with diatoms. Members of Nummulitidae such as *O. complanata* and *P. longisepta* possess planispirally coiled and multilocular tests. Symbiotic relationships of these foraminifera are shown with diatom. The nummulites avoid highly illuminated region due to the flat test that can be damaged by strong water energy thus indicating depth distribution in the lower photic zone.

## 5.2 Results

### 5.2.1 Depth distribution

Ordination by canonical correspondence analysis (Figure 5.0) shows the relationship between the distributions of larger foraminifera with depth, inclination and sedimentological parameters, i.e., mean grain size, sorting, skewness, proportion of the main component, proportion of gravel and proportion of silt and clay. Depth, proportion of silt and clay, skewness and mean grain size are important based on their positions near to the first axis (eigenvalues of 43.41%). Proportion of the main component, inclination, sorting and proportion of gravel are less important based on their positions near to the second axis (eigenvalues of 33.60%). Increasing depth correlates with increasing proportion of silt and clay, increasing skewness, increasing mean grain size and increasing proportion of the main component. Distributions of *A. bicirculata*, *O. complanata* and *P. longisepta* show correlations with these factors. Increasing inclination shows correlations with increasing sorting and increasing proportion of gravel.

Distributions of *C. hispida* and *A. radiata* have shown correlations with increasing sorting and increasing proportion of gravel based on their positions very near to these parameters. *A. papillosa* and *A. lessonii* do not show any correlations with any sedimentological parameters.

Distribution of *Amphistegina bicirculata* shows a correlation with increasing depth. This indicates that the optimal distribution of *A. bicirculata* is in the deeper water region. Optimal distributions of *Operculina complanata* and *Planostegina longisepta* also show correlations with increasing depth based on their positions at the bottom of axis 1. Distributions of *A. papillosa* and *A. lessonii* show correlations with decreasing depth. This indicates that the optimal distributions are in the shallow water region based on their positions at the end of axis 1. Distributions of *C. hispida* and *A. radiata* also show correlations with decreasing depth thus indicating optimal distributions in the shallow water region. In summary, optimal distributions of *A. bicirculata*, *O. complanata* and *P. longisepta* are located in the deeper water region. Optimal distributions of *A. lessonii, A. papillosa*, *C. hispida* and *A. radiata* are located in the shallow water region.

Correspondence analysis (Figure 5.1) shows the distributions of larger foraminiferal species according to depth. *C. hispida*, *A. lessonii* and *A. papillosa* are located at the positive end of axis 1 between the values of 0 and 0.6. Their positions indicate that these species are distributed at the shallow water region. The position of *A. radiata* is at the lowest negative end of axis 2 indicating distribution in the shallow water region. *A. bicirculata*, *O. complanata* and *P. longisepta* are located at the negative end of axis 1 between values of 0 and -0.9 thus indicating that these species are distributed in the deeper water region. Depth distributions of optimally preserved larger benthic foraminifera derived from both canonical correspondence and correspondence analyses are in agreement with each other.

Histograms are used to depict the experienced depth distributions of optimally preserved larger foraminifera fitted by power transformed normal distributions (Figure 5.2). Depth distributions of *A. lessonii* and *C. hispida* show asymmetric pattern with right-side skewness. Depth distributions of *A. bicirculata, A. radiata, A. papillosa, O. complanata* and *P. longisepta* show bimodal pattern that have been broken into two unimodal normal distributions. The depth distributions are explained according to depth zonation that has been defined. Mid sublittoral is defined as the depth from 50 to less than 100m. Deeper sublittoral is defined as the depth from 100 to less than 200m. Uppermost bathyal is defined as the depth from 200 to less than 300m.

Depth distribution of *A. lessonii* is located in the mid sublittoral with an optimum at 73m (standard deviation = 19m). Distribution in the deeper sublittoral shows an optimum at 167m (standard deviation = 87m). The range between the optima is 94m. Depth distribution of *C. hispida* shows an optimum at 67m (standard deviation = 15m) and in the deeper sublittoral the optimum is at 181m (standard deviation = 76m). The range between the optima is 114m. Right-side skewness of the depth distributions of *A. lessonii* and *C. hispida* indicates low depth transport of these two species.

Bimodal pattern is shown by the depth distributions of *A. bicirculata, A. radiata, A. papillosa, O. complanata* and *P. longisepta*. The first components of these bimodal distributions indicate optimal depth distributions located in the mid sublittoral and the second component demonstrates depth transport in the deeper sublittoral. The second

component is composed of optimal tests that have been picked between the 125 - 250μm sieve fraction.

Depth distribution of *A. bicirculata* in the mid sublittoral shows an optimum at 89m (standard deviation = 8m). Optimal depth distribution in the deeper sublittoral is located at 206m, with standard deviation of 50m. The range between the optima is 117m. Depth distribution of *A. radiata* in the mid sublittoral shows that an optimum is attained at 83m (standard deviation = 18m). Second component of the depth distribution of *A. radiata* in the deeper sublittoral shows an optimum at 243m (standard deviation = 16m). The range between the optima is 160m. Depth distribution of *A. papillosa* in the mid sublittoral shows an optimum at 89m (standard deviation = 20m). Distribution in the deeper sublittoral shows an optimum at 205m (standard deviation = 28m). The range between the optima is 115m. Depth distribution of *O. complanata* in the mid sublittoral shows an optimum at 85m (standard deviation = 15m). Distribution in the deeper sublittoral shows an optimum at 202m (standard deviation = 30m). The range between the optima is 117m. Depth distribution of *P. longisepta* shows an optimum at 105m (standard deviation = 20m). Second optimum in the deeper sublittoral is located at 187m, with standard deviation of 18m. The range between the optima is 82m.

The first components of the depth distributions of *A. lessonii, C. hispida, A. bicirculata, A. radiata, A. papillosa* and *O. complanata* demonstrate optimal depth distributions occurring in the mid sublittoral zone. *P. longisepta* demonstrates optimum in the deeper sublittoral. Low depth transport is demonstrated by *A. lessonii* and *C. hispida*. High depth transports occurring at 210m are shown by *A. bicirculata, A. papillosa, O. complanata* and *P. longisepta* thus indicating similar test buoyancies of these species. Highest depth transport at 270m is demonstrated by *A. radiata*.

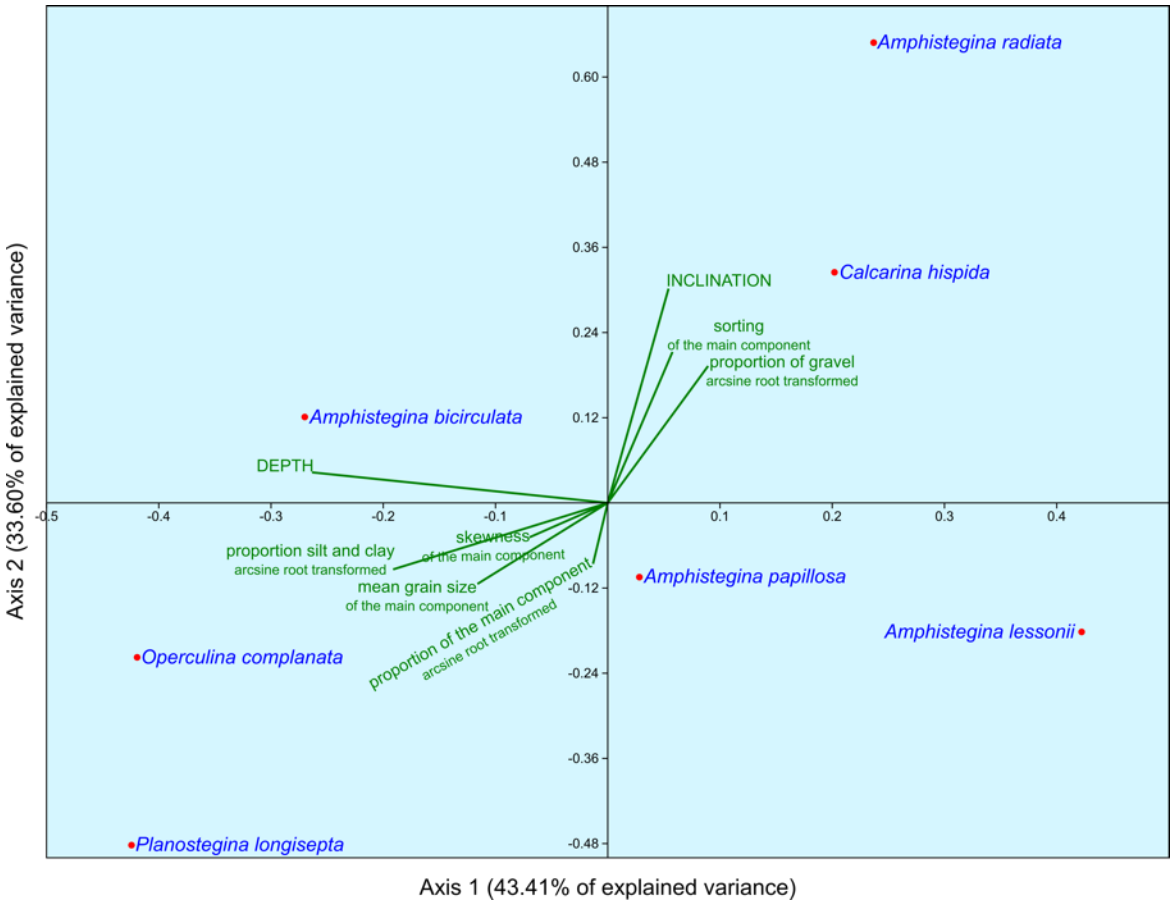


Figure 5.0 Ordination of canonical correspondence analysis showing the relationship of *Amphistegina lessonii, A. bicirculata, A. radiata, A. papillosa, Calcarina hispida, Operculina complanata* and *Planostegina longisepta* with depth, inclination, mean grain size, sorting, skewness, proportion of the main component, proportion of gravel and proportion of silt and clay

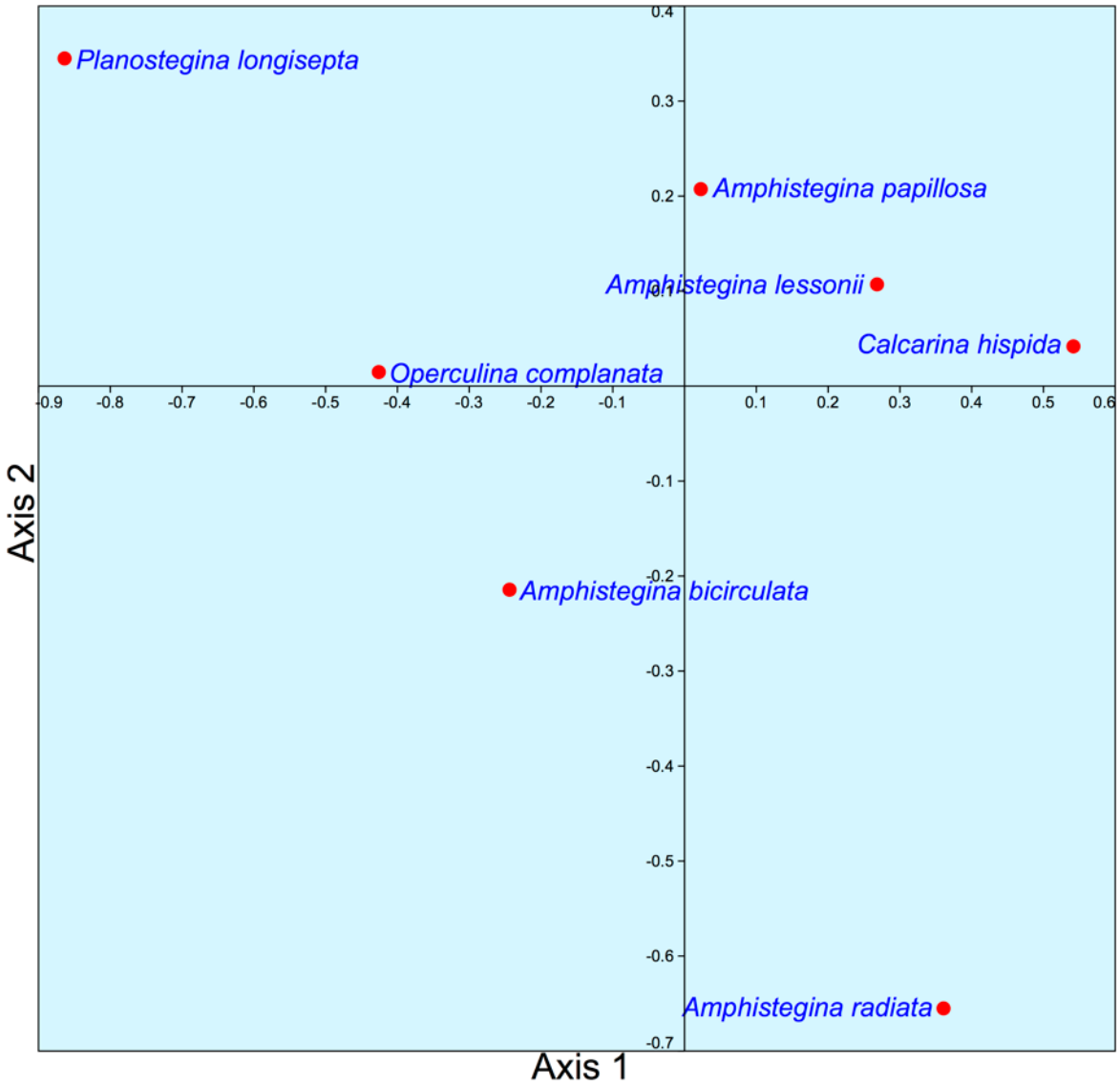


Figure 5.1 Ordination of correspondence analysis showing the distributions of *Amphistegina lessonii, A. bicirculata, A. radiata, A. papillosa, Calcarina hispida, Operculina complanata* and *Planostegina longisepta* according to depth

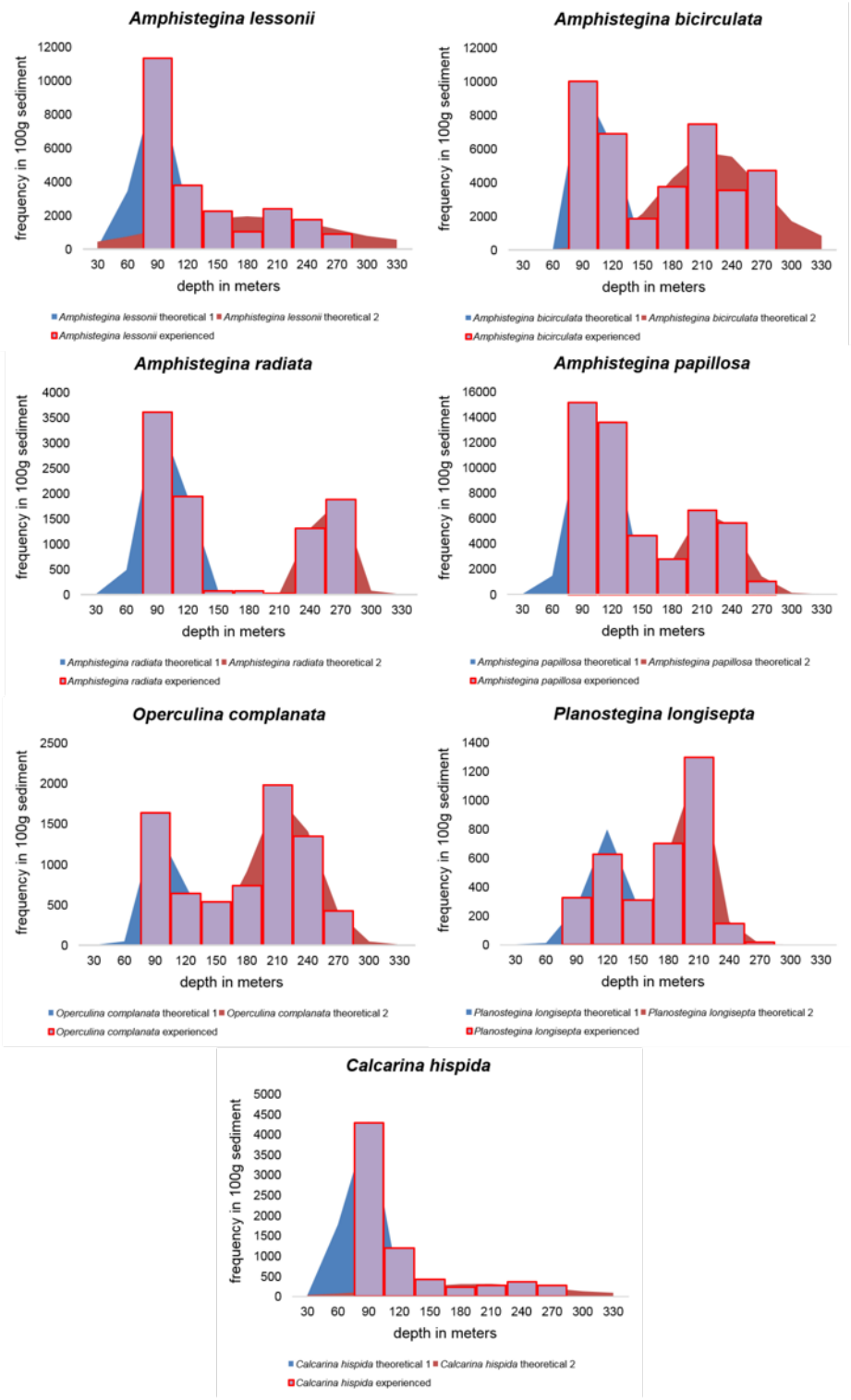


Figure 5.2 Experienced depth distributions (column) fitted by power transformed normal distributions. Abundances of *Amphistegina lessonii, A. bicirculata, A. radiata, A. papillosa, Operculina complanata, Planostegina longisepta* and *Calcarina hispida* are shown in frequency distributions

### 5.2.2 Distribution in grain size

Correspondence analysis of larger benthic foraminifera and grain size classes has identified four groups of species corresponding to the coarse sand, medium sand, fine sand and very fine sand (Figure 5.3). Species located between the values of 0.3 to 0.5 on axis 1 correspond to coarse sand class, i.e., *Amphistegina radiata* and *Calcarina hispida*. Between values of 0 and 0.2 on axis 1, the species in this region correspond to medium sand. The species are *A. papillosa* and *A. bicirculata*. Between values of 0 and -0.2 on axis 1, *A. lessonii* shows correspondence with fine sand class. At the negative end of axis 1, located between values of -0.3 and -0.5 there are two species showing correspondences with very fine sand class. The species are *Planostegina longisepta* and *Operculina complanata*.

Circle graphs are used to depict abundant distributions of larger foraminifera in grain size classes (Figure 5.4). *Amphistegina lessonii* shows abundant distribution in fine sand class as demonstrated by the highest percentage (33% of the samples). This species shows low abundance in very fine, coarse and medium sand classes as demonstrated by the percentages in these classes. Abundant distribution in coarse sand is demonstrated by 32% of the samples of *A. bicirculata*. Low abundance of the samples in other grain size classes are as follows, 28% in very fine sand, 19% in fine sand and 21% in medium sand. *A. radiata* shows abundant distribution in coarse sand as demonstrated by 45% of the samples. *A. papillosa* does not show abundant distribution in any grain size classes. The highest abundance of 27% shows that *A. papillosa* is distributed in the medium sand class. Distribution in coarse sand is represented by 25% of the samples. Distribution in fine and very fine sand classes show similar abundances in each class (24% of the samples). Abundant distributions of *Operculina complanata* and *Planostegina longisepta* are shown in very fine sand class as demonstrated by 47% of the samples of *O. complanata* and 45% of the samples of *P. longisepta*. Abundant distribution of *Calcarina hispida* is shown in coarse sand (46% of the samples). Distributions in other grain size classes are as follows, 20% of the samples in medium sand, 16% of the samples in fine sand and 18% of the samples in very fine sand.

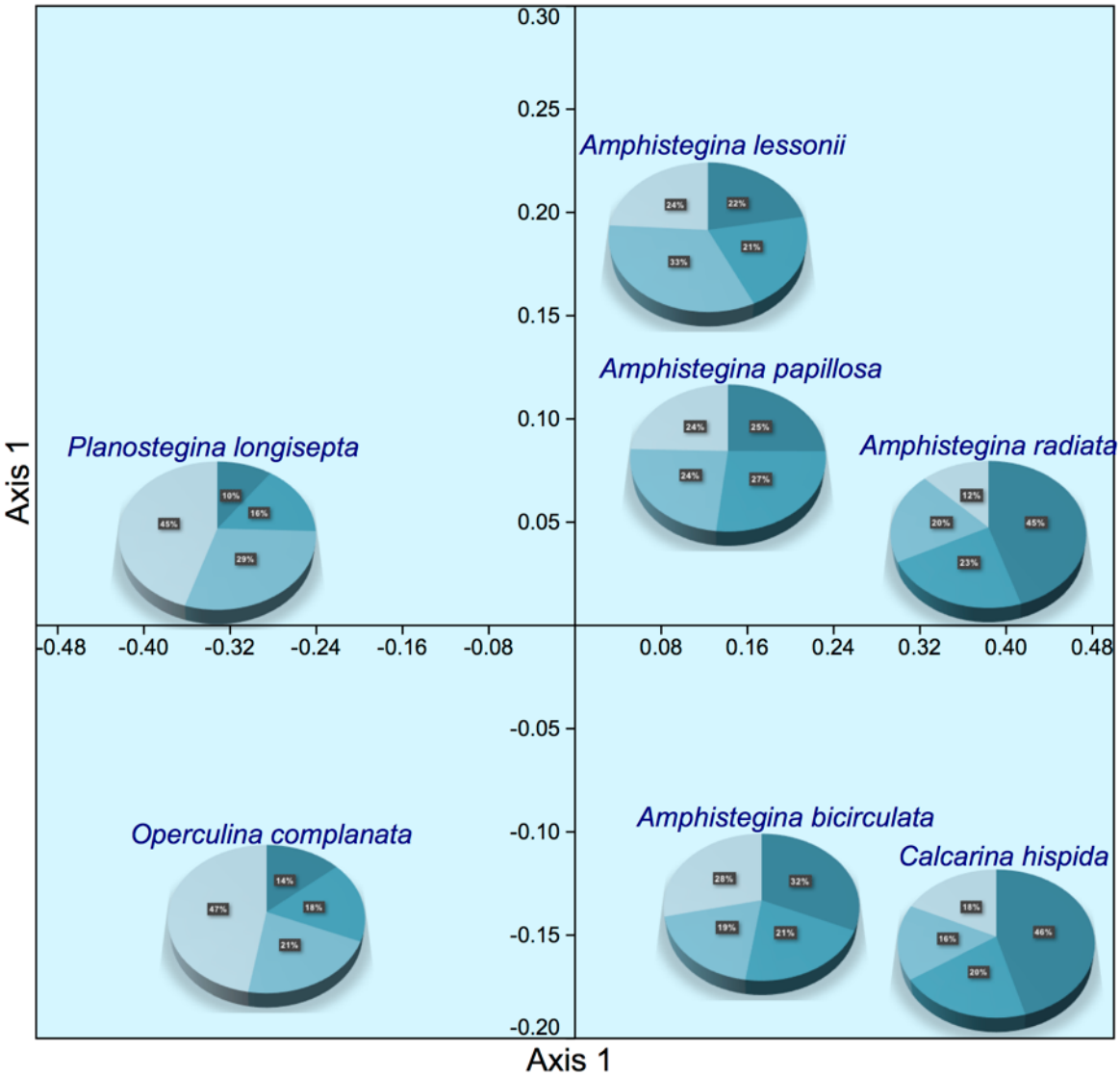


Figure 5.3 Ordination of correspondence analysis showing distributions of *Amphistegina lessonii, A. bicirculata, A. radiata, A. papillosa, Operculina complanata, Planostegina longisepta* and *Calcarina hispida* in grain size classes

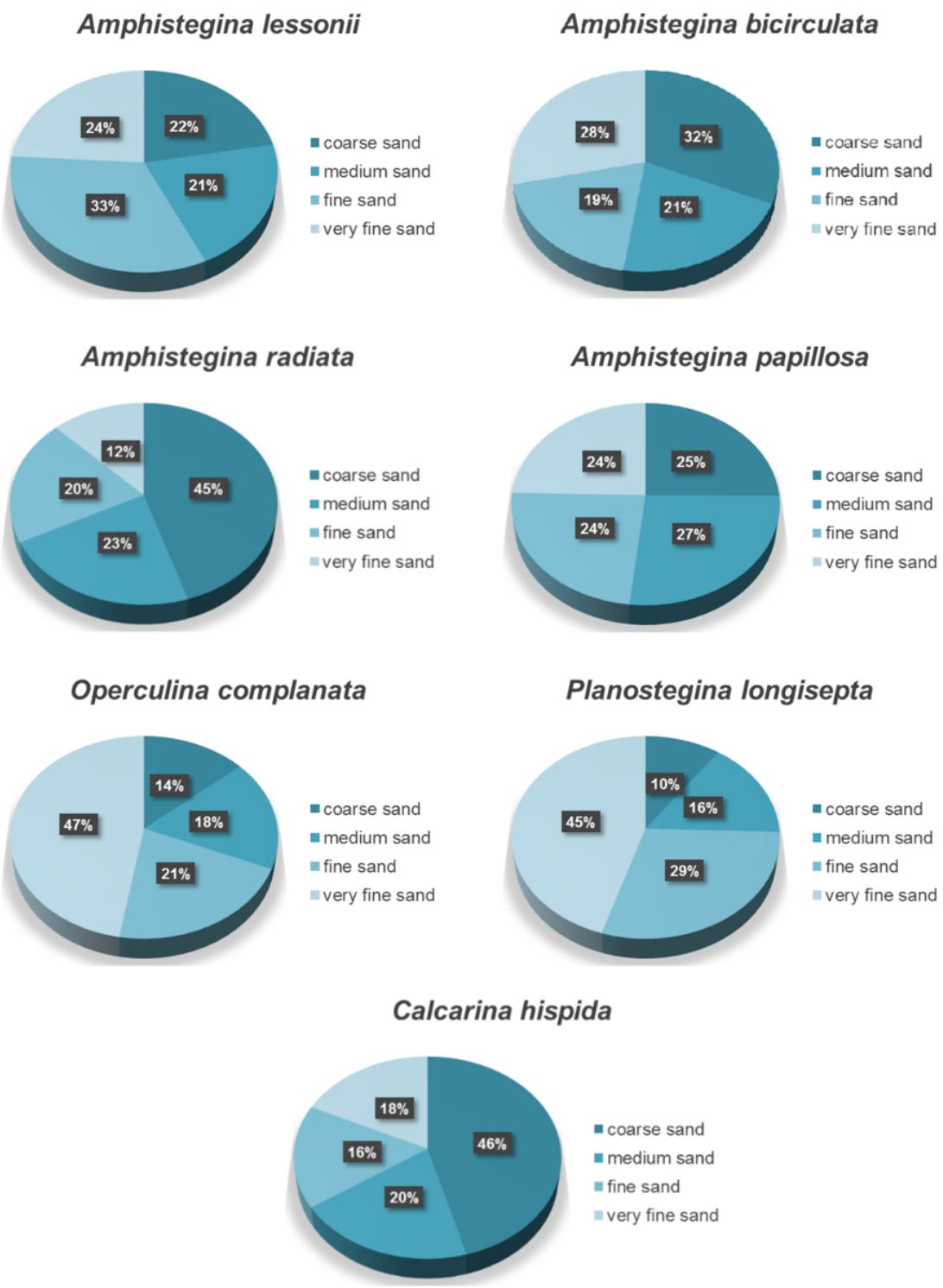


Figure 5.4 Dependence on grain size classes of *Amphistegina lessonii, A. bicirculata, A. radiata, A. papillosa, Operculina complanata, Planostegina longisepta* and *Calcarina hispida*

## 5.3 Discussion

*Amphistegina lessonii*

Shallowest optimal distribution of Amphisteginidae is shown by *A. lessonii*. Distribution of *A. lessonii* was restricted in the upper fore reef zone with optimal distribution of living individuals at 20m with lower limit at 70m (Hallock 1984; Hohenegger 1994; Hohenegger et al. 1999). Depth distribution in the investigation shows an optimum at 73m in the mid sublittoral and 167m in the deeper sublittoral. Optimum attained in mid sublittoral is shifted thus indicating disagreement with the optimum of living distribution. Umbiliconvex form of the living test that was dominant in the reef edge showed preference to firm substrates (Hohenegger et al. 1999). Biconvex form that was more dominant throughout the depth gradient preferred sandy substrate (Hohenegger 1994; Hohenegger et al. 1999). Dependence on fine sand shown by 33% of the samples is in agreement with the substrate preference of the living biconvex form. Depth distribution of *A. lessonii* demonstrates right-side skewness pattern indicating low depth transport of the tests. Influence of submarine topography, storm and current-induced distribution of empty tests lead to different displacement intensities (Hohenegger & Yordanova 2001b). Traction force and slope steepness lead to varying displacement due to the different test buoyancies. Low depth transport of *A. lessonii* is related to low buoyancies of the thick-lenticular test shape (Yordanova & Hohenegger 2007).

*Amphistegina bicirculata*

Upper limit of the depth distribution of living *A. bicirculata* was located at 30m and the lower limit was below 100m (Hohenegger 1994). Optimum of the depth distribution of living *A. bicirculata* was attained at 80m (Hohenegger 2004). Depth distribution of *A. bicirculata* in the investigation shows an optimum at 89m in the mid sublittoral. In the deeper sublittoral, the depth distribution shows an optimum at 206m. Optimal depth distribution of *A. bicirculata* is in agreement with the living distribution. Living distribution of this species preferred firm substrates and showed abundant distribution on macroids (Hohenegger et al. 1999). Small sand (fine to medium) is insufficient for pseudopodial attachment of the living distribution (Hohenegger 2002). This species is characterized by interiomarginal apertural field with numerous papillae suited for strong pseudopodial attachment. Dependence on coarse sand shown by *A. bicirculata* in this study is in agreement with firm/coarse substrate preference demonstrated by the living individuals. Depth distribution of *A. bicirculata* shows a bimodal pattern demonstrating transport at 210m depth. Depth transport of the tests is related to high buoyancies of the thin-lenticular test shape (Yordanova & Hohenegger 2007).

*Amphistegina radiata*

Depth distribution of *A. radiata* shows that the optimum is located at 83m in the mid sublittoral and 243m in the deeper sublittoral. Niche optimum of the living distribution was attained at 20-30m. Distribution of living individuals in the uppermost slope gives values of upper limit at 10m and lower limit at 80m (Hohenegger 1994; Hohenegger et al. 1999). Optimum attained in this study is highly shifted to a deeper depth thus demonstrating disagreement with the niche optimum of living distribution. This also indicates high depth transport of the tests. Depth distribution of *A. radiata* demonstrates bimodal pattern indicating high depth transport of the tests at 270m. Living individuals of *A. radiata* were

abundantly distributed in coarse or medium sand (Hohenegger et al. 1999). Dependence on coarse sand in this study demonstrates agreement with previous studies of living *A. radiata*. Preference to sandy substrate of the living individuals was attributed to the small apertural field that resulted in low pseudopodial attachment (Hohenegger et al. 1999).

*Amphistegina papillosa*

The broadest niche width among all living larger foraminifera was shown by *A. papillosa* (Hohenegger 2004) with the upper limit at 30m, optimal distribution at 80-90m and lower limit below 100m (Hohenegger et al. 1999). The bimodal depth distribution pattern of this species shows an optimum at 89m in mid sublittoral and 205m in the deeper sublittoral. Bimodal pattern of the depth distribution of *A. papillosa* demonstrates transport at 210m. Depth transport of this species is related to the high buoyancies of the lenticular tests (Yordanova & Hohenegger 2007). The shallower optimum attained in this study is in agreement with studies on living individuals. Symmetrical and biconvex shape characterize the small and flat tests of this species. Small apertural field of this test indicates low pseudopodial attachment of the living individuals (Hohenegger 1994) thus demonstrating preference to sandy bottom. Abundant distribution in medium sand is shown in this study thus it is in agreement with preference to sandy substrate of the living *A.papillosa*.

*Operculina complanata*

*O. complanata* possess flat and involute tests, very similar to *O. ammonoides* (Hohenegger 2000b; Briguglio & Hohenegger 2011). All chambers are visible from the lateral sides and the chamber arrangement follows a logarithmic spiral which means that chambers increase in height during growth. Optimal distribution of living individuals was attained at 80m with lower limit at 140m on preferably middle to fine grained substrates (Hohenegger et al. 1999; Hohenegger 2004). The bimodal depth distribution of this species shows an optimum at 85m in mid sublittoral and 202m in the deeper sublittoral. The shallower optimum attained in this study is in agreement with studies on living individuals (Hohenegger 2000a). Bimodal pattern of the depth distribution of *O. complanata* demonstrates transport at 210m. Depth transport of this species is related to the high buoyancies of the thin tests (Yordanova & Hohenegger 2007). Dependence on very fine sand demonstrated by the species in the investigation demonstrates agreement with substrate preference shown by the living individuals.

*Planostegina longisepta*

The genus *Planostegina* demonstrates transition to the genus *Operculina* in terms of test form and surface. Complete division into chamberlets shown by this genus is similar to *Heterostegina*. Living *Planostegina* was known to inhabit the deepest light depleted region of the photic zone. Depth distribution of living *Planostegina* showed that the upper limit was attained at 60m and lower limit was below 120m with niche optimum at 90-100m (Hohenegger 2004). Depth distribution of *P. longisepta* in this study shows the optimal distribution is located at 105m and it is similar to the niche optimum demonstrated by living *P. operculinoides*. Bimodal pattern of the depth distribution of *P. longisepta* demonstrates transport at 210m. Depth transport of this species is related to the high buoyancies of the thin tests (Yordanova & Hohenegger 2007). Substrate preference shown by *P. longisepta* is with very fine sand thus demonstrating correlation with fine

sediment grains in the deeper water region. Living *P. operculinoides* (Hohenegger 2004) also showed substrate preference with fine sand thus demonstrating agreements among members of the genus *Planostegina*.

*Calcarina hispida*

The tests of *Calcarina hispida* are thick, flat and trochospirally coiled. Strong and large tubercles cover the spiral and umbilical sides (Hohenegger et al. 1999). Small spines are densely scattered on the test surface and spines. These small spines are also covered by ultra spikes. Depth distribution of the living individuals shows that the niche width was narrow, with lower limit at 70m. Niche optimum of the living individuals was attained at the shallowest water region (Hohenegger 2004). Depth distribution of *C. hispida* in this study shows that the optimum occurs at 67m in the mid sublittoral and 181m in the deeper sublittoral. Niche optimum of the species in this study is shifted to deeper depth thus indicating disagreement with the niche optimum of living distribution. Depth distribution of *C. hispida* demonstrates right-side skewness pattern indicating low depth transport of the tests. Low depth transport of *C. hispida* is related to the low test buoyancies. Living *C. hispida* was known to inhabit the firm substrate of reef moats, small hole of coral fragments or attachment on corallinacean algae (Hohenegger 1994). Dependence on coarse sand shown by *C. hispida* in this study demonstrate agreement with substrate preference of the living individuals.

## 5.4 Conclusion

Depth distributions of *Amphistegina lessonii* and *Calcarina hispida* show asymmetric pattern with right-side skewness. Depth distributions of *A. bicirculata, A. radiata, A. papillosa, Operculina complanata* and *Planostegina longisepta* show bimodal pattern that have been broken into two unimodal normal distributions. The first components of these bimodal distributions indicate optimal depth distributions located in the mid sublittoral and the second component demonstrates depth transport in the deeper sublittoral.

Optimal depth distributions of *A. lessonii, A. bicirculata, A. radiata, A. papillosa, O. complanata* and *C. hispida* are located in the mid sublittoral. Only *P. longisepta* demonstrates an optimum in the deeper sublittoral. Optimal depth distributions of the optimally preserved tests are in agreement with the optima of living individuals except for *A. lessonii, A. radiata* and *C. hispida* where the optima are shifted. Dependence on substrate type shown by the tests is in agreement with substrate preference of the living larger benthic foraminifera. Agreements on optimal depth distribution and dependence on substrate type of living larger foraminifera signalizes the potential use of optimally preserved tests in understanding the distribution of benthic foraminifera.

Low depth transport is demonstrated by *A. lessonii* and *C. hispida* thus demonstrating low test buoyancies. Depth transport at 210m is shown by *A. bicirculata, A. papillosa, O. complanata* and *P. longisepta*. Similar depth transport of these species is related to similar buoyancies of these tests. High depth transport at 270m is demonstrated by *A. radiata*. High transport of *A. radiata* is influenced by the highly shifted optimum in the mid sublittoral.

# CHAPTER 6

# DEPTH DISTRIBUTION OF SMALLER BENTHIC FORAMINIFERA

## 6.1 Introduction

The niches of benthic foraminifera have not been satisfactorily defined due to ecological complexities (Murray 2006). There are no two microenvironments that are exactly the same therefore it is difficult to make generalizations on which environmental factors controlling distribution pattern. A species must be sufficiently adapted to survive and compete in a niche and not necessarily have to be perfectly adapted to it (Hallock et al. 1991). Critical thresholds of environmental factors control species distribution (Murray 2001). It is defined by the upper and lower limits of the distribution function. An organism is not able to survive outside of these limits. Distribution of benthic foraminifera is influenced by a wide array of abiotic and biotic factors (Jorissen et al. 1995; Murray 2006). Abiotic factors such as temperature, salinity, substrate, oxygen concentration and organic carbon contents are related to changes in water depth (Hohenegger 2000a; Annin 2001). Water depth acts as a composite factor influencing these single factors.

### 6.1.1 Background

Depth distribution of living larger symbiont bearing benthic foraminifera has been successfully investigated using rigorous statistical techniques (Hallock 1984; Hohenegger 1994). Illumination and hydrodynamics are the two most important single factors influencing the depth distribution of living larger benthic foraminifera (Hottinger 1983; Hallock et al. 1991; Hohenegger 2004). Larger foraminifera build specialized wall structures to adapt to illumination intensity and strengthened test structures to handle water movement in the euphotic zone (Hohenegger et al. 1999). Functional morphologies of larger foraminiferal tests are understood better (Hallock et al. 1991) than smaller benthic foraminifera, thus depth distribution of living larger foraminifera can be used as a test case to investigate the depth distribution of optimally preserved smaller benthic foraminifera in the sublittoral and uppermost bathyal. Depth distribution of smaller benthic foraminifera in the sublittoral and uppermost bathyal has never been investigated. Previously, attentions were given to understand the distribution pattern of the deep sea benthic foraminifera by Corliss 1985; Lutze & Thiel 1989; Corliss & Emerson 1990; Corliss 1991; Buzas et al. 1993; Hunt & Corliss 1993; Linke & Lutze 1993; Jorissen et al. 1994; Jorissen et al. 1995; Jorissen et al. 1998; Schmiedl et al. 2000.

### 6.1.2 Dependence on substrate type

Distribution of benthic foraminifera is influenced by substrate type. Investigation on the substrate dependence of smaller benthic foraminifera is performed based on their distribution in grain size classes. The density of living larger foraminifera is different between hard and soft substrate (Hohenegger 1994). Community composition is controlled by substrate preference and competition for space (Hottinger 1983). Different substrates produce different biosystems which are inhabited by different species of benthic foraminifera. Grain size distribution is an indicator of water energy; coarse sand

indicates high water energy and contrarily distribution of fine sand indicates low water energy (Hohenegger et al. 1999).

### 6.1.3 Life position

There are two types of benthic foraminiferal microdistribution pattern, i.e., spatial and temporal (Murray 2006). Spatial microdistribution of benthic foraminifera is characterized by lateral or vertical position in sediments (infaunal) and elevated position above the sediments (epifaunal). Temporal microdistribution pattern is related to reproduction cycle of benthic foraminifera. The two main control of microdistribution pattern are microenvironmental condition and reproduction (Murray 2006). Studies have shown that microhabitat of benthic foraminifera is controlled by pore water oxygen concentration (Jorissen et al. 1995; Jorissen 2002) and food availability (Corliss & Emerson 1990; Jorissen et al. 1992; Hohenegger et al. 1993; Linke & Lutze 1993). Microhabitats of bethic foraminifera are highly variable due to environmental conditions (Murray 2006). Vertical zonation within sediments strongly corresponds to depth related distribution of oxic respiration, nitrate and sulphate reductase (Jorissen et al. 1994; Jorissen et al. 1998).

Even though there is no clear pattern of benthic foraminiferal depth distribution within sediments, studies have shown that there is different morphotype that corresponds to different depths within sediments (Corliss 1985; Corliss 1991; Corliss & Emerson 1990). Epifaunal foraminifera live on top of firm substrates or sediments and it also includes foraminifera living in the top 1cm. Three modes of epifaunal lifestyle have been shown, i.e., sessile, clinging or free living. Infaunal foraminifera living in top few centimetres of the sediments also show attached, clinging or free living life modes. This study investigates life positions of smaller benthic foraminifera, either on sediments (epifaunal) or within sediments (infaunal) based on their distributions in the silt and clay content. Silt and clay content in the sediments can contain and stabilize organic matter such as carbon and nitrogen (Hassink 1997). Organic rich fine sediments provide the best habitat for infaunal foraminifera (Kitazato 1995). Coarse and medium sediments provide shelter and attachment for epifaunal foraminifera (Diz et al. 2004). Preference to epifaunal or infaunal life positions of the smaller benthic foraminifera in a shallow water region may be caused by food availability. In the shallow water region, there is a relatively high organic carbon flux in the seafloor resulting in a shallow oxic layer (Corliss & Emerson 1990) thus eliminating the control of porewater oxygen content as a limiting factor.

### 6.1.4 Aim of the chapter

This chapter investigates the depth distributions, dependence on substrate type and life positions of optimally preserved smaller benthic foraminifera. Canonical correspondence analysis is performed to determine important factors influencing the distributions of 45 smaller benthic foraminiferal species (Table 6.0). The factors are depth, inclination and sedimentological parameters, i.e., mean grain size, sorting, skewness, proportion of the main component, proportion of gravel and proportion of silt and clay. Species distributions according to depth, substrate type and percentages of silt and clay are conducted in correspondence analysis. Frequency distributions are used to depict the experienced depth distributions fitted by power transformed normal distribution. Circle graphs are used

to demonstrate dependence on substrate type and dominance in percentages of silt and clay.

### 6.1.5 Benthic foraminifera with agglutinated tests

Agglutinated foraminifera in the investigation are grouped into two orders based on the type of cement that holds together the particles that are used to build the tests (Table 6.0). The orders are Lituolida and Textulariida. Members of Lituolida, i.e., Spiroplectamminidae are characterized by agglutinated wall with particles attached to a proteinaceous or mineralized matrix (Sen Gupta 2002). Chamber arrangements are planispiral with coiling throughout or uncoiling during later stages (Mikhalevich 2004). Members of the family Spiroplectamminidae possess planispiral or streptospiral chamber arrangements during early stage and biserial or uniserial during later stage. Members of the order Textulariida are characterized by agglutinated wall structures with low-Mg calcite cement (Sen Gupta 2002). There are two families of Textulariida that have been included, Pseudogaudryinidae and Textulariidae. Members of the family Pseudogaudryinidae possess triserial tests in the early part, biserial or uniserial in the later part. Apertural position is interiomarginal. Members of the family Textulariidae possess biserial or uniserial tests. Test is biserial throughout or uniserial in the later part. Apertures of the tests exist in singular or multiple and are located in the interiomargin or areal parts.

### 6.1.6 Benthic foraminifera with secreted $CaCO_3$ tests

Smaller benthic foraminifera with secreted $CaCO_3$ tests are consisted of calcite and aragonite tests (Table 6.0). Calcite tests are divided into high-Mg and low-Mg which belong to the orders Miliolida, Lagenida and Rotaliida. Aragonite test belongs to the order Robertinida. Members of the order Miliolida are characterized by high-Mg calcite tests (Sen Gupta 2002). The larger miliolids are able to survive the environmental condition of the shallow euphotic zone (Hohenegger 1994). Surface texture of the tests is porcelaneous with imperforate chambers. Two families represent Miliolida in this study; Hauerinidae and Spiroloculinidae. Initial chamber in Hauerinidae tests is rounded with succeeding chambers arranged in one or several planes (Sen Gupta 2002). Each chamber covers one-half coil or less. Uncoiling may occur in later parts of the test. Apertural position is terminal, either toothed or partly covered. The test may also be covered with agglutinated outer layer. Members of Spiroloculinidae are characterized by rounded initial chamber and coiled tubular second chamber (Sen Gupta 2002). Apertural position is terminal, either toothed or partly covered.

There are two orders that show possession of the low-Mg calcite test, i.e., Lagenida and Rotaliida (Sen Gupta 2002). Larger foraminifera with hyaline tests have shown preference to inhabit the deeper euphotic zone in order to avoid the high illumination rate of the shallow euphotic zone (Hohenegger 2004). Lagenida is characterized by monolamellar and perforate wall (Sen Gupta 2002). The test is single or multichambered with serial or planispiral chamber arrangement. Family Vaginulinidae representing this order can be characterized by coiled tests that occur throughout or during the early stage.

Members of Rotaliida are characterized by bilamellar and perforate wall (Sen Gupta 2002). Chamber arrangements of the tests are low or high trochospiral, planispiral,

annular or irregular. There are 13 families representing Rotaliida in the investigation; Cibicididae, Elphidiidae, Eponididae, Reussellidae, Anomalinidae, Cassidulinidae, Epistomariidae, Nonionidae, Planorbulinidae, Bolivinitidae, Mississippinidae, Siphogenerinoididae and Rosalinidae. Chamber arrangement in Cibicididae is low trochospiral. Sometimes the chambers are arranged in uniserial or biserial in the later part. Chambers can also be planispiral or annular. Apertural position is interiomarginal in trochospiral form, extending from ventral to dorsal side. Chambers in Elphidiidae tests are arranged planispiral or low trochospiral. The test surface is covered by sutures and pores forming a canal system. Chamber arrangement in Eponididae tests is low trochospiral. The aperture is interiomarginal and slit-like or areal and cribrate. Members of Reussellidae possess triserial tests but then changed into biserial or uniserial arrangement in the later part. Periphery of the test is angular. Apertural position is interiomarginal or terminal. Apertural shape is slitlike or cribrate. Anomalinidae is characterized by low trochospiral test. The primary aperture is interiomarginal and the secondary aperture is sutural on both side of the test. Cassidulinidae is characterized by biserial test with planispiral coil. Members of Epistomariidae are characterized by trochospiral tests. The chambers have complete or incomplete chamberlets. Chamber arrangement in Nonionidae test is planispiral, either throughout or in the early part. The shape of the aperture is slit-like or a series of pores. Chamber arrangement in Planorbulinidae test is planispiral or trochospiral. Sometimes the chamber arrangement is annular or irregular multispiral in the later part. Apertural position in adult form is peripheral and in multiple. Bolivinitidae is characterized by biserial test with interiomarginal aperture and optically radial wall. Members of Mississippinidae are characterized by low trochospiral test. The aperture is umbilical and interiomarginal. Some tests acquire supplementary apertures. The wall structure is optically radial. The periphery of the test is covered by translucent or opaque bands on one or both side. Members of Siphogenerinoididae are characterized by triserial or biserial test in early part, biserial or uniserial in later part. Apertural position is interiomarginal. The aperture is shaped like a loop with internal toothplate. Wall of the test is optically radial. Members of Rosalinidae are characterized by simple interior chamber. The apertural shape is a low interiomarginal arch. The umbilicus is partly or completely covered by chamber extensions.

Smaller benthic foraminifera with aragonite tests belong to the order Robertinida (Sen Gupta 2002). Tests are perforate and multichambered. The chambers are arranged in a trochospiral coil with internal partitions. Apertural position is areal or interiomarginal. Two families represent this order; Ceratobuliminidae and Epistominidae. Primary aperture in Ceratobuliminidae tests is entirely interiomarginal or with areal extension. The shape of the primary aperture in Epistominidae tests is slit-like and located on the test margin.

| **Agglutinated tests** | | **Secreted calcium carbonate tests** | | |
|---|---|---|---|---|
| Lituolida | Textulariida | Miliolida | Lagenida & Rotaliida | Robertinida |
| Organic cemented test | Inorganic cemented test | Porcelaneous test | Hyaline test | Aragonite test |
| *Spirotextularia floridana* | *Pseudogaudryina atlanta pacifica* | *Triloculina affinis* | *Asanonella tubulifera* | *Hoeglundina elegans* |
| *S. fistulosa* | *Textularia crenata* | *T. tricarinata* | *Bolivina vadescens* | *Lamarckina ventricosa* |
| | *T. agglutinans* | *Miliolinella* cf. *M. chiastocytis* | *Caribeanella celsusraphes* | |
| | *T. foliacea* | *M. circularis* | *C. shimabarensis* | |
| | *T. neorugosa* | *M. subrotunda* | *Cellanthus craticulatus* | |
| | | *Quinqueloculina bicarinata* | *Cibicides* cf. *C. refulgens* | |
| | | *Q. lamarckiana* | *Cibicidoides pachyderma* | |
| | | *Q. seminulum* | *Elphidium crispum* | |
| | | *Q. venusta* | *Eponides repandus* | |
| | | *Spirosigmoilina speciosa* | *Fijella simplex* | |
| | | *Spiroloculina manifesta* | *Globocassidulina bisecta* | |
| | | *Pyrgo denticulata* | *Lenticulina limbosa* | |
| | | *P. sarsi* | *L. vortex* | |
| | | | *Melonis nicobarense* | |
| | | | *Neoconorbina communis* | |
| | | | *N. tuberocapitata* | |
| | | | *Paracassidulina neocarinata* | |
| | | | *Paracibicides hebeslucidus* | |
| | | | *Planorbulinella larvata* | |
| | | | *Rectobolivina raphana* | |
| | | | *Rosalina petasiformis* | |
| | | | *R. vilardeboana* | |
| | | | *Stomatorbina concentrica* | |

Table 6.0 Smaller benthic foraminiferal species under investigation

## 6.2 Results

### 6.2.1 Depth distribution

Relationship between the distribution of smaller benthic foraminifera and environmental factors such as depth, inclination and sedimentological parameters is investigated in canonical correspondence analysis (Figure 6.0 and Table 6.1). Depth is more important than inclination in the ordination due to its location nearest to axis 1. Axis 1 holds more importance than axis 2 based on the eigenvalues. Similar directions of increasing inclination, increasing proportion of the main component and increasing depth indicate that these parameters are correlated with each other (bottom-right of the ordination). In the upper-right of the ordination, it is demonstrated that increasing proportion of silt and clay correlates with increasing mean grain size and increasing skewness. In the upper-left of the ordination, increasing sorting is correlated with increasing proportion of gravel. Detailed correspondences between benthic foraminiferal distributions and environmental factors are summarized in table 6.1.

Correspondence analysis between smaller benthic foraminifera and depth is performed to determine their distributions according to the depth zonations (Figure 6.1 and Table 6.2). Species that are located along the positive end of axis 1 between values of 0 and 0.9 and axis 2 between values of 0.84 and -0.60 are the species that corresponds to deeper water region. Species that are located along the negative end of axis 1 between values of 0 and -1.5 and axis 2 between values of 0.84 and -0.60 are showing distributions in shallow water region. The depth distributions are further summarized according to depth zonation that has been defined (Table 6.2). Mid sublittoral is defined as the depth from 50 to less than 100m. Deeper sublittoral is defined as the depth from 100 to less than 200m. Uppermost bathyal is defined as the depth from 200 to less than 300m.

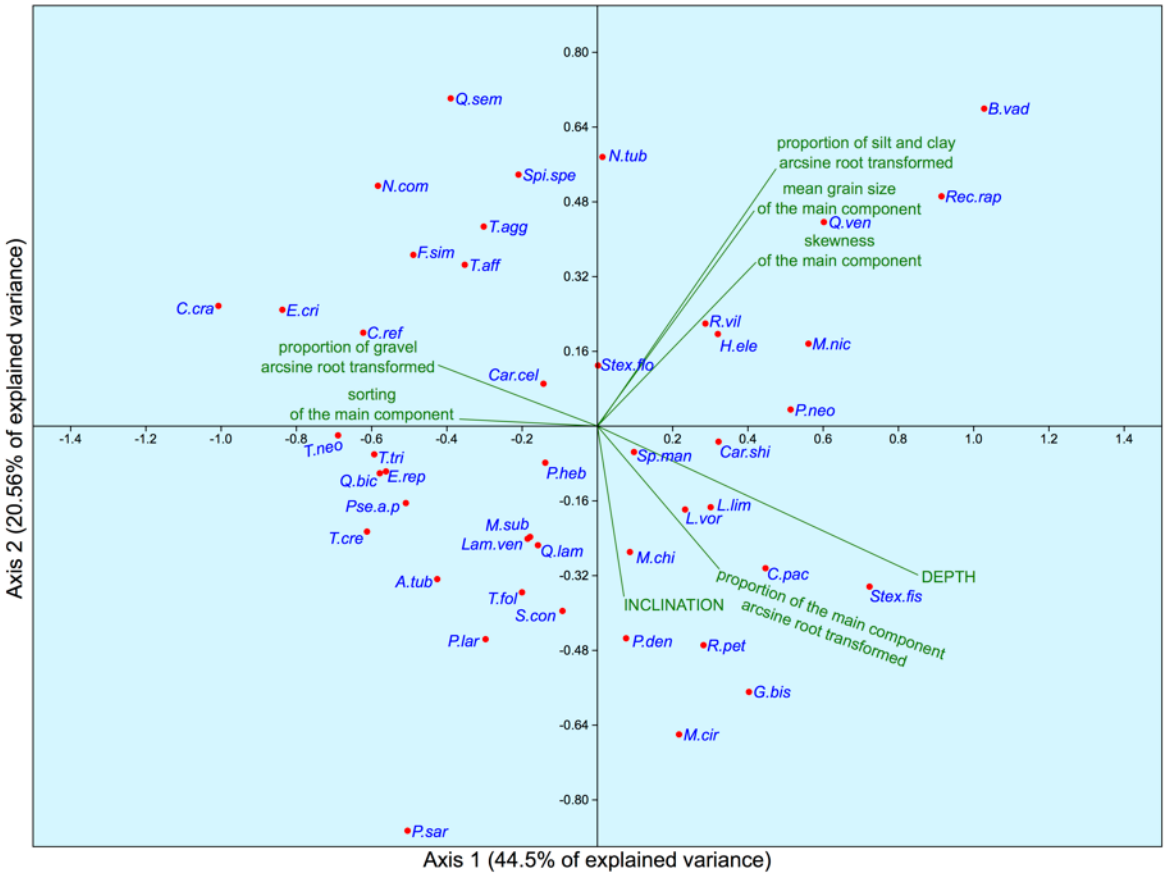


Figure 6.0 Ordination of canonical correspondence analysis showing relationship between smaller benthic foraminifera with depth, inclination, mean grain size, sorting, skewness, proportion of the main component, proportion of gravel and proportion of silt and clay. Acronyms representing the species names are in brackets *Cellanthus craticulatus (C.cra)*, *Elphidium crispum (E.cri)*, *Cibicides* cf. *C. refulgens (C.ref)*, *Caribeanella celsusraphes (Car.cel)*, *Triloculina affinis (T.aff)*, *Fijella simplex (F.sim)*, *Textularia agglutinans (T.agg)*, *Neoconorbina communis (N.com)*, *Spirosigmoilina speciosa (Spi.spe)*, *Quinqueloculina seminulum (Q.sem)*, *Pyrgo sarsi (P.sar)*, *Planorbulinella larvata (P.lar)*, *Stomatorbina concentrica (S.con)*, *Textularia foliacea (T.fol)*, *Asanonella tubulifera (A.tub)*, *Quinqueloculina lamarckiana (Q.lam)*, *Lamarckina ventricosa (Lam.ven)*, *Miliolinella subrotunda (M.sub)*, *Textularia crenata (T.cre)*, *Pseudogaudryina atlanta pacifica (Pse.a.p)*, *Quinqueloculina bicarinata (Q.bic)*, *Eponides repandus (E.rep)*, *Paracibicides hebeslucidus (P.heb)*, *Triloculina tricarinata (T.tri)*, *Textularia neorugosa (T.neo), Spirotextularia fistulosa (Stex.fis)*, *Cibicidoides pachyderma (C.pac)*, *Rosalina petasiformis (R.pet)*, *Globocassidulina bisecta (G.bis)*, *Miliolinella circularis (M.cir)*, *Pyrgo denticulata (P.den)*, *Miliolinella* cf. *M. chiastocytis (M.chi)*, *Lenticulina vortex (L.vor)*, *Lenticulina limbosa (L.lim)*, *Spiroloculina manifesta (Sp.man)*, *Caribeanella shimabarensis (Car.shi)*, *Bolivina vadescens (B.vad)*, *Rectobolivina raphana (Rec.rap)*, *Quinqueloculina venusta (Q.ven)*, *Neoconorbina tuberocapitata (N.tub)*, *Rosalina vilardeboana (R.vil)*, *Hoeglundina elegans (H.ele)*, *Melonis nicobarense (M.nic)*, *Spirotextularia floridana (Stex.flor)* and *Paracassidulina neocarinata (P.neo)*

| Species | Depth | Inclination | Sedimentological parameters |
|---|---|---|---|
| *Bolivina vadescens*<br>*Rectobolivina raphana*<br>*Quinqueloculina venusta*<br>*Rosalina vilardeboana*<br>*Hoeglundina elegans*<br>*Paracassidulina neocarinata*<br>*Melonis nicobarense*<br>*Spirotextularia floridana*<br>*Neoconorbina tuberocapitata* | Deeper region | Less steep slope | High proportion of silt and clay |
| | | | Dominance of finer sediment grains |
| *Spirotextularia fistulosa*<br>*Cibicidoides pachyderma*<br>*Lenticulina vortex*<br>*L. limbosa*<br>*Spiroloculina manifesta*<br>*Caribeanella shimabarensis*<br>*Miliolinella* cf. *M. chiastocytis*<br>*Pyrgo denticulata*<br>*Rosalina petasiformis*<br>*Globocassidulina bisecta*<br>*Miliolinella circularis* | Deeper region | Steep slope | High proportion of sand |
| *Pyrgo sarsi*<br>*Planorbulinella larvata*<br>*Stomatorbina concentrica*<br>*Textularia foliacea*<br>*Asanonella tubulifera*<br>*Quinqueloculina lamarckiana*<br>*Lamarckina ventricosa*<br>*Miliolinella subrotunda*<br>*Paracibicides hebeslucidus* | Deeper region | Steep slope | Low proportion of silt and clay |
| | | | Dominance of coarser sediment grains |
| *Quinqueloculina seminulum*<br>*Triloculina affinis*<br>*Fijella simplex* | Shallow region | Less steep slope | High proportion of sand |
| *Spirosigmoilina speciosa*<br>*Neoconorbina communis*<br>*Textularia agglutinans* | Deeper region | | |
| *Cibicides* cf. *C. refulgens*<br>*Elphidium crispum*<br>*Cellanthus craticulatus*<br>*Triloculina tricarinata*<br>*Eponides repandus*<br>*Quinqueloculina bicarinata*<br>*Pseudogaudryina atlanta pacifica* | Shallow region | Steep slope | High proportion of gravel |
| | | | Dominance of coarser sediment grains |
| *Caribeanella celsusraphes*<br>*Textularia neorugosa*<br>*T. crenata* | Deeper region | | |

Table 6.1 Relationship between smaller benthic foraminiferal distributions and environmental factors derived from canonical correspondence analysis

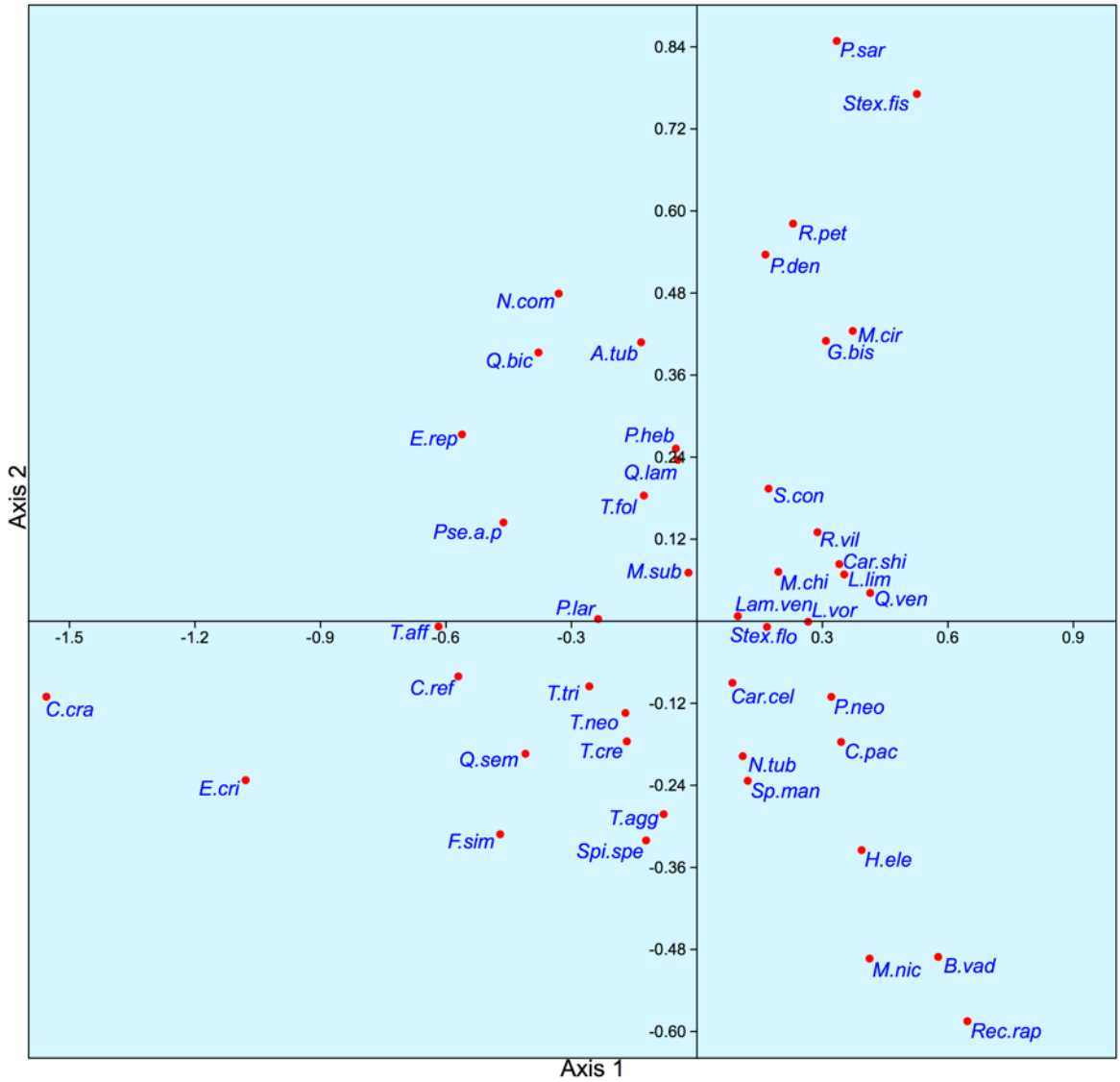


Figure 6.1 Ordination of correspondence analysis showing distributions of smaller benthic foraminifera according to depth. Acronyms representing the species names are in brackets *Cellanthus craticulatus (C.cra)*, *Elphidium crispum (E.cri)*, *Cibicides* cf. *C. refulgens (C.ref)*, *Caribeanella celsusraphes (Car.cel)*, *Triloculina affinis (T.aff)*, *Fijella simplex (F.sim)*, *Textularia agglutinans (T.agg)*, *Neoconorbina communis (N.com)*, *Spirosigmoilina speciosa (Spi.spe)*, *Quinqueloculina seminulum (Q.sem)*, *Pyrgo sarsi (P.sar)*, *Planorbulinella larvata (P.lar)*, *Stomatorbina concentrica (S.con)*, *Textularia foliacea (T.fol)*, *Asanonella tubulifera (A.tub)*, *Quinqueloculina lamarckiana (Q.lam)*, *Lamarckina ventricosa (Lam.ven)*, *Miliolinella subrotunda (M.sub)*, *Textularia crenata (T.cre)*, *Pseudogaudryina atlanta pacifica (Pse.a.p)*, *Quinqueloculina bicarinata (Q.bic)*, *Eponides repandus (E.rep)*, *Paracibicides hebeslucidus (P.heb)*, *Triloculina tricarinata (T.tri)*, *Textularia neorugosa (T.neo), Spirotextularia fistulosa (Stex.fis)*, *Cibicidoides pachyderma (C.pac)*, *Rosalina petasiformis (R.pet)*, *Globocassidulina bisecta (G.bis)*, *Miliolinella circularis (M.cir)*, *Pyrgo denticulata (P.den)*, *Miliolinella* cf. *M. chiastocytis (M.chi)*, *Lenticulina vortex (L.vor)*, *Lenticulina limbosa (L.lim)*, *Spiroloculina manifesta (Sp.man)*, *Caribeanella shimabarensis (Car.shi)*, *Bolivina vadescens (B.vad)*, *Rectobolivina raphana (Rec.rap)*, *Quinqueloculina venusta (Q.ven)*, *Neoconorbina tuberocapitata (N.tub)*, *Rosalina vilardeboana (R.vil)*, *Hoeglundina elegans (H.ele)*, *Melonis nicobarense (M.nic)*, *Spirotextularia floridana (Stex.flor)* and *Paracassidulina neocarinata (P.neo)*

| Depth distribution | Species |
|---|---|
| **Mid sublittoral** | *Cellanthus craticulatus*<br>*Elphidium crispum*<br>*Eponides repandus*<br>*Pseudogaudryina atlanta pacifica*<br>*Triloculina affinis*<br>*Cibicides* cf. *C. refulgens*<br>*Quinqueloculina seminulum*<br>*Fijella simplex*<br>*Quinqueloculina bicarinata* |
| **Deeper sublittoral** | *Planorbulinella larvata*<br>*Triloculina tricarinata*<br>*Asanonella tubulifera*<br>*Paracibicides hebeslucidus*<br>*Quinqueloculina lamarckiana*<br>*Textularia foliacea*<br>*Miliolinella subrotunda*<br>*Textularia neorugosa*<br>*Textularia crenata*<br>*Spirosigmoilina speciosa*<br>*Caribeanella celsusraphes*<br>*Cibicidoides pachyderma*<br>*Hoeglundina elegans*<br>*Lamarckina ventricosa*<br>*Lenticulina vortex*<br>*Melonis nicobarense*<br>*Miliolinella* cf. *M. chiastocytis*<br>*Paracassidulina neocarinata*<br>*Spiroloculina manifesta* |
| **Uppermost bathyal** | *Bolivina vadescens*<br>*Caribeanella shimabarensis*<br>*Globocassidulina bisecta*<br>*Lenticulina limbosa*<br>*Textularia agglutinans*<br>*Miliolinella circularis*<br>*Neoconorbina tuberocapitata*<br>*Neoconorbina communis*<br>*Pyrgo denticulata*<br>*Pyrgo sarsi*<br>*Quinqueloculina venusta*<br>*Rectobolivina raphana*<br>*Rosalina petasiformis*<br>*Rosalina vilardeboana*<br>*Spirotextularia floridana*<br>*Spirotextularia fistulosa*<br>*Stomatorbina concentrica* |

Table 6.2 Depth distributions of smaller benthic foraminifera derived from correspondence analysis. Mid sublittoral is between 50 to < 100m, deeper sublittoral is between 100 to < 200m and uppermost bathyal is between 200 to < 300m

Detailed analysis on the depth distribution of optimally preserved smaller benthic foraminifera is conducted by fitting the experienced distributions with power transformed normal distributions (Figures 6.2, 6.3, 6.4a, 6.4b and 6.5). Values of the mean, upper limit, lower limit and range gained from the fitting of the depth distributions are presented in table 6.3.

There are seven agglutinated foraminifera included in this depth distribution investigation (Figure 6.2). They are *Spirotextularia floridana, S. fistulosa, Pseudogaudryina atlanta pacifica, Textularia foliacea, T. crenata, T. neorugosa* and *T. agglutinans*. Agglutinated foraminifera in the investigation are distributed from the mid sublittoral to the uppermost bathyal (Figure 6.2) with mean values demonstrating optimal depth distributions (Table 6.3). *S. floridana* shows that the optimal distribution occurs in the uppermost bathyal at 230m. *S. fistulosa* is optimally distributed slightly deeper than *S. floridana* in the uppermost bathyal at 260m. Optimal distribution of *P. atlanta pacifica* occurs at the shallowest depth among all other agglutinated foraminifera. The optimal distribution is located in the mid sublittoral at 96m. *T. foliacea* shows that the optimal distribution occurs at the shallowest depth in the deeper sublittoral among all other members of the genus *Textularia* with an optimum at 103m. Optimal depth distributions of *T. crenata* and *T. neorugosa* are located very close to one another in the deeper sublittoral. *T. crenata* shows that the optimum is located at 140m. Optimal depth distribution of *T. neorugosa* occurs at 150m. Deepest optimal distribution among all members of the genus *Textularia* is shown by *T. agglutinans*. The optimum is located in the uppermost bathyal at 202m.

There are 13 porcelaneous foraminiferal species included in the depth distribution investigation. The porcelaneous foraminifera are distributed from the mid sublittoral to the uppermost bathyal (Figure 6.3) with mean values demonstrating optimal depth distributions (Table 6.3). The shallowest optimal depth distribution of porcelaneous foraminifera is shown by *Triloculina affinis*. The optimum is located in the mid sublittoral at 86m. *T. affinis* is one of the three porcelaneous species showing optimal depth distributions in the mid sublittoral. The other two species are *Quinqueloculina bicarinata* and *Q. seminulum*. *Q. bicarinata* and *Q. seminulum* show that their optima occur very near to one another, at 94m and 99m respectively. Porcelaneous foraminifera showing optimal disributions in the deeper sublittoral are *T. tricarinata, Q. lamarckiana, Spirosigmoilina speciosa, Miliolinella subrotunda, M.* cf. *M. chiastocytis* and *Spiroloculina manifesta*. *T. tricarinata* shows that the optimal distribution is located at 109m. *Q. lamarckiana* and *S. speciosa* show optimal distributions near to one another, occurring at 127m and 133m respectively. Optimal distributions of *M. subrotunda* and *M.* cf. *M. chiastocytis* are also located very near to each other at 160m and 166m respectively. Deepest optimal distribution in the deeper sublittoral is shown by *S. manifesta*, which occurs at 175m. Optimal depth distributions occurring in the uppermost bathyal are shown by *Q. venusta, Pyrgo sarsi, P. denticulata* and *M. circularis*. The optima of these four porcelaneous species in the uppermost bathyal are located near to each other. *Q. venusta* shows that the optimum is located at 235m. *P. sarsi* shows an optimum of the depth distribution at 239m. Optima of the depth distributions of *P. denticulata* and *M. circularis* are located at 247m and 249m respectively.

Altogether there are 23 hyaline foraminiferal species that have been included in the depth distribution investigation. Depth distributions of the hyaline foraminifera starts in the mid sublittoral to uppermost bathyal (Figures 6.4a and 6.4b) with mean values demonstrating optimal depth distributions (Table 6.3). Optimal depth distributions which occur in the mid

sublittoral are demonstrated by *Fijella simplex, Cellanthus craticulatus, Elphidium crispum, Cibicides* cf. *C. refulgens* and *Eponides repandus* (Figure 6.4a). Shallowest optimum among all hyaline species is demonsrated by *F. simplex*, located at 69m. *C. craticulatus* shows that the optimal distribution is located at 79m. Depth distribution of *E. crispum* shows an optimum at 82m. *C.* cf. *C. refulgens* shows optimal depth distribution at 86m and *E. repandus* shows that the optimum is located at 88m.

*Planorbulinella larvata* and *Asanonella tubulifera* demonstrate almost similar optimal depth distributions in the deeper sublittoral (Figure 6.4a). Optima for *P. larvata* and *A. tubulifera* are located at 146m and 147m respectively. Optimal depth distribution of *Cibicidoides pachyderma* is located at 170m. Similar optima are shown by the depth distributions of *Caribeanella celsusraphes* and *Paracibicides hebeslucidus*, both located at 177m. Optimal distribution of *Paracassidulina neocarinata* is located at 184m. *Melonis nicobarense* shows the optimal distribution occurs at the base of deeper sublittoral, at 199m. Another species whose optimal distribution located at the base of the deeper sublittoral is *Lenticulina vortex* with an optimum at 192m (Figure 6.4b).

The remaining ten hyaline species show optimal depth distributions in the uppermost bathyal (Figure 6.4b). The shallowest optimum in the uppermost bathyal is demonstrated *by Bolivina vadescens*, located at 201m. Similar optima in the uppermost bathyal are demonstrated by *Neoconorbina tuberocapitata* and *Stomatorbina concentrica*, with both optima occurring at 211 and 214m respectively. *Rectobolivina raphana* shows optimal depth distribution in the uppermost bathyal occurring at 226m. Depth distribution of *Lenticulina limbosa* shows an optimum at 232m. Optimal depth distributions in the uppermost bathyal of two members of the genus *Rosalina*, *R. vilardeboana* and *R. petasiformis* are located at 247m and 257m respectively. The other member of the genus *Neoconorbina*, *N. communis* has an optimal depth distribution at 271m. Deepest optima in the uppermost bathyal are demonstrated by *Caribeanella shimabarensis* and *Globocassidulina bisecta*. Both species have their optima at 290m.

There are only two aragonite species included in the depth distribution investigation. The species are *Lamarckina ventricosa* and *Hoeglundina elegans*. Depth distributions of the aragonite foraminifera starts in the mid sublittoral to uppermost bathyal (Figure 6.5) with mean values demonstrating optimal depth distributions (Table 6.3). Both aragonite species demonstrate optimal depth distributions in the deeper sublittoral. Depth distribution of *L. ventricosa* shows an optimum at 174m. *H. elegans* shows that the optimal depth distribution is located at the base of the deeper sublittoral which occurs at 199m.

| Species | Mean (m) | Upper limit (m) | Lower limit (m) | Range (m) |
|---|---|---|---|---|
| *Asanonella tubulifera* | 147.4 | 13 | 1738 | 1725 |
| *Bolivina vadescens* | 201.3 | 134 | 303 | 170 |
| *Caribeanella celsusraphes* | 176.8 | 53 | 588 | 535 |
| *Caribeanella shimabarensis* | 290.0 | 44 | 1924 | 1880 |
| *Cellanthus craticulatus* | 78.9 | 36 | 171 | 135 |
| *Cibicides* cf. *C. refulgens* | 85.6 | 11 | 692 | 681 |
| *Cibicidoides pachyderma* | 169.5 | 65 | 444 | 379 |
| *Elphidium crispum* | 82.4 | 14 | 477 | 463 |
| *Eponides repandus* | 88.1 | 13 | 579 | 566 |
| *Fijella simplex* | 68.5 | 3 | 1562 | 1559 |
| *Globocassidulina bisecta* | 290.8 | 35 | 2435 | 2401 |
| *Hoeglundina elegans* | 198.6 | 123 | 321 | 198 |
| *Lamarckina ventricosa* | 173.6 | 57 | 525 | 468 |
| *Lenticulina limbosa* | 232.0 | 48 | 1131 | 1083 |
| *Lenticulina vortex* | 192.2 | 59 | 629 | 570 |
| *Melonis nicobarense* | 199.5 | 107 | 373 | 266 |
| *Miliolinella* cf. *M. chiastocytis* | 165.9 | 54 | 510 | 456 |
| *Miliolinella circularis* | 248.4 | 55 | 1131 | 1077 |
| *Miliolinella subrotunda* | 158.8 | 27 | 928 | 901 |
| *Neoconorbina communis* | 271.7 | 173 | 427 | 254 |
| *Neoconorbina tuberocapitata* | 211.2 | 129 | 345 | 215 |
| *Paracassidulina neocarinata* | 184.2 | 81 | 419 | 337 |
| *Paracibicides hebeslucidus* | 177.6 | 7 | 4486 | 4479 |
| *Planorbulinella larvata* | 145.6 | 73 | 289 | 216 |
| *Pseudogaudryina atlanta pacifica* | 96.3 | 15 | 637 | 622 |
| *Pyrgo denticulata* | 247.1 | 22 | 2811 | 2789 |
| *Pyrgo sarsi* | 238.8 | 100 | 572 | 472 |
| *Quinqueloculina bicarinata* | 93.5 | 8 | 1147 | 1140 |
| *Quinqueloculina lamarckiana* | 126.5 | 38 | 418 | 380 |
| *Quinqueloculina seminulum* | 99.5 | 14 | 686 | 671 |
| *Quinqueloculina venusta* | 234.6 | 137 | 402 | 266 |
| *Rectobolivina raphana* | 226.4 | 132 | 389 | 257 |
| *Rosalina petasiformis* | 257.1 | 96 | 692 | 597 |
| *Rosalina vilardeboana* | 247.2 | 110 | 554 | 443 |
| *Spiroloculina manifesta* | 175.2 | 97 | 318 | 221 |
| *Spirotextularia floridana* | 229.8 | 27 | 1938 | 1910 |
| *Spirotextularia fistulosa* | 260.2 | 164 | 414 | 250 |
| *Spirosigmoilina speciosa* | 133.1 | 13 | 1342 | 1329 |
| *Stomatorbina concentrica* | 214.2 | 35 | 1322 | 1288 |
| *Textularia agglutinans* | 202.0 | 93 | 439 | 347 |
| *Textularia crenata* | 139.3 | 15 | 1265 | 1249 |
| *Textularia foliacea* | 102.5 | 0 | 23882 | 23881 |
| *Textularia neorugosa* | 149.1 | 10 | 2170 | 2160 |
| *Triloculina affinis* | 86.0 | 15 | 508 | 493 |
| *Triloculina tricarinata* | 108.8 | 7 | 1779 | 1772 |

Table 6.3 Depth distributions of smaller benthic foraminifera. Mean indicates optimal distribution. Upper limit, lower limit and range represent 99% of the specimens

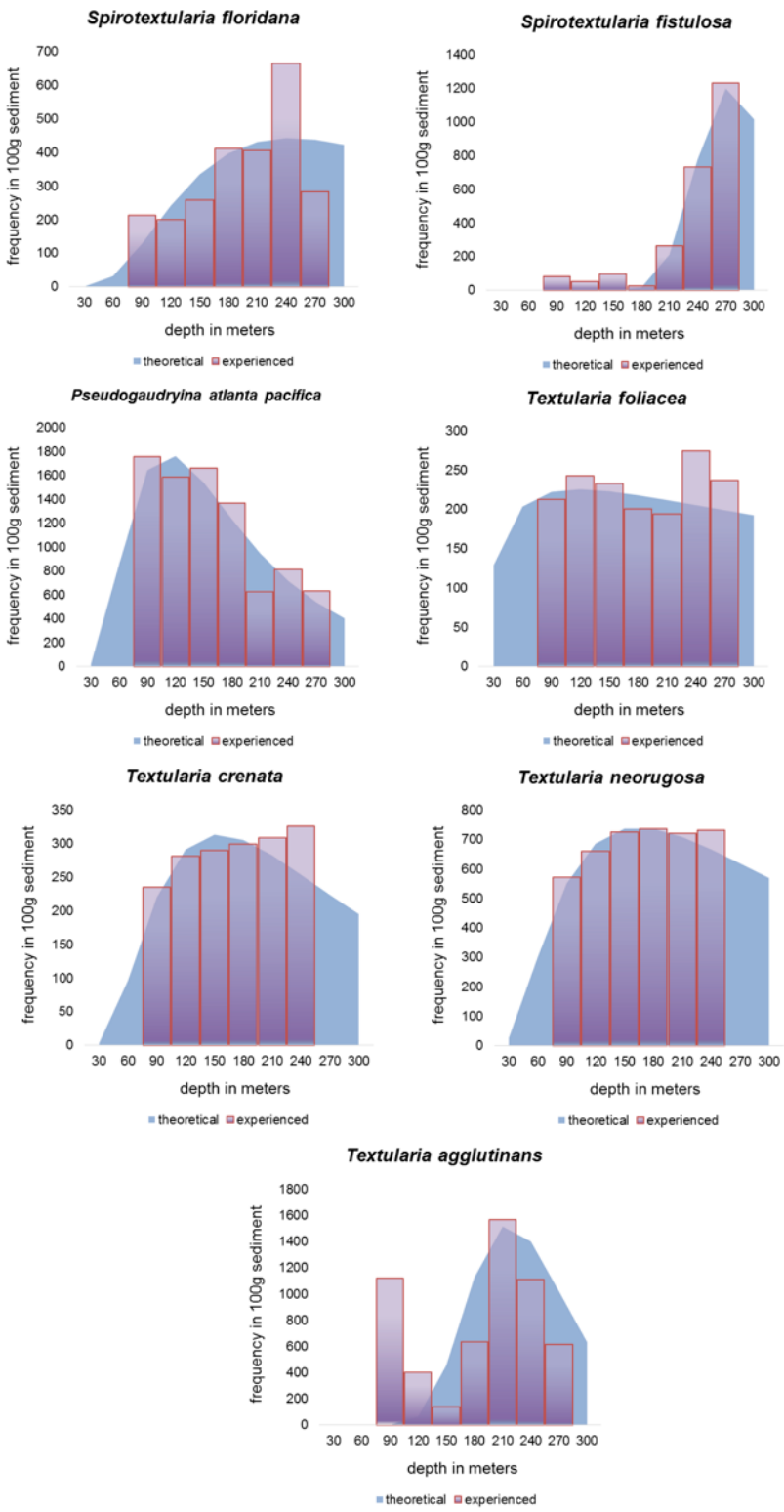


Figure 6.2 Experienced depth distributions (column) fitted by power transformed normal distributions. Abundances of agglutinated foraminifera are shown in frequency distributions

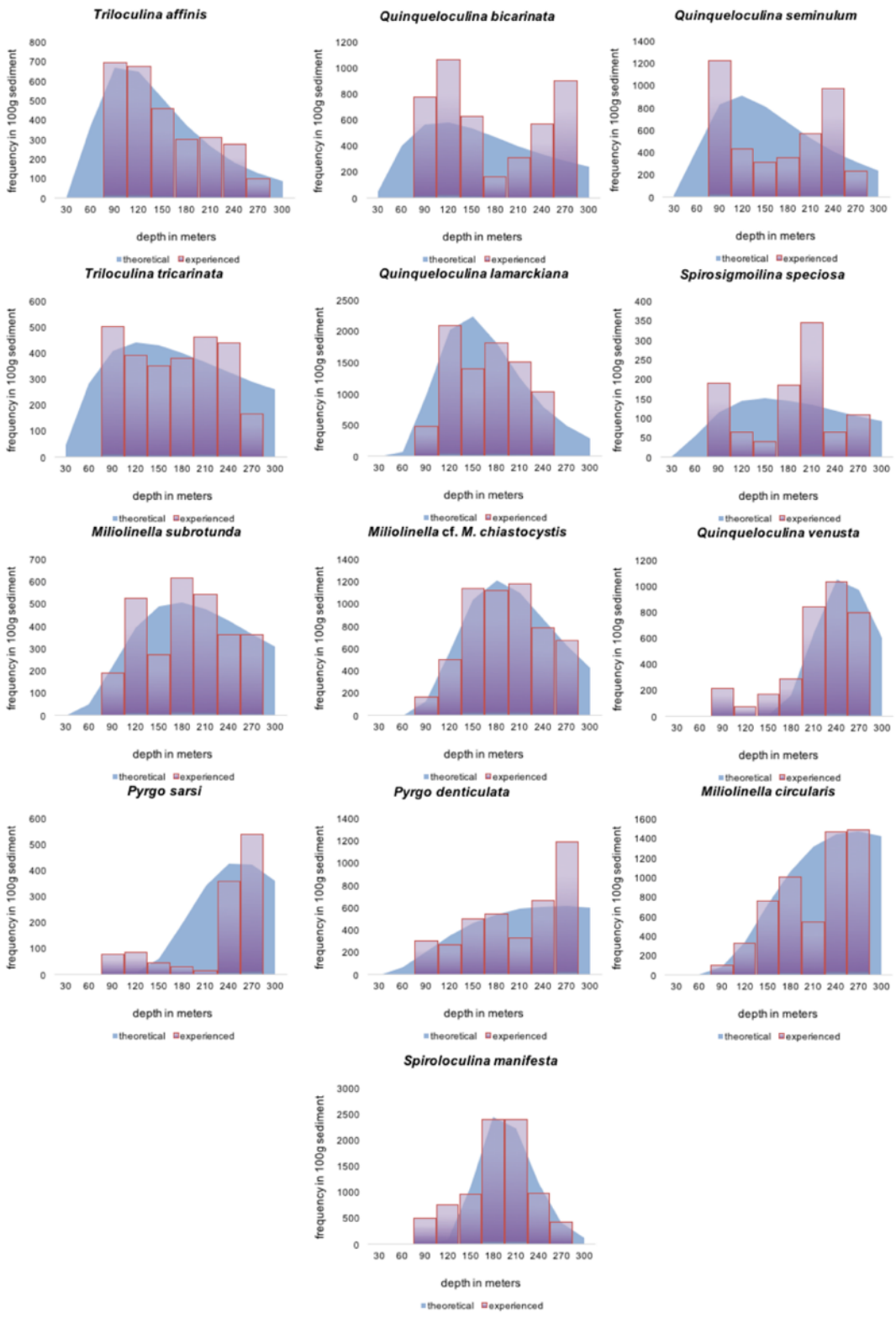


Figure 6.3 Experienced depth distributions (column) fitted by power transformed normal distributions. Abundances of porcelaneous foraminifera are shown in frequency distributions

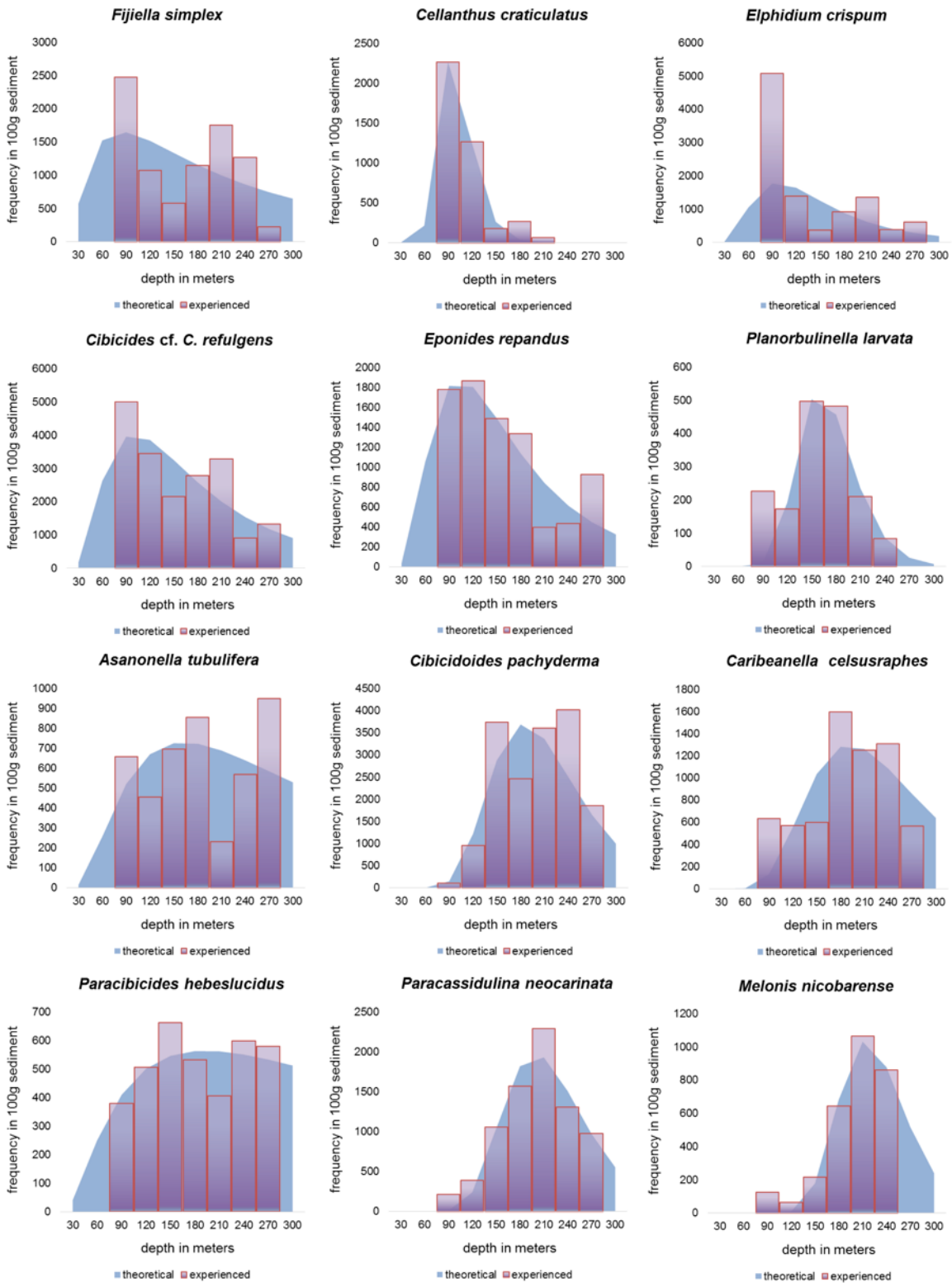


Figure 6.4a Experienced depth distributions (column) fitted by power transformed normal distributions. Abundances of hyaline foraminifera are shown in frequency distributions

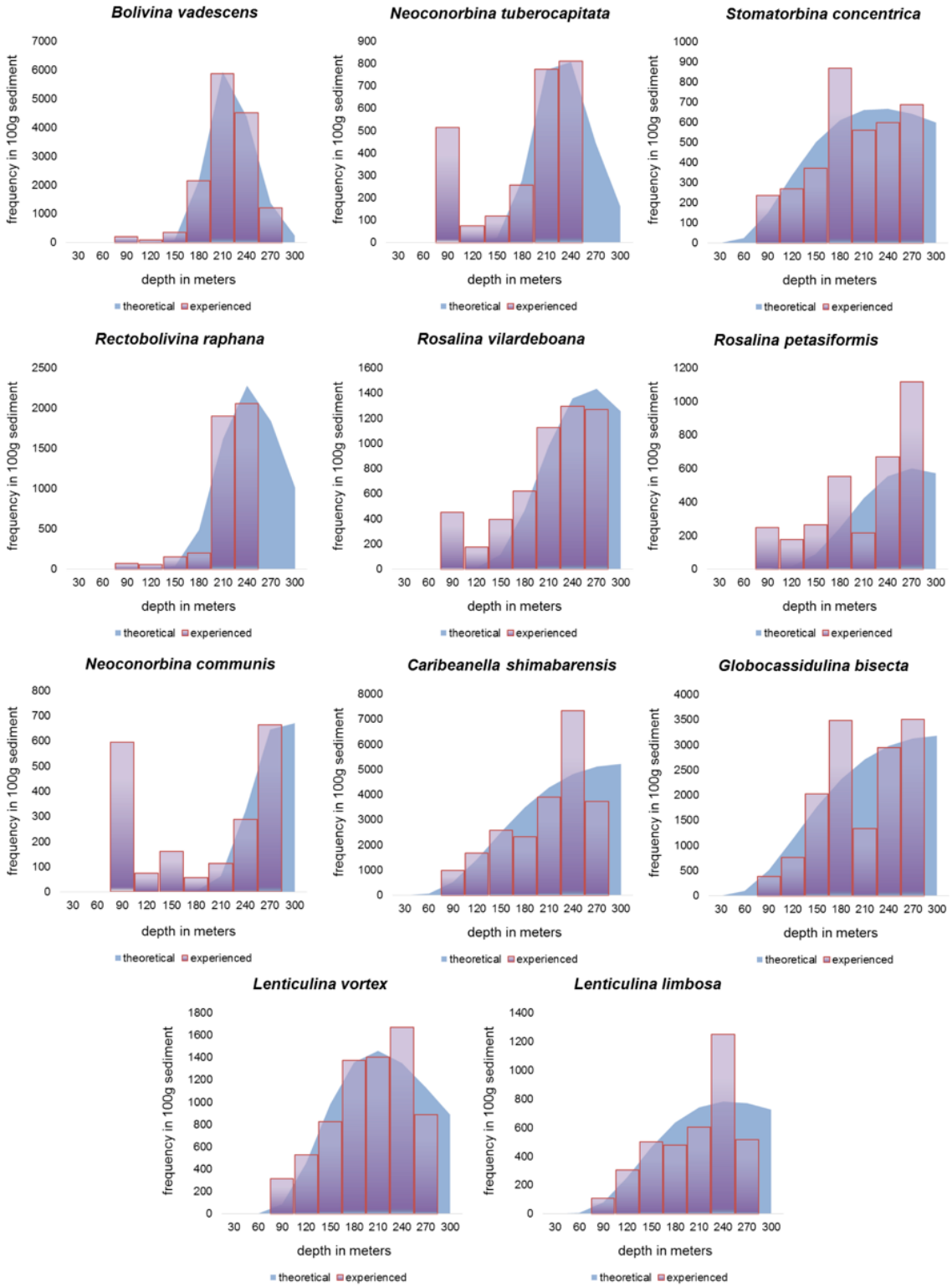


Figure 6.4b Experienced depth distributions (column) fitted by power transformed normal distributions. Abundances of hyaline foraminifera are shown in frequency distributions

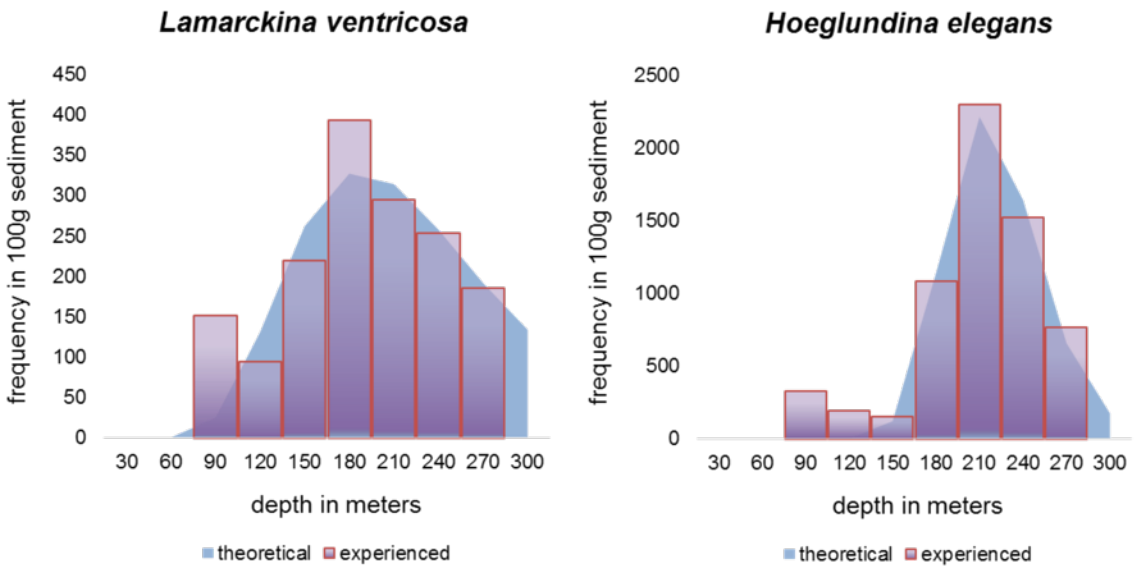


Figure 6.5 Experienced depth distributions (column) fitted by power transformed normal distributions. Abundances of aragonite foraminifera are shown in frequency distributions

### 6.2.2 Distribution in grain size

Correspondence analysis of smaller benthic foraminiferal distribution in grain size classes show five distinct groups (Figure 6.6 and Table 6.4). Each group corresponds to a grain size class. The grain size classes are coarse sand, medium sand, fine sand and very fine sand. One remaining group of species does not correspond to a specific grain size class.

Circle graphs representing distributions in coarse sand are located between values of 0.6 and 1.0 along axis 1. Species distributed in coarse sand are *Elphidium crispum, Caribeanella celsusraphes, Stomatorbina concentrica, Planorbulinella larvata, Textularia neorugosa* and *T. crenata*. Circle graphs that are located along axis 1 between values of 0 and 0.4 and axis 2 between values of 0.4 and -0.5 represent species with distributions in medium sand class. Species are *Pyrgo sarsi, Miliolinella circularis, Asanonella tubulifera* and *Textularia foliacea*. Distributions in fine sand class are located along axis 1 between values of 0 and -0.6 and axis 2 between values of 0 and -0.7. Species corresponding to fine sand class are *Cellanthus craticulatus* and *Spirotextularia fistulosa*. Smaller benthic foraminiferal species showing distributions in very fine sand class are located along axis 1 between values of 0 and -1.2 and axis 2 between values of 0 and -0.5. The species are *Quinqueloculina seminulum, Q. venusta, Spiroloculina manifesta, Lenticulina limbosa, Triloculina affinis, Textularia agglutinans, Spirotextularia floridana, Melonis nicobarense, Cibicidoides pachyderma, Paracassidulina neocarinata, Hoeglundina elegans, Caribeanella shimabarensis, Spirosigmoilina speciosa, Rosalina vilardeboana, Neoconorbina tuberocapitata, Fijella simplex, Bolivina vadescens* and *Rectobolivina raphana*. Species that do not show any correspondence to a specific grain size class are *Lenticulina vortex, Lamarckina ventricosa, M. subrotunda, M.* cf. *M. chiastocytis, Pseudogaudryina atlanta pacifica, Eponides repandus, Globocassidulina bisecta, Q. lamarckiana, Q. bicarinata, Paracibicides hebeslucidus, Cibicides* cf. *C. refulgens, Triloculina tricarinata, Rosalina petasiformis, Pyrgo denticulata* and *N. communis.*

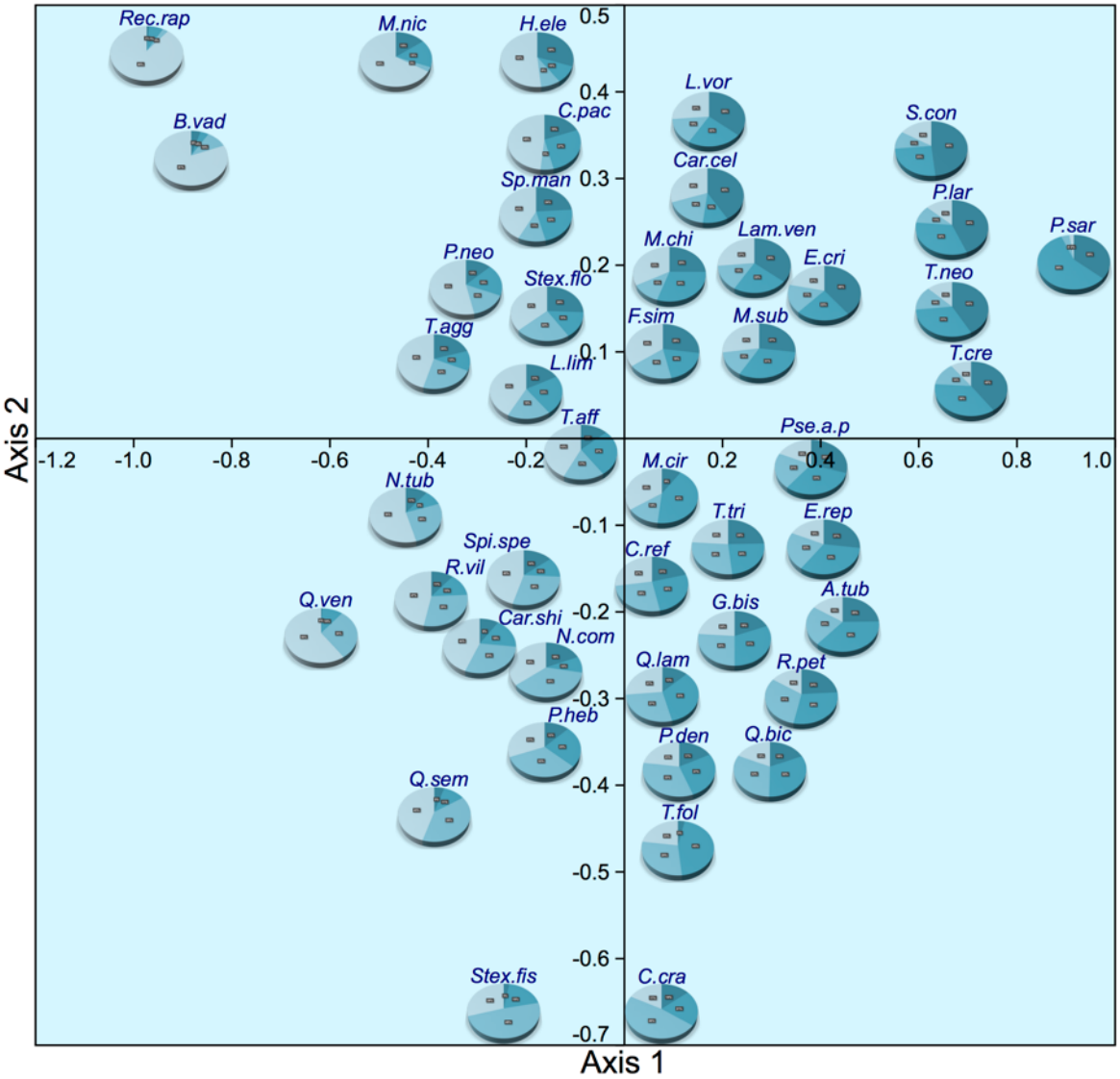


Figure 6.6 Ordination of correspondence analysis showing the distributions of smaller benthic foraminifera in grain size classes. Acronyms representing the species names are in brackets *Cellanthus craticulatus (C.cra)*, *Elphidium crispum (E.cri)*, *Cibicides* cf. *C. refulgens (C.ref)*, *Caribeanella celsusraphes (Car.cel)*, *Triloculina affinis (T.aff)*, *Fijella simplex (F.sim)*, *Textularia agglutinans (T.agg)*, *Neoconorbina communis (N.com)*, *Spirosigmoilina speciosa (Spi.spe)*, *Quinqueloculina seminulum (Q.sem)*, *Pyrgo sarsi (P.sar)*, *Planorbulinella larvata (P.lar)*, *Stomatorbina concentrica (S.con)*, *Textularia foliacea (T.fol)*, *Asanonella tubulifera (A.tub)*, *Quinqueloculina lamarckiana (Q.lam)*, *Lamarckina ventricosa (Lam.ven)*, *Miliolinella subrotunda (M.sub)*, *Textularia crenata (T.cre)*, *Pseudogaudryina atlanta pacifica (Pse.a.p)*, *Quinqueloculina bicarinata (Q.bic)*, *Eponides repandus (E.rep)*, *Paracibicides hebeslucidus (P.heb)*, *Triloculina tricarinata (T.tri)*, *Textularia neorugosa (T.neo), Spirotextularia fistulosa (Stex.fis)*, *Cibicidoides pachyderma (C.pac)*, *Rosalina petasiformis (R.pet)*, *Globocassidulina bisecta (G.bis)*, *Miliolinella circularis (M.cir)*, *Pyrgo denticulata (P.den)*, *Miliolinella* cf. *M. chiastocytis (M.chi)*, *Lenticulina vortex (L.vor)*, *Lenticulina limbosa (L.lim)*, *Spiroloculina manifesta (Sp.man)*, *Caribeanella shimabarensis (Car.shi)*, *Bolivina vadescens (B.vad)*, *Rectobolivina raphana (Rec.rap)*, *Quinqueloculina venusta (Q.ven)*, *Neoconorbina tuberocapitata (N.tub)*, *Rosalina vilardeboana (R.vil)*, *Hoeglundina elegans (H.ele)*, *Melonis nicobarense (M.nic)*, *Spirotextularia floridana (Stex.flor)* and *Paracassidulina neocarinata (P.neo)*

| Grain size class | Species |
|---|---|
| **Coarse sand** | *Elphidium crispum*<br>*Stomatorbina concentrica*<br>*Planorbulinella larvata*<br>*Textularia neorugosa*<br>*Textularia crenata*<br>*Caribeanella celsusraphes* |
| **Medium sand** | *Pyrgo sarsi*<br>*Miliolinella circularis*<br>*Asanonella tubulifera*<br>*Textularia foliacea* |
| **Fine sand** | *Cellanthus craticulatus*<br>*Spirotextularia fistulosa* |
| **Very fine sand** | *Quinqueloculina seminulum*<br>*Bolivina vadescens*<br>*Cibicidoides pachyderma*<br>*Hoeglundina elegans*<br>*Lenticulina limbosa*<br>*Melonis nicobarense*<br>*Paracassidulina neocarinata*<br>*Rectobolivina raphana*<br>*Spiroloculina manifesta*<br>*Spirotextularia floridana*<br>*Textularia agglutinans*<br>*Triloculina affinis*<br>*Quinqueloculina venusta*<br>*Caribeanella shimabarensis*<br>*Spirosigmoilina speciosa*<br>*Rosalina vilardeboana*<br>*Neoconorbina tuberocapitata*<br>*Fijella simplex* |
| **No preference** | *Lamarckina ventricosa*<br>*Lenticulina vortex*<br>*Miliolinella subrotunda*<br>*Miliolinella* cf. *M. chiastocytis*<br>*Pseudogaudryina atlanta pacifica*<br>*Eponides repandus*<br>*Globocassidulina bisecta*<br>*Quinqueloculina lamarckiana*<br>*Quinqueloculina bicarinata*<br>*Paracibicides hebeslucidus*<br>*Cibicides* cf. *C. refulgens*<br>*Triloculina tricarinata*<br>*Rosalina petasiformis*<br>*Pyrgo denticulata*<br>*Neoconorbina communis* |

Table 6.4 Smaller benthic foraminiferal distributions in grain size classes derived from correspondence analysis

Distribution in grain size classes is investigated because depth distribution is influenced by substrate type. Results from the investigation are presented in circle graphs (Figures 6.7, 6.8, 6.9a, 6.9b and 6.10).

Abundant distributions of agglutinated foraminifera in grain size classes are demonstrated by *Spirotextularia floridana, S. fistulosa, Pseudogaudryina atlanta pacifica, Textularia foliacea, T. crenata, T. neorugosa* and *T. agglutinans* (Figure 6.7). Abundant distributions in the very fine sand class are shown by *S. floridana* (37% of the samples) and *T. agglutinans* (46% of the samples). Abundant distribution in the fine sand class is represented by *S. fistulosa* (49% of the samples). In the medium sand class, abundant distribution is demonstrated by *T. foliacea* (45% of the samples). No abundant distribution in any grain size classes is demonstrated by *Pseudogaudryina atlanta pacifica.* Abundant distributions in the coarse sand class are demonstrated by *T. crenata* (40% of the samples) and *T. neorugosa* (42% of the samples).

Distributions of porcelaneous foraminifera in grain size classes are represented by 13 species (Figure 6.8). Most of the species, i.e., *Triloculina tricarinata, Miliolinella subrotunda, M.* cf. *M. chiastocytis, Quinqueloculina bicarinata, Q. lamarckiana* and *Pyrgo denticulata* do not show abundant distributions in any grain size classes. Distributions in the medium sand class are demonstrated by *M. circularis* (42% of the samples) and *P. sarsi* (58% of the samples). The remaining five porcelaneous species demonstrate abundant distributions in the very fine sand class, i.e., *T. affinis* (43% of the samples)*, Q. seminulum* (45% of the samples)*, Q. venusta* (60% of the samples)*, Spirosigmoilina speciosa* (45% of the samples) and *Spiroloculina manifesta* (43% of the samples).

Distributions of hyaline foraminifera in grain size classes are represented by 23 species (Figures 6.9a and 6.9b). Abundant distributions in the coarse sand class are demonstrated by *Elphidium crispum* (40% of the samples)*, Caribeanella celsusraphes* (42% of the samples)*, Stomatorbina concentrica* (48% of the samples) and *Planorbulinella larvata* (44% of the samples). The only species demonstrating abundant distribution in the medium sand class is *Asanonella tubulifera,* with 36% of the samples. Many of the hyaline species show abundant distributions in the very fine sand class, i.e., *Cibicidoides pachyderma* (49% of the samples)*, Paracassidulina neocarinata* (53% of the samples)*, Melonis nicobarense* (66% of the samples)*, Bolivina vadescens* (81% of the samples)*, Neoconorbina tuberocapitata* (54% of the samples)*, Rectobolivina raphana* (89% of the samples)*, Rosalina vilardeboana* (47% of the samples)*, Caribeanella shimabarensis* (44% of the samples)*, Lenticulina limbosa* (42% of the samples) and *Fijella simplex* (35% of the samples). Only *Cellanthus craticulatus* shows abundant distribution in the fine sand class, with 48% of the samples. Most of the species also do not show abundant distributions in any grain size classes. Hyaline foraminifera that do not demonstrate abundant distributions in grain size classes are *Cibicides* cf. *C. refulgens, Eponides repandus, Paracibicides hebeslucidus, Rosalina petasiformis, Neoconorbina communis, Globocassidulina bisecta* and *Lenticulina vortex*.

Aragonite foraminifera showing distributions in grain size classes are demonstrated by *Lamarckina ventricosa* and *Hoeglundina elegans* (Figure 6.10). *L. ventricosa* does not show any abundant distribution in the grain size classes. *H. elegans* demonstrates abundant distribution in the very fine sand class, with 52% of the samples.

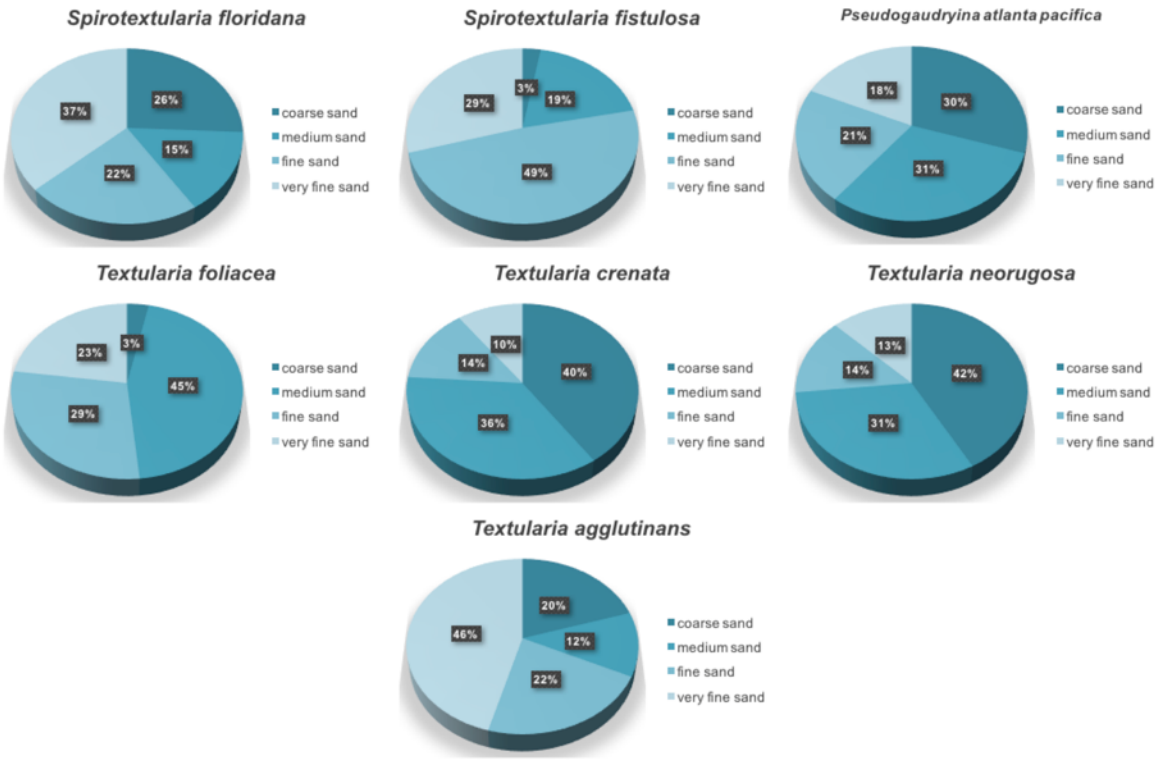


Figure 6.7 Distributions of agglutinated foraminifera in grain size classes

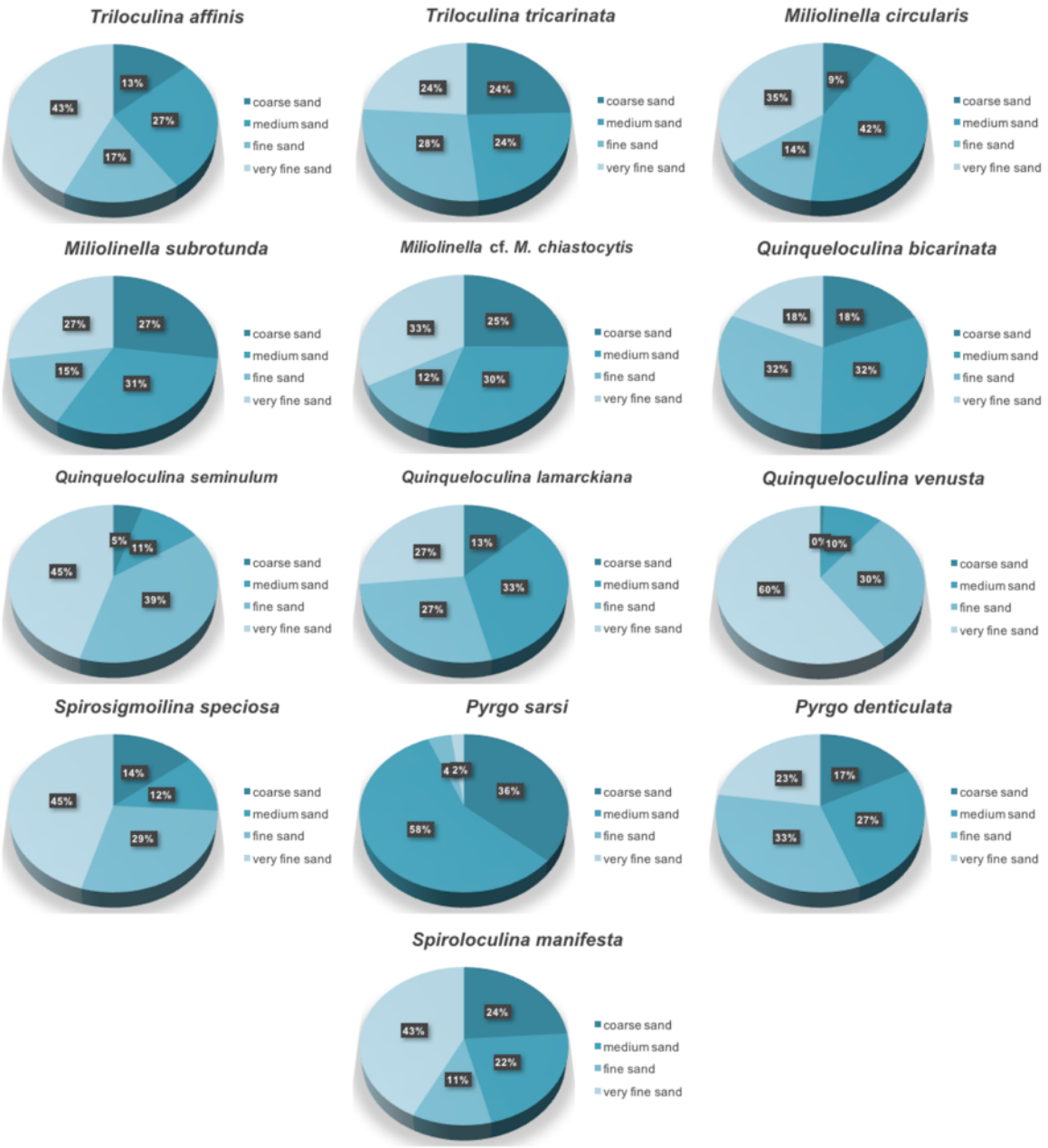


Figure 6.8 Distributions of porcelaneous foraminifera in grain size classes

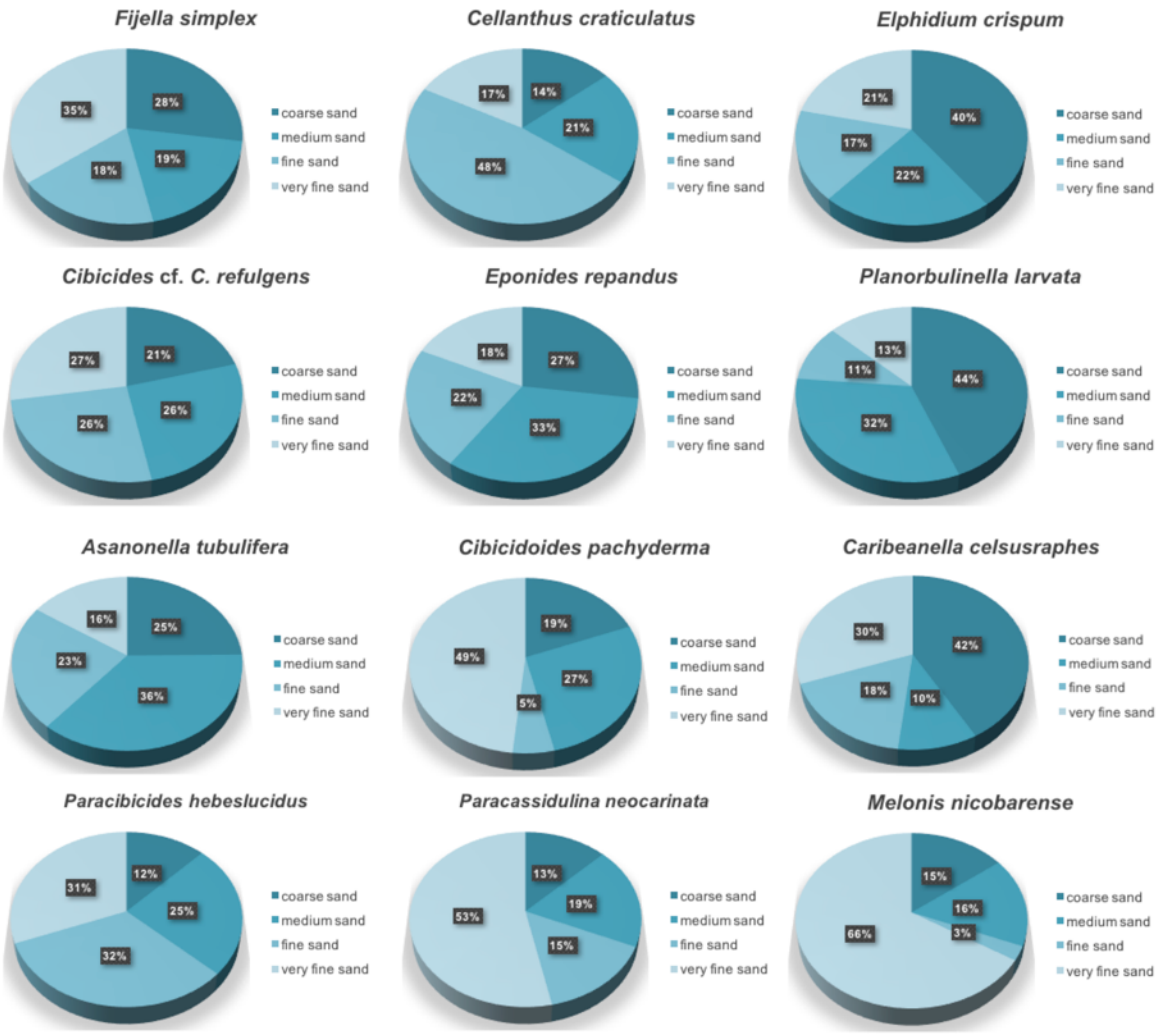


Figure 6.9a Distributions of hyaline foraminifera in grain size classes

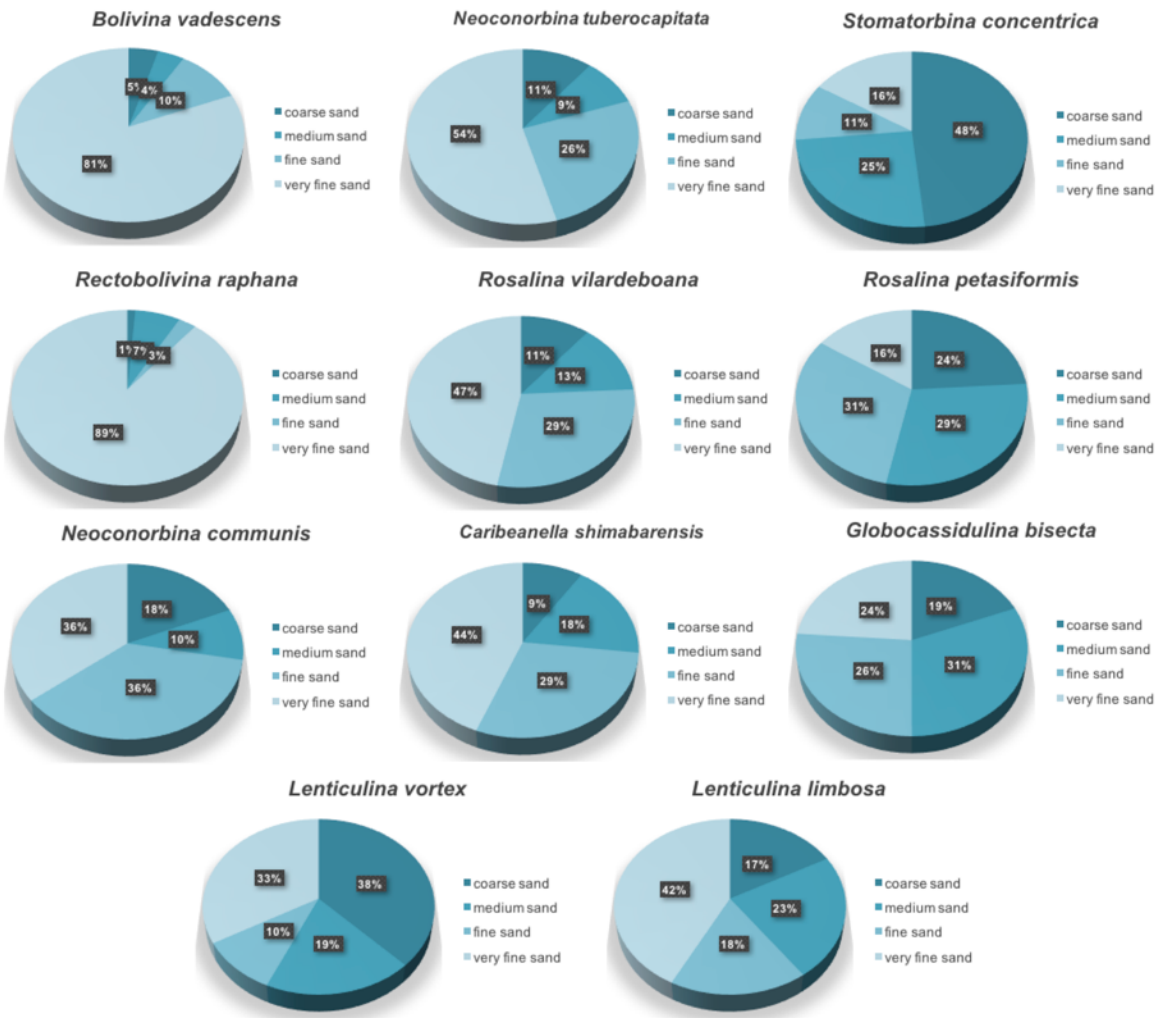


Figure 6.9b Distributions of hyaline foraminifera in grain size classes

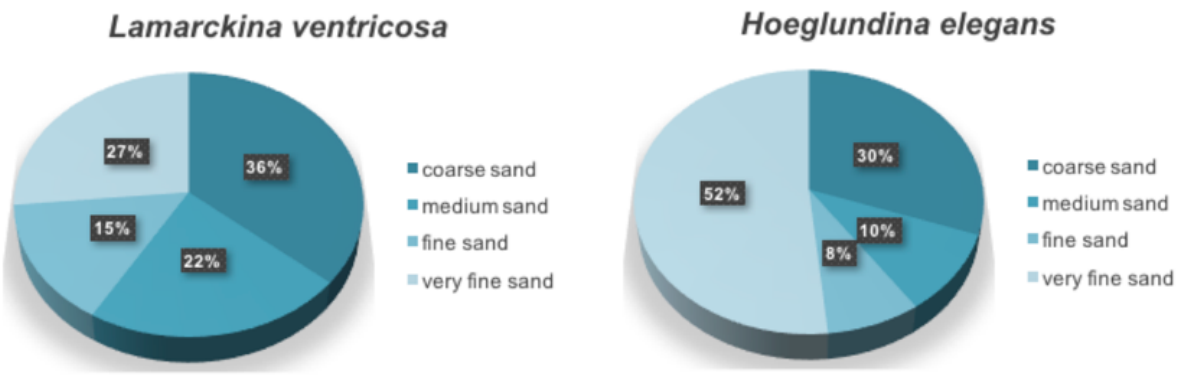


Figure 6.10 Distributions of aragonite foraminifera in grain size classes

### 6.2.3 Distribution in percentages of silt and clay

Correspondence analysis of smaller benthic foraminiferal distribution in the percentages of silt and clay shows six groups (Figure 6.11 and Table 6.5). Each group corresponds to highest percentages, high percentages, lowest percentages, low percentages, medium percentages and no abundant distributions. The group showing correspondence to highest and high percentages of silt and clay is located between values of -1.2 and -0.2 on axis 1 and between values of 0.6 and -0.6 on axis 2. Species that are located in this region are *Fijella simplex, Bolivina vadescens, Cibicidoides pachyderma, Lenticulina limbosa, Melonis nicobarense, Paracassidulina neocarinata, Rectobolivina raphana, Spiroloculina manifesta, Spirotextularia floridana, Triloculina affinis, Caribeanella shimabarensis, Quinqueloculina venusta, Q. seminulum, Textularia agglutinans, Neoconorbina tuberocapitata, Hoeglundina elegans, Rosalina vilardeboana* and *Spirosigmoilina speciosa*.

Smaller benthic foraminiferal species corresponding to medium percentages of silt and clay is located between the values of 0 and 0.4 on axis 1 and between values of 0.5 and -0.7 on axis 2. Species located in this region is *Pyrgo denticulata.* Species that show correspondences to low and lowest percentages of silt and clay are located between the values of 0.4 and 1.0 on axis 1 and between values of 0.6 and -0.7 on axis 2. These species are *Planorbulinella larvata, Quinqueloculina bicarinata, Cellanthus craticulatus, Textularia crenata, T. neorugosa* and *Pyrgo sarsi*.

Species that do not show any correspondence to percentages of silt and clay are *Asanonella tubulifera, Textularia foliacea, Stomatorbina concentrica, C. celsusraphes, Miliolinella circularis, Elphidium crispum, Lenticulina vortex, Lamarckina ventricosa, Spirotextularia fistulosa, Miliolinella subrotunda, M.* cf. *M. chiastocytis, Pseudogaudryina atlanta pacifica, Eponides repandus, Globocassidulina bisecta, Q. lamarckiana, Paracibicides hebeslucidus, Cibicides* cf. *C. refulgens, Triloculina tricarinata, Rosalina petasiformis* and *N. communis.*

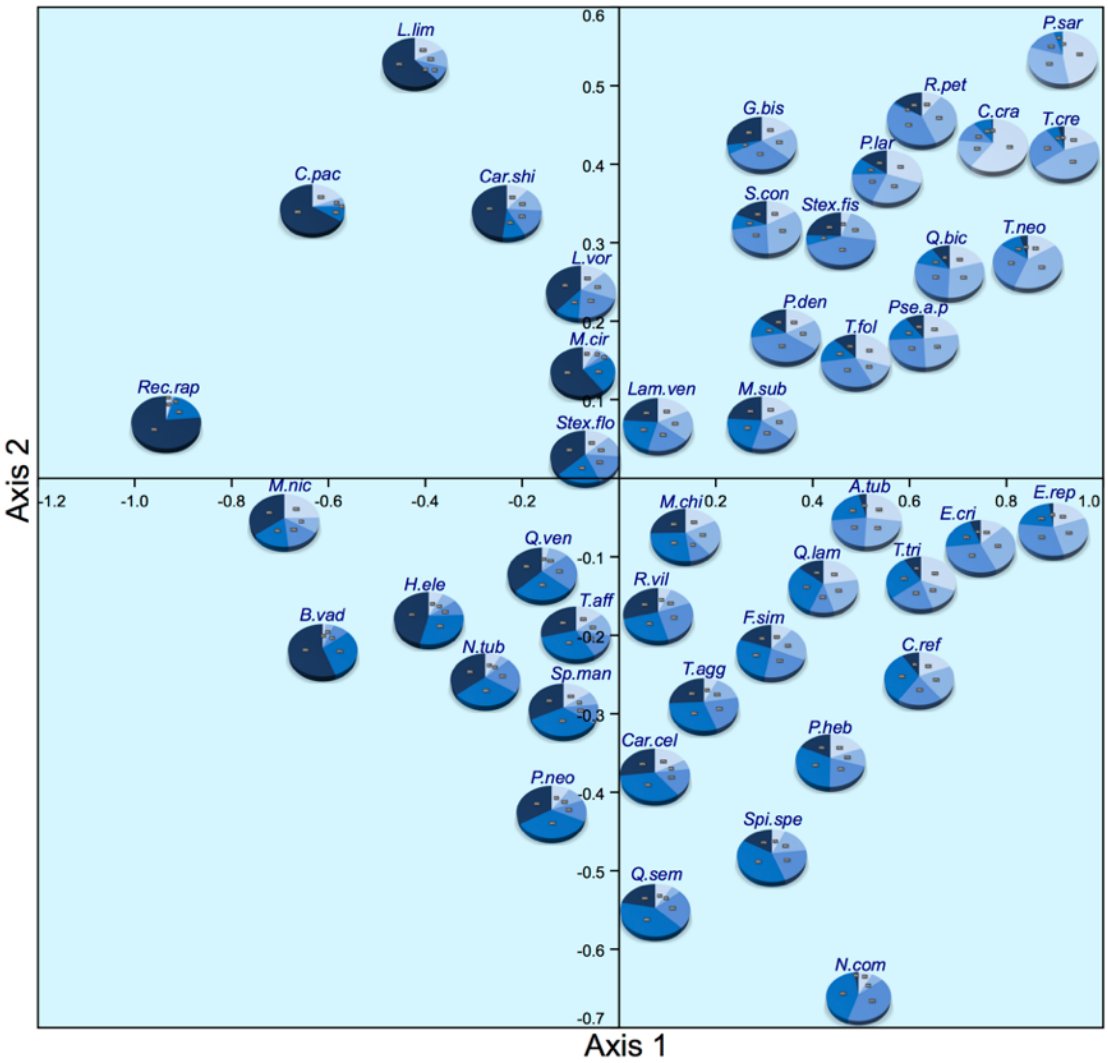


Figure 6.11 Ordination of correspondence analysis showing the distributions of smaller benthic foraminifera in percentages of silt and clay. Acronyms representing the species names are in brackets *Cellanthus craticulatus (C.cra)*, *Elphidium crispum (E.cri)*, *Cibicides* cf. *C. refulgens (C.ref)*, *Caribeanella celsusraphes (Car.cel)*, *Triloculina affinis (T.aff)*, *Fijella simplex (F.sim)*, *Textularia agglutinans (T.agg)*, *Neoconorbina communis (N.com)*, *Spirosigmoilina speciosa (Spi.spe)*, *Quinqueloculina seminulum (Q.sem)*, *Pyrgo sarsi (P.sar)*, *Planorbulinella larvata (P.lar)*, *Stomatorbina concentrica (S.con)*, *Textularia foliacea (T.fol)*, *Asanonella tubulifera (A.tub)*, *Quinqueloculina lamarckiana (Q.lam)*, *Lamarckina ventricosa (Lam.ven)*, *Miliolinella subrotunda (M.sub)*, *Textularia crenata (T.cre)*, *Pseudogaudryina atlanta pacifica (Pse.a.p)*, *Quinqueloculina bicarinata (Q.bic)*, *Eponides repandus (E.rep)*, *Paracibicides hebeslucidus (P.heb)*, *Triloculina tricarinata (T.tri)*, *Textularia neorugosa (T.neo), Spirotextularia fistulosa (Stex.fis)*, *Cibicidoides pachyderma (C.pac)*, *Rosalina petasiformis (R.pet)*, *Globocassidulina bisecta (G.bis)*, *Miliolinella circularis (M.cir)*, *Pyrgo denticulata (P.den)*, *Miliolinella* cf. *M. chiastocytis (M.chi)*, *Lenticulina vortex (L.vor)*, *Lenticulina limbosa (L.lim)*, *Spiroloculina manifesta (Sp.man)*, *Caribeanella shimabarensis (Car.shi)*, *Bolivina vadescens (B.vad)*, *Rectobolivina raphana (Rec.rap)*, *Quinqueloculina venusta (Q.ven)*, *Neoconorbina tuberocapitata (N.tub)*, *Rosalina vilardeboana (R.vil)*, *Hoeglundina elegans (H.ele)*, *Melonis nicobarense (M.nic)*, *Spirotextularia floridana (Stex.flor)* and *Paracassidulina neocarinata (P.neo)*

| Percentages of silt and clay | Species |
|---|---|
| **Low percentages** | *Quinqueloculina bicarinata*<br>*Textularia neorugosa*<br>*Textularia crenata* |
| **Lowest percentages** | *Planorbulinella larvata*<br>*Pyrgo sarsi*<br>*Cellanthus craticulatus* |
| **Medium percentages** | *Pyrgo denticulata* |
| **High percentages** | *Fijella simplex*<br>*Spiroloculina manifesta*<br>*Triloculina affinis*<br>*Quinqueloculina seminulum*<br>*Textularia agglutinans*<br>*Spirosigmoilina speciosa* |
| **Highest percentages** | *Rosalina vilardeboana*<br>*Bolivina vadescens*<br>*Cibicidoides pachyderma*<br>*Hoeglundina elegans*<br>*Lenticulina limbosa*<br>*Spirotextularia floridana*<br>*Melonis nicobarense*<br>*Paracassidulina neocarinata*<br>*Rectobolivina raphana*<br>*Caribeanella shimabarensis*<br>*Quinqueloculina venusta*<br>*Neoconorbina tuberocapitata* |
| **No dominance** | *Neoconorbina communis*<br>*Asanonella tubulifera*<br>*Rosalina petasiformis*<br>*Lamarckina ventricosa*<br>*Globocassidulina bisecta*<br>*Miliolinella subrotunda*<br>*Stomatorbina concentrica*<br>*Quinqueloculina lamarckiana*<br>*Cibicides* cf. *C. refulgens*<br>*Triloculina tricarinata*<br>*Elphidium crispum*<br>*Eponides repandus*<br>*Spirotextularia fistulosa*<br>*Pseudogaudryina atlanta pacifica*<br>*Textularia foliacea*<br>*Lenticulina vortex*<br>*Miliolinella circularis*<br>*Caribeanella celsusraphes*<br>*Miliolinella* cf. *M. chiastocytis*<br>*Paracibicides hebeslucidus* |

Table 6.5 Smaller benthic foraminiferal distributions in percentages of silt and clay derived from correspondence analysis

Distribution in percentages of silt and clay gives account into the life position of optimally preserved smaller benthic foraminifera. Results from the investigation are presented in circle graphs (Figures 6.12, 6.13, 6.14a, 6.14b and 6.15).

Abundant distributions of agglutinated foraminifera in percentages of silt and clay are demonstrated by *Spirotextularia floridana, S. fistulosa, Pseudogaudryina atlanta pacifica, Textularia foliacea, T. crenata, T. neorugosa* and *T. agglutinans* (Figure 6.12). Abundant distribution in the highest percentages of silt and clay is shown by *S. floridana* (38% of the samples). Abundant distribution in the high percentages of silt and clay is shown by *T. agglutinans* (30% of the samples). Abundant distribution in the medium percentages of silt and clay is represented by *S. fistulosa* (42% of the samples). In the low percentages of silt and clay, abundant distributions are demonstrated by *T. crenata* (45% of the samples) and *T. neorugosa* (40% of the samples). No abundant distribution in any percentages of silt and clay is demonstrated by *Pseudogaudryina atlanta pacifica* and *T. foliacea*.

Distributions of porcelaneous foraminifera in percentages of silt and clay are represented by 13 species (Figure 6.13). Abundant distributions in the high percentages of silt and clay are demonstrated by *Q. seminulum* (40% of the samples), *Spiroloculina manifesta* (33% of the samples), *Spirosigmoilina speciosa* (39% of the samples) and *Triloculina affinis* (29% of the samples). Abundant distribution in the highest percentages of silt and clay is demonstrated by *Q. venusta* (38% of the samples). Abundant distribution in medium percentages of silt and clay is demonstrated by *Pyrgo denticulata* (37% of the samples). Abundant distribution in low percentages of silt and clay are demonstrated by *Q. bicarinata*, with 30% of the samples. Abundant distribution in the lowest percentages of silt and clay is demonstrated by *Pyrgo sarsi* (47% of the samples). The remaining porcelaneous species, i.e., *Miliolinella subrotunda, M.* cf. *M. chiastocytis, M. circularis, T. tricarinata* and *Q. lamarckiana* do not show abundant distributions in percentages of silt and clay.

Distributions of hyaline foraminifera in percentages of silt and clay are represented by 23 species (Figures 6.14a and 6.14b). Abundant distributions in the highest percentages of silt and clay are demonstrated by *Cibicidoides pachyderma* (65% of the samples), *Paracassidulina neocarinata* (34% of the samples) and *Melonis nicobarense,* with 60% of the samples (Figure 6.14a). Abundant distribution in high percentages of silt and clay is demonstrated by *Fijella simplex*, with 28% of the samples. Abundant distributions in the lowest percentages of silt and clay are shown by *Cellanthus craticulatus* (60% of the samples) and *Planorbulinella larvata* (30% of the samples). There are no abundant distributions in percentages of silt and clay as demonstrated by *Elphidium crispum, Cibicides* cf. *C. refulgens, Eponides repandus, Asanonella tubulifera, Caribeanella celsusraphes* and *Paracibicides hebeslucidus* (Figure 6.14a).

Most of the hyaline species in figure 6.14b demonstrate high abundances in highest percentages of silt and clay. Such distributions are shown by *Bolivina vadescens* (55% of the samples), *Neoconorbina tuberocapitata* (36% of the samples), *Rectobolivina raphana* (76% of the samples), *Rosalina vilardeboana* (30% of the samples), *Caribeanella shimabarensis* (48% of the samples) and *Lenticulina limbosa* (61% of the samples). *Stomatorbina concentrica, Rosalina petasiformis, L. vortex*, *Neoconorbina communis* and *Globocassidulina bisecta* do not demonstrate abundant distributions in any percentages of silt and clay.

Aragonite foraminifera showing distributions in percentages of silt and clay are demonstrated by *Lamarckina ventricosa* and *Hoeglundina elegans* (Figure 6.15). *L. ventricosa* does not show any abundant distribution in the percentages of silt and clay. *H. elegans* demonstrates abundant distribution in the highest percentages of silt and clay, with 46% of the samples.

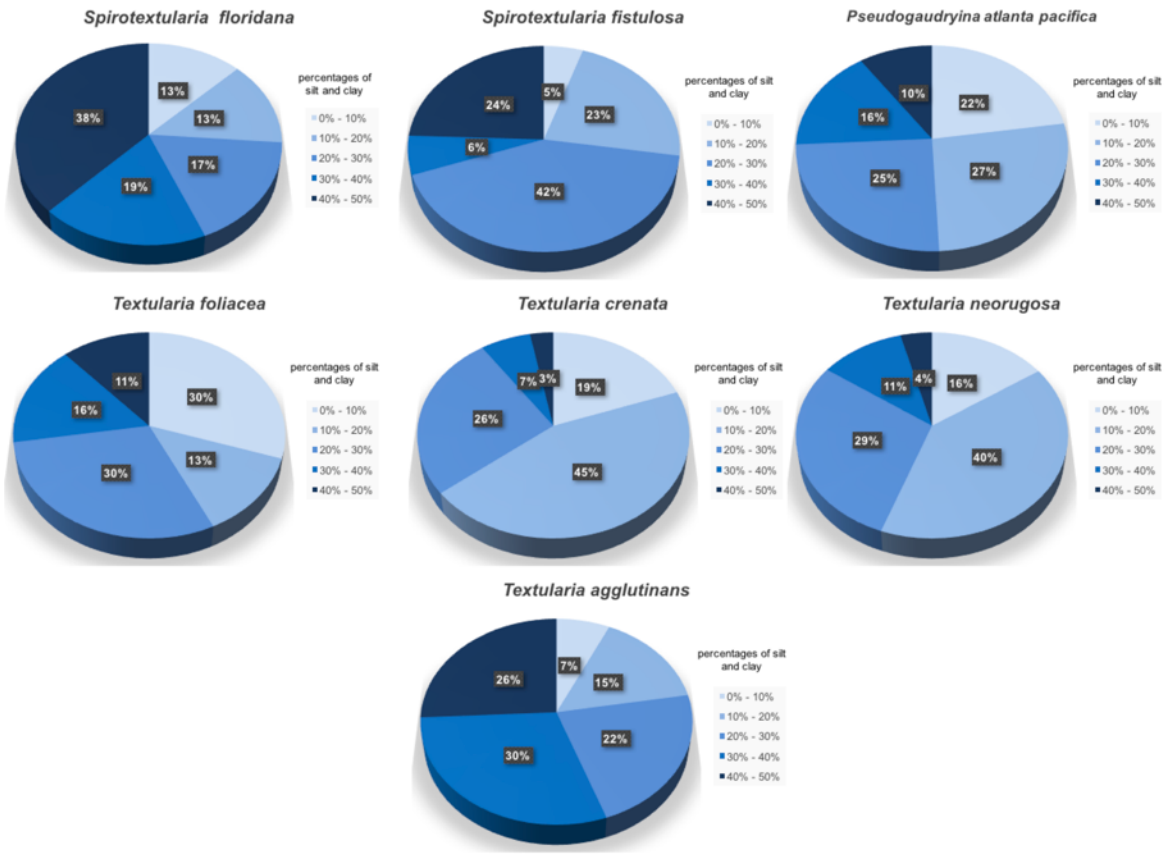


Figure 6.12 Distributions of agglutinated foraminifera in percentages of silt and clay

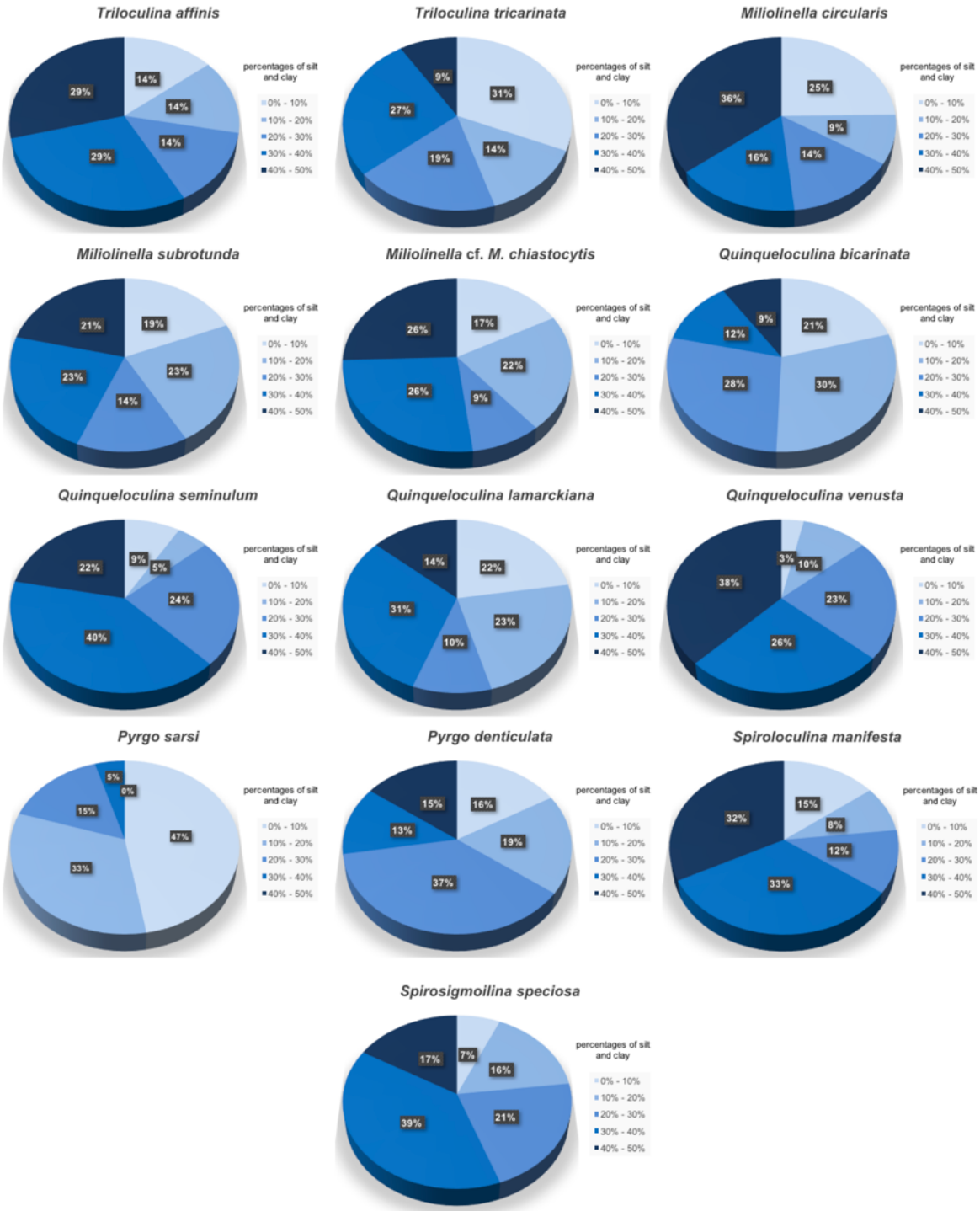


Figure 6.13 Distributions of porcelaneous foraminifera in percentages of silt and clay

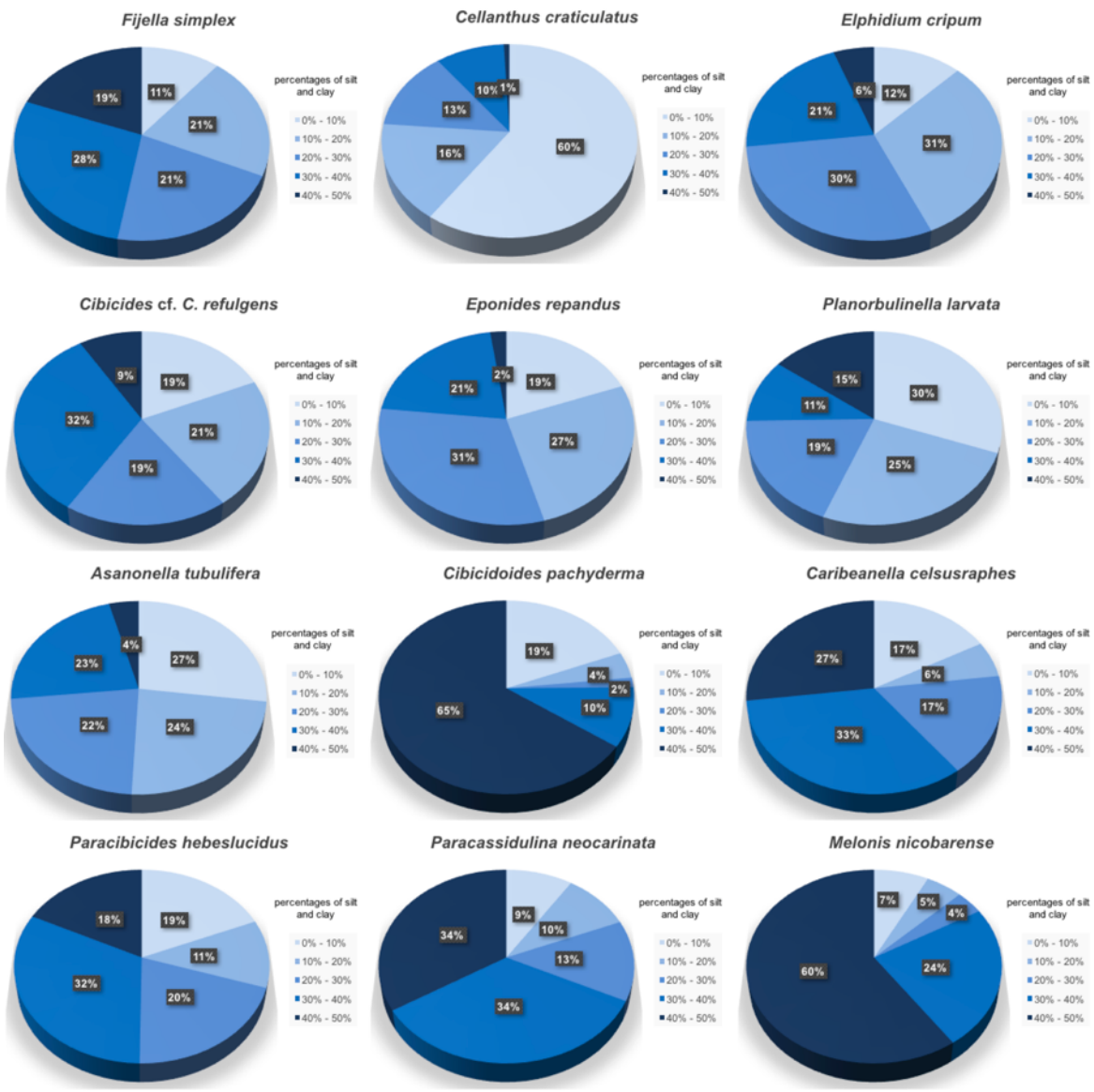


Figure 6.14a Distributions of hyaline foraminifera in percentages of silt and clay

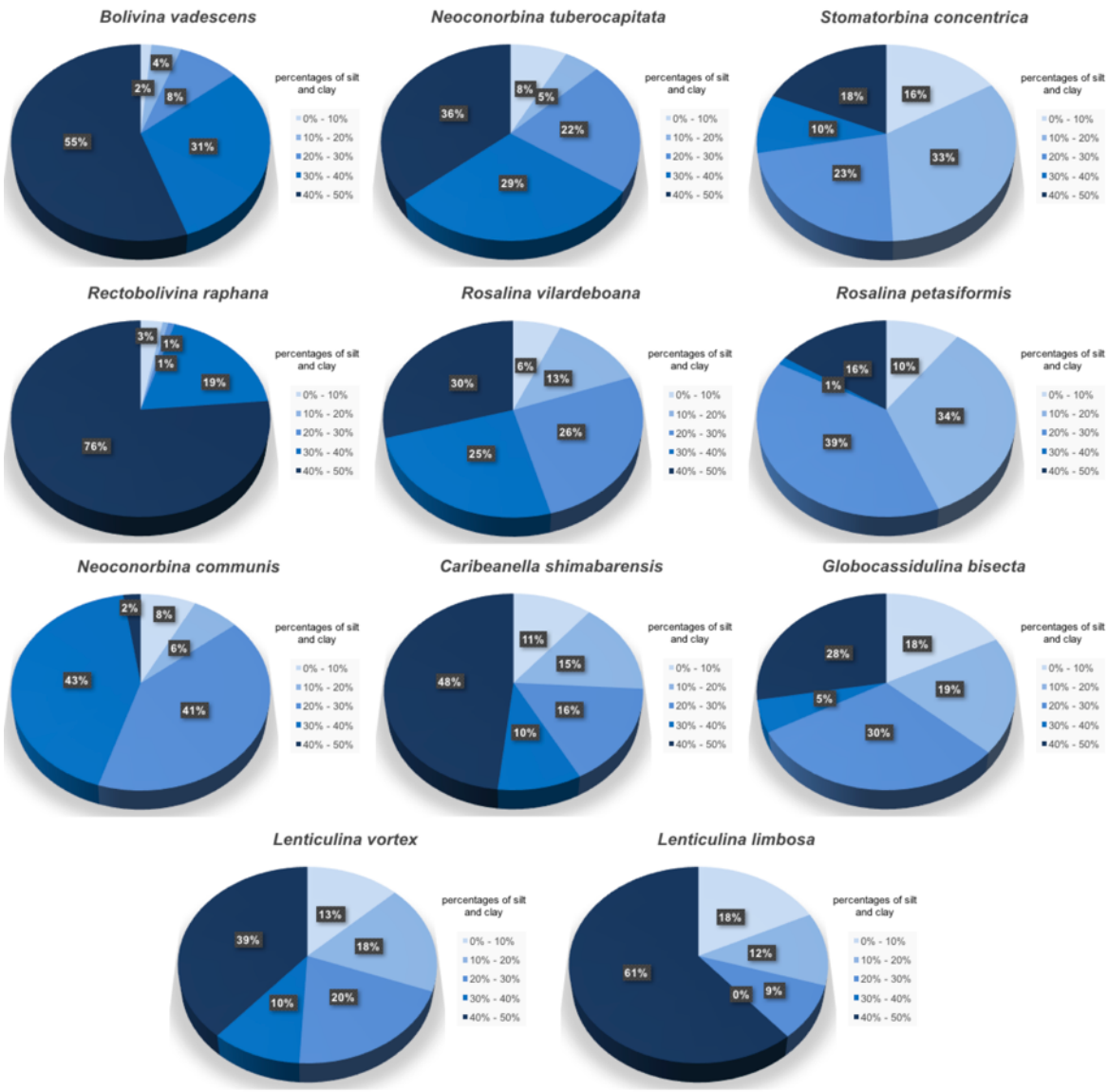


Figure 6.14b Distributions of hyaline foraminifera in percentages of silt and clay

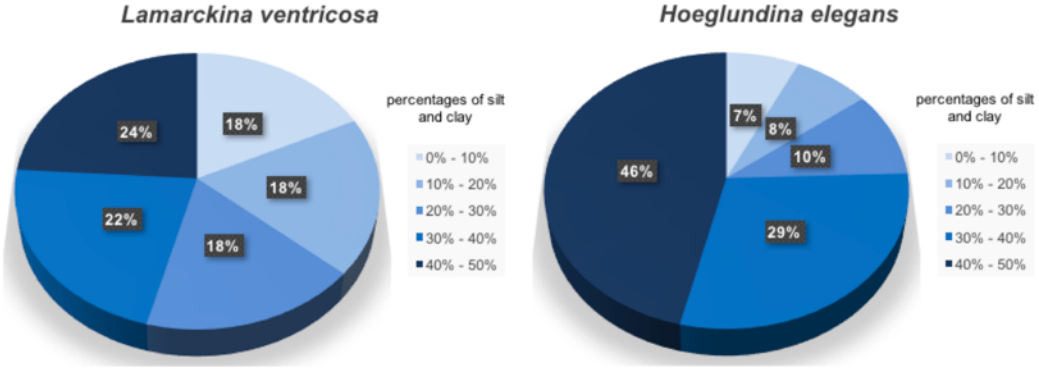


Figure 6.15 Distributions of aragonite foraminifera in percentages of silt and clay

## 6.3 Discussion

### 6.3.1 Agglutinated foraminifera

*Spirotextularia floridana* (Plate 1, Fig. 7a-b.) is distributed from the mid sublittoral to uppermost bathyal. Optimal depth distribution is located in the uppermost bathyal at 230m (Figure 6.2, Table 6.3). Highest abundance is shown in very fine sand, with 37% of the samples distributed in this grain size class (Table 6.4, Figure 6.7). Distribution in silt and clay demonstrates highest abundance (38% of the samples) in the highest percentages of silt and clay of 40-50% (Table 6.5, Figure 6.12). The decrease in sample proportions is continuous with decreasing silt and clay percentages thus indicating no dominance is shown in other percentages classes. This dependence on very fine sand substrate is in agreement with the dominance in highest percentages of silt and clay. It reflects on the preference to infaunal life position of *S. floridana*.

*Spirotextularia fistulosa* (Plate 1, Fig. 8a-b) is distributed from the mid sublittoral to uppermost bathyal. Optimal depth distribution is located in the uppermost bathyal at 260m (Figure 6.2, Table 6.3). Highest abundance is shown in fine sand, with 49% of the samples distributed in this grain size class (Table 6.4, Figure 6.7). Distribution in silt and clay demonstrates highest abundance (42% of the samples) in the medium percentages of silt and clay of 20-30% (Table 6.5, Figure 6.12). 24% of the samples is distributed in the 40-50% class (highest percentages) and 23% in the 10-20% class (low percentages) thus indicating no dominance in these classes. Dominance in medium percentages of silt and clay is not in agreement with the dependence on fine sand substrate of *S. fistulosa*. Dominance in medium percentages of silt and clay reflects on preference to either epifaunal or infaunal life position of *S. fistulosa*.

*Pseudogaudryina atlanta pacifica* (Plate 2, Fig. 3a-b) is distributed from the mid sublittoral to uppermost bathyal with an optimum at 96m in the mid sublittoral (Figure 6.2, Table 6.3). Distribution in grain size classes does not show preference on substrate type due to 31% of the samples is distributed in medium sand and 30% in coarse sand (Table 6.4, Figure 6.7). Distribution in silt and clay does not demonstrate any high abundance in percentages classes (Table 6.5, Figure 6.12). 22% of the samples is distributed in the 0-10% class (lowest percentages), 25% in the 20-30% class (medium percentages), 10% in the 40-50% class (highest percentages) thus indicating no dominance. No dependence on substrate type and no dominance in percentages of silt and clay demonstrates preference to either epifaunal or infaunal life position of *P. atlanta pacifica*.

*Textularia foliacea* (Plate 3, Fig. 6a-b) is distributed from the mid sublittoral to uppermost bathyal with an optimum at 103m in the deeper sublittoral (Figure 6.2, Table 6.3). Highest abundance is shown in medium sand, with 45% of the samples distributed in this grain size class (Table 6.4, Figure 6.7). Distribution in silt and clay does not demonstrate any high abundance in percentages classes (Table 6.5, Figure 6.12). 30% of the samples is distributed in the 0-10% class (lowest percentages), 30% in the 20-30% class (medium percentages) and 11% in 40-50% class (highest percentages) thus indicating no dominance. Dependence on medium sand substrate is in agreement with no dominance in percentages of silt and clay classes. Medium sandy substrate indicates unstable depositional environment (Kitazato 1994) thus it reflects on the preference to either epifaunal or infaunal life position of *T. foliacea*.

*Textularia crenata* (Plate 3, Fig. 2a-b, 3) is distributed from the mid sublittoral to uppermost bathyal with an optimum at 139m in the deeper sublittoral (Figure 6.2, Table 6.3). Highest abundance is shown in coarse sand, with 40% of the samples distributed in this grain size class (Table 6.4, Figure 6.7). Distribution in silt and clay demonstrates highest abundance (45% of the samples) in the low percentages class of 10-20% (Table 6.5, Figure 6.12). Proportion of samples decreases continuously with the increase of silt and clay percentages thus no dominance in other classes is detected. Dependence on coarse sand substrate is in agreement with the dominance in low percentages of silt and clay. Dominance in low percentages of silt and clay reflects on the preference to epifaunal life position of *T. crenata*.

*Textularia neorugosa* (Plate 3, Fig. 8a-c) is distributed from the mid sublittoral to uppermost bathyal with an optimum at 149m in the deeper sublittoral (Figure 6.2, Table 6.3). Highest abundance is shown in coarse sand, with 42% of the samples distributed in this grain size class (Table 6.4, Figure 6.7). Distribution in silt and clay demonstrates highest abundance (40% of the samples) in the low percentages class of 10-20% (Table 6.5, Figure 6.12). Proportion of samples decreases continuously with the increase of silt and clay percentages thus no dominance in other classes is detected. Dependence on coarse sand substrate is in agreement with the dominance in low percentages of silt and clay. Dominance in low percentages of silt and clay reflects on the preference to epifaunal life position of *T. neorugosa*.

*Textularia agglutinans* (Plate 2, Fig. 7a-c) is distributed from the mid sublittoral to uppermost bathyal. Optimal depth distribution is located at 202m of the uppermost bathyal (Figure 6.2, Table 6.3). Highest abundance is shown in very fine sand, with 46% of the samples distributed in this grain size class (Table 6.4, Figure 6.7). Distribution in silt and clay demonstrates highest abundances in the 40-50% and 30-40% classes (Table 6.5, Figure 6.12), with 26% of the samples in the highest percentages and 30% of the samples in the high percentages classes. Proportion of samples decreases continuously with the decrease of silt and clay percentages thus no dominance in other classes is detected. Dependence on very fine sand substrate is in agreement with the dominance in high percentages of silt and clay thus reflecting on the preference to infaunal life position of *T. agglutinans*.

### 6.3.2 Porcelaneous foraminifera

*Miliolinella circularis* (Plate 4, Fig. 12a-b) is distributed from the mid sublittoral to uppermost bathyal. Optimal depth distribution is located at 248m of the uppermost bathyal (Figure 6.3, Table 6.3). Highest abundance is shown in medium sand, with 42% of the samples distributed in this grain size class (Table 6.4, Figure 6.8). Distribution in silt and clay demonstrates highest abundance (36% of samples) in the highest percentages class of 40-50% (Table 6.5, Figure 6.13). The decrease in the proportion of samples is not continuous with decreasing silt and clay percentages where the second highest sample proportion of 25% is distributed in the lowest percentages class of 0-10%. This demonstrates another dominance in silt and clay percentages. Dependence on medium sand substrate is in agreement with no dominance in silt and clay percentages thus reflecting on the preference to either epifaunal or infaunal life position of *M. circularis*.

*Miliolinella subrotunda* (Plate 5, Fig. 1a-b) is distributed from the mid sublittoral to uppermost bathyal with an optimum at 160m in the deeper sublittoral (Figure 6.3, Table 6.3). Distribution in grain size classes does not show preference on substrate type due to 31% of the samples is distributed in medium sand and 27% in coarse sand (Table 6.4, Figure 6.8). Distribution in silt and clay does not demonstrate any high abundance in percentages classes (Table 6.5, Figure 6.13). 19% of the samples is distributed in the 0-10% class (lowest percentages), 14% in the 20-30% class (medium percentages), 21% in the 40-50% class (highest percentages) thus indicating no dominance in these classes. No dependence on substrate type and no dominance in percentages of silt and clay demonstrates preference to either epifaunal or infaunal life position of *M. subrotunda*.

*Miliolinella* cf. *M. chiastocytis* (Plate 4, Fig. 11a-c) is distributed from the mid sublittoral to uppermost bathyal with an optimum at 166m in the deeper sublittoral (Figure 6.3, Table 6.3). Distribution in grain size classes does not show preference on substrate type due to 33% of the samples is distributed in very fine sand and 30% in medium sand (Table 6.4, Figure 6.8). Distribution in silt and clay does not demonstrate any dominance in percentages classes (Table 6.5, Figure 6.13). Highest abundance (26% of the samples) is recorded in the highest percentages class of 40-50%. The decrease in the proportion of samples is not continuous with decreasing silt and clay percentages where the second highest sample proportion of 22% is distributed in the low percentages class of 10-20%. This demonstrates dominances in the highest and low percentages classes. No dependence on substrate type is in agreement with no dominance in silt and clay percentages thus reflecting on the preference of either epifaunal or infaunal life position of *M.* cf. *M. chiastocytis*.

*Triloculina affinis* (Plate 8, Fig. 1a-b) is distributed from the mid sublittoral to uppermost bathyal. Optimal depth distribution is located at 86m in the mid sublittoral (Figure 6.3, Table 6.3). Highest abundance is shown in very fine sand, with 43% of the samples distributed in this grain size class (Table 6.4, Figure 6.8). Distribution in silt and clay demonstrates highest abundances in the 40-50% and 30-40% classes (Table 6.5, Figure 6.13), with similar sample proportions of 29% dominating the highest and high percentages classes. Proportion of samples decreases continuously with the decrease of silt and clay percentages thus no dominance in other classes is detected. Dependence on very fine sand substrate is in agreement with the dominance in high percentages of silt and clay thus reflecting on the preference to infaunal life position of *T. affinis*.

*Triloculina tricarinata* (Plate 8, Fig. 5a-b) is distributed from the mid sublittoral to uppermost bathyal with an optimum at 109m in the deeper sublittoral (Figure 6.3, Table 6.3). Distribution in grain size classes does not show preference on substrate type due to 28% of the samples is distributed in fine sand and the remaining sample proportion is distributed equally in the other grain size classes, with 24% of sample in each class (Table 6.4, Figure 6.7). Distribution in silt and clay does not demonstrate any dominance in percentages classes (Table 6.5, Figure 6.13). Highest abudance (31% of the samples) is recorded in the lowest percentages class of 0-10%. The decrease in sample proportion is not continuous with the increasing silt and clay percentages where second highest abundance (27% of the samples) is recorded in the high percentages class of 30-40%. This demonstrates dominances in the high and lowest percentages classes. No dependence on substrate type is in agreement with no dominance in silt and clay percentages thus reflecting on the preference to either epifaunal or infaunal life position of *T. tricarinata*.

*Pyrgo sarsi* (Plate 5, Fig. 7a-b) is distributed from the mid sublittoral to uppermost bathyal. Optimal depth distribution is located in the uppermost bathyal at 239m (Figure 6.3, Table 6.3). Highest abundance is shown in medium sand, with 58% of the samples distributed in this grain size class (Table 6.4, Figure 6.8). Distribution in silt and clay demonstrates highest abundance (47% of the samples) in the lowest percentages of silt and clay of 0-10% (Table 6.5, Figure 6.13). Proportion of samples decreases continuously with the decrease of silt and clay percentages thus no dominance in other classes is detected. Dependence on medium sand substrate and dominance in lowest percentages of silt and clay reflects on the preference to epifaunal life position of *P. sarsi*.

*Pyrgo denticulata* (Plate 5, Fig. 6a-b) is distributed from the mid sublittoral to uppermost bathyal. Optimal depth distribution is located in the uppermost bathyal at 247m (Figure 6.3, Table 6.3). Distribution in grain size classes does not show preference on substrate type due to 33% of the samples is distributed in fine sand and 27% in medium sand (Table 6.4, Figure 6.8). Distribution in silt and clay demonstrates highest abundance (37% of the samples) in the medium percentages of silt and clay of 20-30% (Table 6.5, Figure 6.13). No dependence on substrate type and dominance in medium percentages of silt and clay reflects on the preference to either epifaunal or infaunal life position of *P. denticulata*.

*Quinqueloculina bicarinata* (Plate 6, Fig. 2a-b) is distributed from the mid sublittoral to uppermost bathyal. Optimal depth distribution is located in the mid sublittoral at 94m (Figure 6.3, Table 6.3). Distribution in grain size classes does not show preference on substrate type due to similar distributions of 32% of the samples in each medium and fine sand class (Table 6.4, Figure 6.8). Distribution in silt and clay demonstrates highest abundance (30% of the samples) in the low percentages of silt and clay of 10-20% (Table 6.5, Figure 6.13). Proportion of samples decreases continuously with the increasing percentages of silt and clay thus no dominance is detected in other classes. No dependence on substrate type and dominance in low percentages of silt and clay reflects on the preference to epifaunal life position of *Q. bicarinata*.

*Quinqueloculina lamarckiana* (Plate 6, Fig. 8a-c) is distributed from the mid sublittoral to uppermost bathyal with an optimum at 127m in the deeper sublittoral (Figure 6.3, Table 6.3). Distribution in grain size classes does not show preference on substrate type due to 33% of the samples is distributed in medium sand and the remaining sample proportion is distributed equally in the fine and very fine sand classes, with 27% of samples in each class (Table 6.4, Figure 6.7). Distribution in silt and clay does not demonstrate any dominance in percentages classes (Table 6.5, Figure 6.13). Highest abudance (31% of the samples) is recorded in the high percentages class of 30-40%. The decrease in sample proportion is not continuous with the decreasing silt and clay percentages where second highest abundance (23% of the samples) is recorded in the low percentages class of 10-20%. This demonstrates dominances in the high and low percentages classes. No dependence on substrate type is in agreement with no dominance in silt and clay percentages thus reflecting on the preference to either epifaunal or infaunal life position of *Q. lamarckiana*.

*Quinqueloculina seminulum* (Plate 7, Fig. 3a-c) is distributed from the mid sublittoral to uppermost bathyal. Optimal depth distribution is located at 99m in the mid sublittoral (Figure 6.3, Table 6.3). Highest abundance is shown in very fine sand, with 45% of the samples distributed in this grain size class (Table 6.4, Figure 6.8). Distribution in silt and

clay demonstrates highest abundance (40% of the samples) in the high percentages class of 30-40% (Table 6.5, Figure 6.13). Proportion of samples decreases continuously with decreasing silt and clay percentages thus no dominance in other classes is detected. Dependence on very fine sand substrate is in agreement with the dominance in high percentages of silt and clay thus reflecting on the preference to infaunal life position of *Q. seminulum*.

*Quinqueloculina venusta* (Plate 7, Fig. 5a-b) is distributed from the mid sublittoral to uppermost bathyal. Optimal depth distribution is located at 235m in the uppermost bathyal (Figure 6.3, Table 6.3). Highest abundance is shown in very fine sand, with 60% of the samples distributed in this grain size class (Table 6.4, Figure 6.8). Distribution in silt and clay demonstrates highest abundance (38% of the samples) in the highest percentages class of 40-50% (Table 6.5, Figure 6.13). Proportion of samples decreases continuously with decreasing silt and clay percentages thus no dominance in other classes is detected. Dependence on very fine sand substrate is in agreement with the dominance in highest percentages of silt and clay thus reflecting on the preference to infaunal life position of *Q. venusta*.

*Spirosigmoilina speciosa* (Plate 7, Fig. 8a-b) is distributed from the mid sublittoral to uppermost bathyal. Optimal depth distribution is located at 133m in the deeper sublittoral (Figure 6.3, Table 6.3). Highest abundance is shown in very fine sand, with 45% of the samples distributed in this grain size class (Table 6.4, Figure 6.8). Distribution in silt and clay demonstrates highest abundance (39% of the samples) in the high percentages class of 30-40% (Table 6.5, Figure 6.13). Proportion of samples decreases continuously with decreasing silt and clay percentages thus no dominance in other classes is detected. Dependence on very fine sand substrate is in agreement with the dominance in high percentages of silt and clay thus reflecting on the preference to infaunal life position of *S. speciosa*.

*Spiroloculina manifesta* (Plate 9, Fig. 6a-d) is distributed from the mid sublittoral to uppermost bathyal. Optimal depth distribution is located at 175m in the deeper sublittoral (Figure 6.3, Table 6.3). Highest abundance is shown in very fine sand, with 43% of the samples distributed in this grain size class (Table 6.4, Figure 6.8). Distribution in silt and clay demonstrates highest abundances in the 40-50% and 30-40% classes (Table 6.5, Figure 6.13), with 32% of the samples distributed similarly in each class. Proportion of samples decreases continuously with decreasing silt and clay percentages thus no dominance in other classes is detected. Dependence on very fine sand substrate is in agreement with the dominance in high percentages of silt and clay thus reflecting on the preference to infaunal life position of *S. manifesta*.

### 6.3.3 Hyaline foraminifera

*Fijella simplex* (Plate 16, Fig. 17) is distributed from the mid sublittoral to uppermost bathyal. Optimal depth distribution is located at 69m in the mid sublittoral (Figure 6.4a, Table 6.3). Highest abundance is shown in very fine sand, with 35% of the samples distributed in this grain size class (Table 6.4, Figure 6.9a). Distribution in silt and clay demonstrates highest abundances in the 40-50% and 30-40% classes (Table 6.5, Figure 6.14a), with 19% of the samples distributed in the highest percentages class of 40-50% and 28% in the high percentages class of 30-40%. Proportion of samples decreases

continuously with decreasing silt and clay percentages thus no dominance in other classes is detected. Dependence on very fine sand substrate is in agreement with the dominance in high percentages of silt and clay thus reflecting on the preference to infaunal life position of *F. simplex*.

*Cellanthus craticulatus* (Plate 15, Fig. 4) is distributed from the mid sublittoral to uppermost bathyal. Optimal depth distribution is located at 79m in the mid sublittoral (Figure 6.4a, Table 6.3). Highest abundance is shown in very fine sand, with 48% of the samples distributed in this grain size class (Table 6.4, Figure 6.9a). Distribution in silt and clay demonstrates highest abundance (60% of the samples) in the lowest percentages of silt and clay of 0-10% (Table 6.5, Figure 6.14a). The decrease in sample proportion is continuous with increasing silt and clay percentages thus no other dominance is detected. Dominance in the lowest percentages of silt and clay is not in agreement with the dependence on very fine sand substrate. Dominance in the lowest percentages of silt and clay reflects on the preference to epifaunal life position of *C. craticulatus*.

*Elphidium crispum* (Plate 15, Fig. 6a-b) is distributed from the mid sublittoral to uppermost bathyal. Optimal depth distribution is located at 82m in the mid sublittoral (Figure 6.4a, Table 6.3). Highest abundance is shown in coarse sand, with 40% of the samples distributed in this grain size class (Table 6.4, Figure 6.9a). Distribution in silt and clay does not demonstrate any dominance (Table 6.5, Figure 6.14a) with 31% of the samples distributed in the low percentages class of 10-20% and 30% of the samples distributed in the medium percentages class of 20-30%. Dependence on coarse sand is in agreement with no dominance in silt and clay percentages thus reflecting on the preference to either epifaunal or infaunal life position of *E. crispum*.

*Cibicides* cf. *C. refulgens* (Plate 14, Fig. 6a-b) is distributed from the mid sublittoral to uppermost bathyal. Optimal depth distribution is located at 86m in the mid sublittoral (Figure 6.4a, Table 6.3). Distribution in grain size classes does not show preference on substrate type due to 27% of the samples is distributed in very fine sand, 26% of the samples in fine sand, 26% of the samples in medium sand and 21% of the sample in coarse sand (Table 6.4, Figure 6.9a). Distribution in silt and clay does not demonstrate any dominance in percentages classes (Table 6.5, Figure 6.14a). Highest abundance (32% of the samples) is recorded in the high percentages class of 30-40%. The decrease in sample proportion is not continuous with the decreasing silt and clay percentages where second highest abundance (21% of the samples) is recorded in the low percentages class of 10-20%. This demonstrates similar dominance in the high and low percentages classes. No dependence on substrate type is in agreement with no dominance in silt and clay percentages thus reflecting on the preference to either epifaunal or infaunal life position of *C.* cf. *C. refulgens*.

*Paracibicides hebeslucidus* (Plate 14, Fig. 8a-c) is distributed from the mid sublittoral to uppermost bathyal. Optimal depth distribution is located at 178m in the deeper sublittoral (Figure 6.4a, Table 6.3). Distribution in grain size classes does not show preference on substrate type due to 32% of the samples distributed in fine sand and 31% of the samples in very fine sand (Table 6.4, Figure 6.9a). Distribution in silt and clay does not demonstrate any dominance in percentages classes (Table 6.5, Figure 6.14a). Highest abundance (32% of the samples) is recorded in the high percentages class of 30-40%. The decrease in sample proportion is not continuous with decreasing silt and clay percentages where 20% of the samples distributed in the medium percentages class of

20-30% and 19% of the samples in the lowest percentages class of 0-10%. This demonstrates similar dominance in the medium and lowest percentages classes. No dependence on substrate type is in agreement with no dominance in silt and clay percentages thus reflecting on the preference to either epifaunal or infaunal life position of *P. hebeslucidus*.

*Cibicidoides pachyderma* (Plate 12, Fig. 6a-b) is distributed from the mid sublittoral to uppermost bathyal with an optimum at 170m in the deeper sublittoral (Figure 6.4a, Table 6.3). Highest abundance is shown in very fine sand, with 49% of the samples distributed in this grain size class (Table 6.4, Figure 6.9a). Distribution in silt and clay demonstrates dominance (65% of the samples) in the highest percentage class of 40-50% (Table 6.5, Figure 6.14a). Dependence on very fine sand substrate is in agreement with the dominance in highest percentages of silt and clay thus reflecting on the preference to infaunal life position of *C. pachyderma*.

*Caribeanella celsusraphes* (Plate 16, Fig. 7a-b) is distributed from the mid sublittoral to uppermost bathyal with an optimum at 177m in the deeper sublittoral (Figure 6.4a, Table 6.3). Highest abundance is shown in coarse sand, with 42% of the samples distributed in this grain size class (Table 6.4, Figure 6.9a). Distribution in silt and clay does not demonstrate any dominance (Table 6.5, Figure 6.14a). Highest abundance (31% of the samples) is distributed in the high percentages class of 30-40%. The decrease in sample proportion is not continuous with decreasing silt and clay percentages where dominance is detected in the medium and lowest percentages classes. Dependence on coarse sand is in agreement with no dominance in silt and clay percentages thus reflecting on the preference to either epifaunal or infaunal life position of *C. celsusraphes*.

*Caribeanella shimabarensis* (Plate 16, Fig. 10a-b) is distributed from the mid sublittoral to uppermost bathyal. Optimal depth distribution is located at 290m in the uppermost bathyal (Figure 6.4b, Table 6.3). Highest abundance is shown in very fine sand, with 44% of the samples distributed in this grain size class (Table 6.4, Figure 6.9b). Distribution in silt and clay demonstrates dominance (45% of the samples) in the highest percentage class of 40-50% (Table 6.5, Figure 6.14b). Dependence on very fine sand substrate is in agreement with the dominance in highest percentages of silt and clay thus reflecting on the preference to infaunal life position of *C. shimabarensis*.

*Eponides repandus* (Plate 15, Fig. 9a-b) is distributed from the mid sublittoral to uppermost bathyal. Optimal depth distribution is located at 88m in the mid sublittoral (Figure 6.4a, Table 6.3). Distribution in grain size classes does not show preference on substrate type due to 33% of the samples distributed in medium sand and 27% of the samples in coarse sand (Table 6.4, Figure 6.9a). Distribution in silt and clay does not demonstrate any dominance in percentages classes (Table 6.5, Figure 6.14a). Highest abundance (31% of the samples) is recorded in the medium percentages class of 20-30%. The decrease in sample proportion is not continuous with decreasing or increasing percentages of silt and clay, where 27% of the samples distributed in the low percentages class of 10-20% and 21% of the samples in the high percentages class of 30-40%. This demonstrates similar dominance in the low and high percentages classes. No dependence on substrate type is in agreement with no dominance in silt and clay percentages thus reflecting on the preference to either epifaunal or infaunal life position of *E. repandus*.

*Planorbulinella larvata* (Plate 16, Fig. 12a-b) is distributed from the mid sublittoral to uppermost bathyal with an optimum at 146m in the deeper sublittoral (Figure 6.4a, Table 6.3). Highest abundance is shown in coarse sand, with 44% of the samples distributed in this grain size class (Table 6.4, Figure 6.9a). Distribution in silt and clay demonstrates highest abundance (30% of the samples) in the lowest percentages class of 0-10% (Table 6.5, Figure 6.14a). Proportion of samples decreases continuously with the increase of silt and clay percentages thus no dominance in other classes is detected. Dependence on coarse sand substrate is in agreement with the dominance in lowest percentages of silt and clay. Dominance in lowest percentages of silt and clay reflects on the preference to epifaunal life position of *P. larvata*.

*Asanonella tubulifera* (Plate 15, Fig. 7a-b) is distributed from the mid sublittoral to uppermost bathyal with an optimum at 147m in the deeper sublittoral (Figure 6.4a, Table 6.3). Highest abundance is shown in medium sand, with 36% of the samples distributed in this grain size class (Table 6.4, Figure 6.9a). Distribution in silt and clay demonstrates highest abundance (27% of samples) in the lowest percentages class of 0-10% (Table 6.5, Figure 6.14a). The decrease in the proportion of samples is continuous with increasing silt and clay percentages but no dominance is recorded because the samples are equally proportioned in the low, medium and high percentages classes. This demonstrates no dominance in silt and clay percentages. Dependence on medium sand substrate is in agreement with no dominance in silt and clay percentages thus reflecting on the preference to either epifaunal or infaunal life position of *A. tubulifera*.

*Paracassidulina neocarinata* (Plate 14, Fig. 5a-b) is distributed from the mid sublittoral to uppermost bathyal with an optimum at 178m in the deeper sublittoral (Figure 6.4a, Table 6.3). Highest abundance is shown in very fine sand, with 53% of the samples distributed in this grain size class (Table 6.4, Figure 6.9a). Distribution in silt and clay demonstrates highest abundances in the 40-50% and 30-40% classes (Table 6.5, Figure 6.14a), with similar sample proportion of 34% distributed in each percentages class. Proportion of samples decreases continuously with the decrease of silt and clay percentages thus no dominance in other classes is detected. Dependence on very fine sand substrate is in agreement with the dominance in highest percentages of silt and clay thus reflecting on the preference to infaunal life position of *P. neocarinata*.

*Melonis nicobarense* (Plate 16, Fig. 2a-b) is distributed from the mid sublittoral to uppermost bathyal with an optimum at 199m in the deeper sublittoral (Figure 6.4a, Table 6.3). Highest abundance is shown in very fine sand, with 66% of the samples distributed in this grain size class (Table 6.4, Figure 6.9a). Distribution in silt and clay demonstrates dominance (60% of the samples) in the highest percentages class of 40-50% (Table 6.5, Figure 6.14a). Proportion of samples decreases continuously with decreasing silt and clay percentages thus no dominance in other classes is detected. Dependence on very fine sand substrate is in agreement with the dominance in highest percentages of silt and clay thus reflecting on the preference to infaunal life position of *M. nicobarense*.

*Bolivina vadescens* (Plate 13, Fig. 8) is distributed from the mid sublittoral to uppermost bathyal. Optimal depth distribution is located at 201m in the uppermost bathyal (Figure 6.4b, Table 6.3). Highest abundance is shown in very fine sand, with 81% of the samples distributed in this grain size class (Table 6.4, Figure 6.9b). Distribution in silt and clay demonstrates dominance (55% of the samples) in the highest percentages class of 40-50% (Table 6.5, Figure 6.14b). Dependence on very fine sand substrate is in agreement

with the dominance in highest percentages of silt and clay thus reflecting on the preference to infaunal life position of *B. vadescens*.

*Stomatorbina concentrica* (Plate 15, Fig. 11a-b) is distributed from the mid sublittoral to uppermost bathyal. Optimal depth distribution is located at 214m in the uppermost bathyal (Figure 6.4b, Table 6.3). Highest abundance is shown in coarse sand, with 48% of the samples distributed in this grain size class (Table 6.4, Figure 6.9b). Distribution in silt and clay does not demonstrate any dominance (Table 6.5, Figure 6.14b). Highest abundance (33% of the samples) is distributed in the low percentages class of 10-20%. The decrease in sample proportion is not continuous with increasing silt and clay percentages where dominance is detected in the medium and highest percentages classes. Dependence on coarse sand is in agreement with no dominance in silt and clay percentages thus reflecting on the preference to either epifaunal or infaunal life position of *S. concentrica*.

*Rectobolivina raphana* (Plate 16, Fig. 14) is distributed from the mid sublittoral to uppermost bathyal. Optimal depth distribution is located at 214m in the uppermost bathyal (Figure 6.4b, Table 6.3). Highest abundance is shown in very fine sand, with 89% of the samples distributed in this grain size class (Table 6.4, Figure 6.9b). Distribution in silt and clay demonstrates dominance (76% of the samples) in the highest percentages class of 40-50% (Table 6.5, Figure 6.14b). Dependence on very fine sand substrate is in agreement with the dominance in highest percentages of silt and clay thus reflecting on the preference to infaunal life position of *R. raphana*.

*Globocassidulina bisecta* (Plate 14, Fig. 4) is distributed from the mid sublittoral to uppermost bathyal. Optimal depth distribution is located at 291m in the uppermost bathyal (Figure 6.4b, Table 6.3). Distribution in grain size classes does not show preference on substrate type due to 31% of the samples distributed in medium sand and 26% of the samples in fine sand (Table 6.4, Figure 6.9b). Distribution in silt and clay does not demonstrate any dominance in percentages classes (Table 6.5, Figure 6.14b). Highest abundance (30% of the samples) is recorded in the medium percentages class of 20-30%. The decrease in sample proportion is not continuous with decreasing silt and clay percentages where 19% of the samples distributed in the low percentages class of 10-20% and 28% of the samples in the highest percentages class of 40-50%. This demonstrates dominance in the low and highest percentages classes. No dependence on substrate type is in agreement with no dominance in silt and clay percentages thus reflecting on the preference to either epifaunal or infaunal life position of *G. bisecta*.

*Neoconorbina tuberocapitata* (Plate 17, Fig. 2a-b) is distributed from the mid sublittoral to uppermost bathyal. Optimal depth distribution is located at 211m in the uppermost bathyal (Figure 6.4b, Table 6.3). Highest abundance is shown in very fine sand, with 54% of the samples distributed in this grain size class (Table 6.4, Figure 6.9b). Distribution in silt and clay demonstrates highest abundance (36% of the samples) in the highest percentages class of 40-50% (Table 6.5, Figure 6.14b). The decrease in sample proportion is continuous with decreasing silt and clay percentages thus no dominance in other classes is detected. Dependence on very fine sand substrate is in agreement with the dominance in highest percentages of silt and clay thus reflecting on the preference to infaunal life position of *N. tuberocapitata*.

*Neoconorbina communis* (Plate 17, Fig. 1a-b) is distributed from the mid sublittoral to uppermost bathyal. Optimal depth distribution is located at 272m in the uppermost bathyal (Figure 6.4b, Table 6.3). Distribution in grain size classes does not show preference on substrate type due to similar sample abundances in the coarse and medium sand classes (Table 6.4, Figure 6.9b) with 36% of the samples distributed in each class. Distribution in silt and clay does not demonstrate any dominance in percentages classes (Table 6.5, Figure 6.14b). Highest abundance (43% of the samples) is recorded in the high percentages class of 30-40% and another 42% of the samples can be found in the medium percentages class of 20-30%. This demonstrates similar dominance in the high and medium percentages classes. No dependence on substrate type is in agreement with no dominance in silt and clay percentages thus reflecting on the preference to either epifaunal or infaunal life position of *N. communis*.

*Rosalina vilardeboana* (Plate 17, Fig. 7a-b) is distributed from the mid sublittoral to uppermost bathyal. Optimal depth distribution is located at 247m in the uppermost bathyal (Figure 6.4b, Table 6.3). Highest abundance is shown in very fine sand, with 47% of the samples distributed in this grain size class (Table 6.4, Figure 6.9b). Distribution in silt and clay demonstrates highest abundance (30% of the samples) in the highest percentages class of 40-50% (Table 6.5, Figure 6.14b). The decrease in sample proportion is continuous with decreasing silt and clay percentages thus no dominance in other classes is detected. Dependence on very fine sand substrate is in agreement with the dominance in highest percentages of silt and clay thus reflecting on the preference to infaunal life position of *R. vilardeboana*.

*Rosalina petasiformis* (Plate 17, Fig. 6a-b) is distributed from the mid sublittoral to uppermost bathyal. Optimal depth distribution is located at 257m in the uppermost bathyal (Figure 6.4b, Table 6.3). Distribution in grain size classes does not show preference on substrate type due to 31% of the samples distributed in fine sand and 29% of the samples can be found in medium sand classes (Table 6.4, Figure 6.9b). Distribution in silt and clay does not demonstrate any dominance in percentages classes (Table 6.5, Figure 6.14b). Highest abundance (39% of the samples) is recorded in the medium percentages class of 20-30% and second highest abundance (34% of the samples) can be found in the low percentages class of 10-20%. This demonstrates similar dominance in the medium and low percentages classes. No dependence on substrate type is in agreement with no dominance in silt and clay percentages thus reflecting on the preference to either epifaunal or infaunal life position of *R. petasiformis*.

*Lenticulina vortex* (Plate 10, Fig. 14a-b) is distributed from the mid sublittoral to uppermost bathyal. Optimal depth distribution is located at 192m in the deeper sublittoral (Figure 6.4b, Table 6.3). Distribution in grain size classes does not show preference on substrate type due to 38% of the samples distributed in coarse sand and 33% of the samples can be found in very fine sand classes (Table 6.4, Figure 6.9b). Distribution in silt and clay does not demonstrate any dominance in percentages classes (Table 6.5, Figure 6.14b). Highest abundance (39% of the samples) is recorded in the highest percentages class of 40-50%. The decrease in silt and clay percentages is not continuous with decreasing sample proportion where another abundance (20% of the samples) is recorded in the medium percentages class of 20-30%. No dependence on substrate type is in agreement with no dominance in silt and clay percentages thus reflecting on the preference to either epifaunal or infaunal life position of *L. vortex*.

*Lenticulina limbosa* (Plate 10, Fig. 13a-b) is distributed from the mid sublittoral to uppermost bathyal. Optimal depth distribution is located at 232m in the uppermost bathyal (Figure 6.4b, Table 6.3). Highest abundance is shown in very fine sand, with 42% of the samples distributed in this grain size class (Table 6.4, Figure 6.9b). Distribution in silt and clay demonstrates dominance (61% of the samples) in the highest percentages class of 40-50% (Table 6.5, Figure 6.14b). Dependence on very fine sand substrate is in agreement with the dominance in the highest percentages of silt and clay thus reflecting on the preference to infaunal life position of *L. limbosa*.

### 6.3.4 Aragonite foraminifera

*Lamarckina ventricosa* (Plate 11, Fig. 1a-b) is distributed from the mid sublittoral to uppermost bathyal. Optimal depth distribution is located at 174m in the deeper sublittoral (Figure 6.5, Table 6.3). Distribution in grain size classes does not show preference on substrate type due to 36% of the samples distributed in coarse sand and 27% of the samples can be found in very fine sand classes (Table 6.4, Figure 6.10). Distribution in silt and clay does not demonstrate any dominance in percentages classes (Table 6.5, Figure 6.15). Highest abundance (24% of samples) is recorded in the highest percentages of silt and clay class of 40-50%. The samples are equally proportioned in the medium, low and lowest percentages of silt and clay, with 18% of the samples distributed in each class. No dependence on substrate type is in agreement with no dominance in silt and clay percentages thus reflecting on the preference to either epifaunal or infaunal life position of *L. ventricosa*.

*Hoeglundina elegans* (Plate 11, Fig. 2a-b) is distributed from the mid sublittoral to uppermost bathyal. Optimal depth distribution is located at 199m in the deeper sublittoral (Figure 6.5, Table 6.3). Highest abundance is shown in very fine sand, with 52% of the samples distributed in this grain size class (Table 6.4, Figure 6.10). Distribution in silt and clay demonstrates dominance (46% of the samples) in the highest percentages class of 40-50% (Table 6.5, Figure 6.15). The decrease in sample proportion is continuous with decreasing silt and clay percentages thus no other dominance is detected. Dependence on very fine sand substrate is in agreement with the dominance in highest percentages of silt and clay thus reflecting on the preference to infaunal life position of *H. elegans*.

## 6.4 Conclusion

### 6.4.1 Optimal depth distribution and dependence on substrate type of optimally preserved smaller benthic foraminiferal tests

Relationships among depth, inclination and sedimentological parameters have been determined by canonical correspondence analysis. Depth is the most important factor in the ordination. Increasing depth shows positive correlation with increasing skewness indicating dominance of finer sediment components in the deeper water region. Decreasing depth shows positive correlation with increasing sorting indicating dominance of coarser sediment components in the shallow water region. Relationships between depth, inclination and grain size distribution carried out in canonical correspondence analysis have also demonstrated similar results. Sediments in the deepest region are

dominated by silt and clay component. Sandy components have shown dominance in the mid sublittoral region. Coarser sediments dominate the shallowest water region.

Optimal depth distribution of the optimally preserved tests in the mid and deeper sublittoral is related to dependence on coarse sand, medium sand or no dependence on specific substrate type. Optimal depth distribution of the tests in the uppermost bathyal is related to dependence on fine and very fine sand.

Agglutinated tests showing shallowest optimal depth distribution at less than 100m in the mid sublittoral zone, i.e., *Pseudogaudryina atlanta pacifica* does not show dependence on specific substrate type (Table 6.6). Agglutinated tests showing optimal depth distribution in the deeper sublittoral zone from 100m to less than 200m, i.e., *Textularia crenata, T. foliacea* and *T. neorugosa* have shown dependence on coarse and medium sand (Table 6.6). Agglutinated tests showing deepest optimal depth distribution in the uppermost bathyal from 200m to less than 300m, i.e., *T. agglutinans, Spirotextularia floridana* and *S. fistulosa* demonstrate dependence on fine and very fine sand. Agglutinated foraminiferal tests in the investigation have demonstrated agreement between optimal depth distribution and dependence on substrate type.

Porcelaneous and hyaline tests demonstrate partial agreement between optimal depth distribution in the mid sublittoral zone and dependence on substrate type (Table 6.6). Porcelaneous tests showing optimal depth distribution in the mid sublittoral zone demonstrate dependence on very fine sand or no dependence on specific substrate type. For example, *Triloculina affinis* with an optimum at 86m shows dependence on very fine sand and *Quinqueloculina bicarinata* with an optimum at 94m does not demonstrate dependence on any specific substrate type. Hyaline tests showing optimal depth distribution in the mid sublittoral zone demonstrate dependence on very fine sand, coarse sand or no dependence on specific substrate type (Table 6.6). For instance, *Fijella simplex* with an optimum at 69m shows dependence on very fine sand, *Elphidium crispum* with an optimum at 82m shows dependence on coarse sand and *Cibicides* cf. *C. refulgens* with an optimum at 96m does not demonstrate dependence on any specific substrate type. Aragonite tests, i.e., *Hoeglundina elegans* and *Lamarckina ventricosa* do not demonstrate optimal depth distribution in the mid sublittoral zone.

Porcelaneous, hyaline and aragonite tests demonstrate partial agreement between optimal depth distribution in the deeper sublittoral zone and dependence on substrate type (Table 6.6). Porcelaneous tests showing optimal depth distribution in the deeper sublittoral zone demonstrate dependence on very fine sand or no dependence on specific substrate type (Table 6.6). For example, *Spiroloculina manifesta* with an optimum at 175m shows dependence on very fine sand and *Quinqueloculina lamarckiana* with an optimum at 127m does not demonstrate dependence on any specific substrate type. Hyaline tests showing optimal depth distribution in the deeper sublittoral zone demonstrate dependence on coarse sand, medium sand, very fine sand or no dependence on specific substrate type (Table 6.6). For example, *Caribeanella celsusraphes* with an optimum at 177m shows dependence on coarse sand, *Asanonella tubulifera* with an optimum at 147m shows dependence on medium sand, *Cibicidoides pachyderma* with an optimum at 170m shows dependence on very fine sand and *Lenticulina vortex* with an optimum at 192m does not demonstrate dependence on any specific substrate type. Aragonite tests, i.e., *Hoeglundina elegans* and *Lamarckina ventricosa* showing optimal depth distribution in the deeper sublittoral zone demonstrate

dependence on very fine sand or no dependence on specific substrate type (Table 6.6). *H. elegans* with an optimum at 198m shows dependence on very fine sand and *L. ventricosa* with an optimum at 173m does not demonstrate dependence on any specific substrate type.

Porcelaneous and hyaline tests demonstrate partial agreement between optimal depth distribution in the uppermost bathyal and dependence on substrate type (Table 6.6). Porcelaneous tests showing optimal depth distribution in the uppermost bathyal zone demonstrate dependence on very fine sand, medium sand or no dependence on specific substrate type (Table 6.6). For instance, *Quinqueloculina venusta* with an optimum at 235m shows dependence on very fine sand, *Miliolinella circularis* with an optimum at 248m shows dependence on medium sand and *Pyrgo denticulata* with an optimum at 247m does not demonstrate dependence on any specific substrate type. Hyaline tests showing optimal depth distribution in the uppermost bathyal demonstrate dependence on coarse sand, very fine sand or no dependence on specific substrate type (Table 6.6). For example, *Stomatorbina concentrica* with an optimum at 226m shows dependence on coarse sand, *Caribeanella shimabarensis* with an optimum at 290m shows dependence on very fine sand and *Globocassidulina bisecta* with an optimum at 291m does not demonstrate dependence on any specific substrate type.

### 6.4.2 Relationship between dependence on substrate type, dominance in percentages of silt and clay and life position of the optimally preserved smaller benthic foraminiferal tests

Relationships between dependence on substrate type, dominance in percentages of silt and clay and life position of optimally preserved smaller benthic foraminifera are presented in table 6.6. Dependence on fine or very fine sand is related to test dominance in the high or highest percentages of silt and clay. Dominance in the high or highest percentages of silt and clay is reflected on infaunal life position of the species. Dependence on coarse sand, medium sand or no dependence on any specific substrate type is related to test dominance in the low or lowest percentages of silt and clay. Dominance in the low or lowest percentages of silt and clay is reflected on epifaunal life position of the species. Dependence on coarse sand, medium sand or no dependence on any specific substrate type is related to no dominance in percentages of silt and clay. No dominance of the tests in percentages of silt and clay reflects on either epifaunal or infaunal life position of the species. Most of the smaller benthic foraminiferal species have shown agreements to these principles except for *Spirotextularia fistulosa* and *Cellanthus craticulatus* (Table 6.6). *S. fistulosa* has shown dependence on fine sand and dominance in medium percentages of silt and clay of 20-30%. Dominance in medium percentages of silt and clay is reflected on either epifaunal or infaunal life position of this species. *C. craticulatus* has shown dependence on very fine sand and dominance in the lowest percentages of silt and clay of 0-10%. Dominance in the lowest percentages of silt and clay reflects on epifaunal life position of *C. craticulatus*.

| Species | Optima | Substrate | Silt and clay | Life position |
|---|---|---|---|---|
| **Agglutinated foraminifera:** | | | | |
| *Spirotextularia floridana* | 230m | Very fine sand | Highest % | Infaunal |
| *Spirotextularia fistulosa* | 260m | Fine sand | Medium % | Epi/Infaunal |
| *Pseudogaudryina atlanta pacifica* | 96m | No dependence | No dominance | Epi/Infaunal |
| *Textularia agglutinans* | 202m | Very fine sand | Highest % | Infaunal |
| *Textularia crenata* | 139m | Coarse sand | Low % | Epifaunal |
| *Textularia foliacea* | 103m | Medium sand | No dominance | Epi/Infaunal |
| *Textularia neorugosa* | 149m | Coarse sand | Low % | Epifaunal |
| **Porcelaneous foraminifera:** | | | | |
| *Miliolinella* cf. *M. chiastocytis* | 166m | No dependence | No dominance | Epi/Infaunal |
| *Miliolinella circularis* | 248m | Medium sand | No dominance | Epi/Infaunal |
| *Miliolinella subrotunda* | 159m | No dependence | No dominance | Epi/Infaunal |
| *Pyrgo denticulata* | 247m | No dependence | Medium % | Epi/Infaunal |
| *Pyrgo sarsi* | 239m | Medium sand | Lowest % | Epifaunal |
| *Triloculina affinis* | 86m | Very fine sand | High % | Infaunal |
| *Triloculina tricarinata* | 109m | No dependence | No dominance | Epi/Infaunal |
| *Spirosigmoilina speciosa* | 133m | Very fine sand | High % | Infaunal |
| *Spiroloculina manifesta* | 175m | Very fine sand | High % | Infaunal |
| *Quinqueloculina bicarinata* | 94m | No dependence | Low % | Epifaunal |
| *Quinqueloculina lamarckiana* | 127m | No dependence | No dominance | Epi/Infaunal |
| *Quinqueloculina seminulum* | 99m | Very fine sand | High % | Infaunal |
| *Quinqueloculina venusta* | 235m | Very fine sand | Highest % | Infaunal |
| **Hyaline foraminifera:** | | | | |
| *Asanonella tubulifera* | 147m | Medium sand | No dominance | Epi/Infaunal |
| *Bolivina vadescens* | 201m | Very fine sand | Highest % | Infaunal |
| *Caribeanella celsusraphes* | 177m | Coarse sand | No dominance | Epi/Infaunal |
| *Caribeanella shimabarensis* | 290m | Very fine sand | Highest % | Infaunal |
| *Cellanthus craticulatus* | 79m | Fine sand | Lowest % | Epifaunal |
| *Cibicides* cf. *C. refulgens* | 86m | No dependence | No dominance | Epi/Infaunal |
| *Elphidium crispum* | 82m | Coarse sand | No dominance | Epi/Infaunal |
| *Eponides repandus* | 88m | No dependence | No dominance | Epi/Infaunal |
| *Fijella simplex* | 69m | Very fine sand | High % | Infaunal |
| *Cibicidoides pachyderma* | 170m | Very fine sand | Highest % | Infaunal |
| *Globocassidulina bisecta* | 291m | No dependence | No dominance | Epi/Infaunal |
| *Lenticulina limbosa* | 232m | Very fine sand | Highest % | Infaunal |
| *Lenticulina vortex* | 192m | No dependence | No dominance | Epi/Infaunal |
| *Melonis nicobarense* | 199m | Very fine sand | Highest % | Infaunal |
| *Paracassidulina neocarinata* | 184m | Very fine sand | Highest % | Infaunal |
| *Paracibicides hebeslucidus* | 178m | No dependence | No dominance | Epi/Infaunal |
| *Planorbulinella larvata* | 146m | Coarse sand | Lowest % | Epifaunal |
| *Neoconorbina communis* | 272m | No dependence | No dominance | Epi/Infaunal |
| *Neoconorbina tuberocapitata* | 211m | Very fine sand | Highest % | Infaunal |
| *Rosalina petasiformis* | 257m | No dependence | No dominance | Epi/Infaunal |
| *Rosalina vilardeboana* | 247m | Very fine sand | Highest % | Infaunal |
| *Stomatorbina concentrica* | 214m | Coarse sand | No dominance | Epi/Infaunal |
| *Rectobolivina raphana* | 226m | Very fine sand | Highest % | Infaunal |
| **Aragonite foraminifera:** | | | | |
| *Hoeglundina elegans* | 198m | Very fine sand | Highest % | Infaunal |
| *Lamarckina ventricosa* | 173m | No dependence | No dominance | Epi/Infaunal |

Table 6.6 Summary of optimal depth distribution, substrate type dependence and life position of smaller benthic foraminiferal tests in the mid to deeper sublittoral and uppermost bathyal

## Bibliography


Akimoto, K. et al., 2002. *Atlas of Holocene benthic foraminifers of Shimabara Bay, Kyushu, southwest Japan*, The Kagoshima University Museum.

Annin, V.K., 2001. Benthic foraminifera assemblages as bottom environmental indicators Posiet Bay, Sea of Japan. *Journal of Asian Earth Sciences*, 20(1), pp.9–29.

Boggs, S., 2006. *Principles of sedimentology and stratigraphy* Fourth., New Jersey: Pearson Prentice Hall.

Briguglio, A. & Hohenegger, J., 2011. How to react to shallow water hydrodynamics: The larger benthic foraminifera solution. *Marine Micropaleontology*, 81(1-2), pp.63–76. Available at: http://dx.doi.org/10.1016/j.marmicro.2011.07.004.

Buzas, M.A., Culver, S.J. & Jorissen, F.J., 1993. A statistical evaluation of the microhabitats of living (stained) infaunal benthic foraminifera. *Marine Micropaleontology*, 20(3-4), pp.311–320.

Cheetham, M.D. et al., 2008. A comparison of grain-size analysis methods for sand-dominated fluvial sediments. *Sedimentology*, 55(6), pp.1905–1913. Available at: http://doi.wiley.com/10.1111/j.1365-3091.2008.00972.x.

Corliss, B.H., 1985. Microhabitats of benthic foraminifera within deep-sea sediments. *Nature*, 314(6), pp.435–438. Available at: http://adsabs.harvard.edu/cgi-bin/nph-data_query?bibcode=1985Natur.314..435C&link_type=ABSTRACT\npapers2://publication/doi/10.1038/314435a0.

Corliss, B.H., 1991. Morphology and microhabitat preferences of benthic foraminifera from the northwest Atlantic Ocean. *Marine Micropaleontology*, 17(3-4), pp.195–236.

Corliss, B.H. & Emerson, S., 1990. Distribution of rose bengal stained deep-sea benthic foraminifera from the Nova Scotian continental margin and Gulf of Maine. *Deep-Sea Research*, 37(3), pp.381–400.

Debenay, J.P., 2012. *A Guide to 1,000 Foraminifera from Southwestern Pacific: New Caledonia*, IRD Editions.

Diz, P. et al., 2004. Distribution of benthic foraminifera in coarse sediments, Ria de Vigo, NW Iberian Margin. *Journal of Foraminiferal Research*, 34(4), pp.258–275.

Sen Gupta, B.K., 2002. Systematics of modern foraminifera. In B. K. Sen Gupta, ed. *Modern Foraminifera*. Kluwer Academic Publishers, pp. 7–36.

Hallock, P., 1984. Distribution of selected species of living algal symbiont-bearing foraminifera on two Pacific coral reefs. *The Journal of Foraminiferal Research*, 14(4), pp.250–261.

Hallock, P., 1981. Light dependence in Amphistegina. *Journal of Foraminiferal Research*, 11(1), pp.40–46.

Hallock, P., Röttger, R. & Wetmore, K., 1991. Hypotheses on form and function in foraminifera. In *Biology of the Foraminifera*. Academic Press Limited, pp. 41–66.

Hammer, O. & Harper, D.A.T., 2006. *Palaeontological data analysis* First., Blackwell Publishing.

Hassink, J., 1997. The capacity of soils to preserve organic C and N by their association with clay and silt particles. *Plant and Soil*, 191(1), pp.77–87.

Hatta, A. & Ujiie, H., 1992. Benthic foraminifera from coral seas between Ishigaki and Iriomote Islands, southern Ryukyu Island Arc, northwestern Pacific. *Bulletin of the College of Science, University of the Ryukyus*, p.287.

Hohenegger, J., 2000a. Coenoclines of larger foraminifera. *Micropaleontology*, 46, suppl.(2000), pp.127–151.

Hohenegger, J., 2004. Depth coenoclines and environmental considerations of western Pacific larger foraminifera. *The Journal of Foraminiferal Research*, 34(1), pp.9–33.

Hohenegger, J., 1994. Distribution of living larger foraminifera NW of Sesoko-Jima, Okinawa, Japan. *Marine Ecology*, 15, pp.291–334.

Hohenegger, J. et al., 1999. Habitats of larger foraminifera on the upper reef slope of Sesoko Island, Okinawa, Japan. *Marine Micropaleontology*, 36(2-3), pp.109–168.

Hohenegger, J., 2002. Inferences on sediment production and transport at carbonate beaches using larger foraminifera. *Carbonate Beaches 2000*, pp.112–125. Available at: http://ascelibrary.org/doi/abs/10.1061/40640(305)9.

Hohenegger, J., 2011. *Large foraminifera: Greenhouse constructions and gardeners in the oceanic microcosm*, Kagoshima, Japan: The Kagoshima University Museum.

Hohenegger, J., 2006. Morphocoenoclines, character combination and environmental gradients: A case study using symbiont-bearing benthic foraminifera. *Paleobiology*, 32(1), pp.70–99.

Hohenegger, J., 2000b. Remarks on West Pacific Nummulitidae (Foraminifera). *The Journal of Foraminiferal Research*, 30(1), pp.3–28.

Hohenegger, J., Piller, W. & Baal, C., 1993. Horizontal and vertical spatial microdistribution of foraminifers in the shallow subtidal Gulf of Trieste, northern Adriatic Sea. *The Journal of Foraminiferal Research*, 23(2), pp.79–101.

Hohenegger, J. & Yordanova, E.K., 2001a. Depth-transport functions and erosion-deposition diagrams as indicators of slope inclination and time-averaged traction forces: Applications in tropical reef environments. *Sedimentology*, 48(5), pp.1025–1046.

Hohenegger, J. & Yordanova, E.K., 2001b. Displacement of larger foraminifera at the western slope of Motobu Peninsula (Okinawa, Japan). *Palaios*, 16(1), pp.53–72. Available at: http://palaios.sepmonline.org/cgi/doi/10.1669/0883-1351(2001)016<0053:DOLFAT>2.0.CO;2.

Hottinger, L., 1983. Processes determining the distribution of larger foraminifera in space and time. *Utrecht Micropaleontology Bulletin*, 30, pp.239–253.

Hunt, A.S. & Corliss, B.H., 1993. Distribution and microhabitats of living (stained) benthic foraminifera from the Canadian Arctic Archipelago. *Marine Micropaleontology*, 20(3-4), pp.321–345.

Jorissen, F.J., 2002. Benthic foraminiferal microhabitats below the sediment water interface. In B. K. Sen Gupta, ed. *Modern Foraminifera*. Kluwer Academic Publishers, pp. 181–200. Available at: http://www.springerlink.com/content/q534423572544175.

Jorissen, F.J. et al., 1998. Live benthic foraminiferal faunas off Cape Blanc, NW-Africa: Community structure and microhabitats. *Deep-Sea Research Part I: Oceanographic Research Papers*, 45(12), pp.2157–2188.

Jorissen, F.J. et al., 1992. Vertical distribution of benthic foraminifera in the northern Adriatic Sea: The relation with organic flux. *Marine Micropaleontology*, 19, pp.131–146.

Jorissen, F.J. et al., 1994. Vertical distribution of living benthic foraminifera in submarine canyons off New Jersey. *The Journal of Foraminiferal Research*, 24(1), pp.28–36.

Jorissen, F.J., De Stigter, H.C. & Widmark, J.G.V., 1995. A conceptual model explaining benthic foraminiferal microhabitats. *Marine Micropaleontology*, 26(1-4), pp.3–15. Available at: http://linkinghub.elsevier.com/retrieve/pii/037783989500047X.

Kirk, J.T.O., 1994. *Light and photosynthesis in aquatic ecosystems* Second., Canberra.

Kitazato, H., 1995. Recolonization by deep-sea benthic foraminifera: Possible substrate preferences. *Marine Micropaleontology*, 26(1-4), pp.65–74.

Lalli, C. & Parsons, T., 1997. *Biological Oceanography: An Introduction* Second., Elsevier.

Lee, J.J. et al., 1989. Identification and distribution of endosymbiotic diatoms in larger Foraminifera. *Micropaleontology*, 35(4), pp.353–366.

Linke, P. & Lutze, G.F., 1993. Microhabitat preferences of benthic foraminifera: A static concept or a dynamic adaptation to optimize food acquisition? *Marine Micropaleontology*, 20(3-4), pp.215–234.

Loeblich, A. & Tappan, H., 1994. *Foraminifera of the Sahul shelf and Timor sea* Special. S. J. Culver, ed., Cushman Foundation for Foraminiferal Research Inc.

Lutze, G.F. & Thiel, H., 1989. Epibenthic foraminifera from elevated microhabitats; Cibicidoides wuellerstorfi and Planulina ariminensis. *The Journal of Foraminiferal Research*, 19(2), pp.153–158.

Matsuda, S. & Iryu, Y., 2011. Rhodoliths from deep fore-reef to shelf areas around Okinawa-jima, Ryukyu Islands, Japan. *Marine Geology*, 282(3-4), pp.215–230. Available at: http://dx.doi.org/10.1016/j.margeo.2011.02.013.

Mikhalevich, V., 2004. On the new understanding of the order Lituolida Lankester, 1885 (Foraminifera). *Acta Palaeont Romaniae*, 4(July), pp.247–267. Available at: http://www.geo-paleontologica.org/Acta.vol.IV/24Mikhalevich.pdf.

Murray, J., 2006. *Ecology and application of benthic foraminifera* First., Cambridge University Press.

Murray, J., 2001. The niche of benthic foraminifera, critical thresholds and proxies. *Marine Micropaleontology*, 41(1-2), pp.1–7.

Parker, J.H., 2009. *Taxonomy of foraminifera from Ningaloo Reef, western Australia* Memoir 36., Canberra: Association of Australasian Palaeontologists.

Pecheux, M.J.-F., 1995. Ecomorphology of a recent large foraminifer, Operculina Ammonoides. *Geobios*, 28(5), pp.529–566.

Schmiedl, G. et al., 2000. Trophic control of benthic foraminiferal abundance and microhabitat in the bathyal Gulf of Lions, western Mediterranean Sea. *Marine Micropaleontology*, 40(3), pp.167–188.

Yordanova, E.K. & Hohenegger, J., 2007. Studies on settling, traction and entrainment of larger benthic foraminiferal tests: Implications for accumulation in shallow marine sediments. *Sedimentology*, 54(6), pp.1273–1306.

Yordanova, E.K. & Hohenegger, J., 2002. Taphonomy of larger foraminifera: Relationships between living individuals and empty tests on flat reef slopes (Sesoko Island, Japan). *Facies*, 46(1), pp.169–203.

## Species Index